2008-05-23

A Study of Cell Polarity and Fate Specification in Early *C. Elegans* Embryos: A Dissertation

Soyoung Kim
University of Massachusetts Medical School

A Dissertation Presented

By

Soyoung Kim

Submitted to the Faculty of the
University of Massachusetts Graduate School of Biomedical Sciences,
Worcester in partial fulfillment of the requirements for the degree of

DOCTOR OF PHILOSOPHY

May 23, 2008

Interdisciplinary Graduate Program

A STUDY OF CELL POLARITY AND FATE SPECIFICATION IN EARLY *C.ELEGANS* EMBRYOS

A Dissertation Presented

By

Soyoung Kim

Approved as to style and content by:

Charles Sagerstrom, Chair of Committee

Kirsten Hagstrom, Member of Committee

Dannel McCollum, Member of Committee

Heidi Tissenbaum, Member of Committee

Keith Blackwell, Member of Committee

Craig C. Mello, Dissertation Mentor

Anthony Carruthers, Dean of the Graduate School of Biomedical Sciences

Interdisciplinary Graduate Program

May 23, 2008

For my mother, Sunghee Kim

with love

In the vastness of space and the immensity of time, it is my joy to share a planet and an epoch.

- Carl Sagan, *Cosmos*

ACKNOWLEDGEMENTS

I would like to thank all people who have helped and inspired me during my doctoral study. First of all, I would like to express my deepest and sincerest gratitude toward my thesis advisor, Dr. Craig Mello, for his guidance, advice, teaching, support, and inspiration during my study at Umass Medical School. His perpetual energy and enthusiasm in science and his mission for providing "only high-quality work and not less" have made a deep impression on me. He also gave me both shock and pleasure to be close to a "celebrity" by becoming one of the youngest Nobel laureates.

It is difficult to overstate my appreciation to Drs. Masaki Shirayama, Kuniaki Nakamura, and Takao Ishidate with whom I began to learn about the stunning world of "worms". They kept an eye on the progress of my work, taught me extremely patiently, and were always available when I needed their advices, which made me possible to complete my doctoral research.

I am grateful to the members of my thesis committee, Drs. Charles Sagerstrom, Kirsten Hagstrom, Dannel McCollum, Heidi Tissenbaum, and Keith Blackwell for their constant encouragement, guidance, insight and support.

Thanks are due also to the members of Mello lab for providing a stimulating and fun environment for learning and growing. Drs. Elaine Youngman, Darryl Conte, and Ji liu sacrificed

their valuable time to read and comment my thesis. Particularly, Tuba Bas helped me get through difficult times by providing constant laugh and fun, and has always believed in me and become one of my best friends.

I would also like to thank my new and old friends Soo-Ryun Lee, Hyung-Jin Kim, Lanzo Kim, Mikyung Lim, Miyoung Jung, Sang Oh, Chul-Hwa Jung, Haihong Shen, and Hark Jung for "resonating" with me at crucial times in my life, and thereby contributing in various and sundry ways to this work. I am especially indebted to my dearest friend, Dr. Hopi Lee for his support and friendship. This work would not have been possible without him.

It would have been just heinous to deal with the pressure of graduate study without the fun of reading "Harry Potter". Thereby I would also like to express my appreciation to J.K. Rowling, the author of famous "Harry Potter" series, for sustaining my mental health by providing such a tantalizing world.

I cannot finish without saying how grateful I am with my family: grandmother, uncles, aunts, and cousins (all together about three dozens) all have given me their love and encouragement. Particular thanks to Hun, my little 6 feet tall brother, such a cutie. Lastly, and most importantly, I wish to thank my parents, Taesoo Kim and Sunghee Kim. They bore me, taught me, and loved me, which wasn't an easy feat. To them I dedicate this thesis.

ABSTRACT

Asymmetric cell divisions constitute a basic foundation of animal development, providing a mechanism for placing specific cell types at defined positions in a developing organism. In a 4-cell stage embryo in *Caenorhabditis elegans* the EMS cell divides asymmetrically to specify intestinal cells, which requires a polarizing signal from the neighboring P2 cell. Here we describe how the extracellular signal from P2 is transmitted from the membrane to the nucleus during asymmetric EMS cell division, and present the identification of additional components in the pathways that accomplish this signaling.

P2/EMS signaling involves multiple inputs, which impinge on the Wnt, MAPK-like, and Src pathways. Transcriptional outputs downstream of these pathways depend on a homolog of β-catenin, WRM-1. Here we analyze the regulation of WRM-1, and show that the MAPK-like pathway maintains WRM-1 at the membrane, while its release and nuclear translocation depend on Wnt/Src signaling and sequential phosphorylation events by the major cell-cycle regulator CDK-1 and by the membrane-bound GSK-3 during EMS cell division. Our results provide novel mechanistic insights into how the signaling events at the cortex are coupled to the asymmetric EMS cell division through WRM-1.

To identify additional regulators in the pathways governing gut specification, we performed suppressor genetic screens using temperature-sensitive alleles of the gutless mutant *mom-2*/Wnt, and extra-gut mutant *cks-1*. Five intragenic suppressors and three semi-dominant suppressors were isolated in *mom-2* suppressor screens. One extragenic suppressor was mapped to the locus *ifg-1*, eukaryotic translation initiation factor *eIF4G*. From the suppressor screen using *cks-1(ne549)*, an allele of the self-cleaving nucleopore protein *npp-10* was identified as a suppressor of *cks-1(ne549)* and other extra-gut mutants.

Taken together, these results help us better understand how the fate of intestinal cells are specified and regulated in early *C. elegans* embryos and broaden our knowledge of cell polarity and fate specification.

TABLE OF CONTENTS

LIST OF TABLES

LIST OF FIGURES

CHAPTER I

INTRODUCTION

I) Introduction to early *C. elegans* embryogenesis

Embryogenesis is the process by which an embryo is formed and develops - that is, the process whereby a living thing transforms itself from a single cell into a vastly complicated multicellular organism, with all cells able to work correctly in relation to each other. How is this remarkable feat accomplished? One answer to this question is asymmetrical cell division, which produces two daughter cells with different properties, leading to the expansion in cell type diversity.

Caenorhabditis elegans is an ideal model system for studying asymmetric cell division because all somatic cells are generated in a stereotyped cell lineage (Sulston et al., 1983). This invariance of the *C. elegans* cell lineage indicates that there is a link between the pattern of cell divisions and the ultimate fate that each cell assumes. Therefore *C. elegans* has been especially useful to address questions of patterning mechanisms in a simple metazoan system.

Characteristics of *C. elegans*

C. elegans is a free-living nematode, about 1mm in length (Figure 1). At 20°C, the laboratory strain of *C. elegans* has an average life span of approximately 2–3 weeks, a generation

time of approximately 4 days (Figure 2), and a brood size about 300 eggs. Its transparent body and embryo can be easily observed and characterized in a great detail under the light microscope (Figure 3). Although it has only around 1000 somatic cells (959 in the adult hermaphrodite; 1031 in the adult male; 558 cells when hatching), it presents all of the major types of differentiated tissues found in other animals (e.g., intestine, muscles, germ-line, epidermis, and a nervous system) (Figure 1). What is unique about this organism is that wild type individuals contain a constant 959 cells, and the position of cells is constant as is the cell number. In addition, it was the first multicellular organism to have its genome completely sequenced, contributing to its well-established genetic tools.

Early embryogenesis in *C. elegans*

C. elegans reproduces primarily as a self-fertilizing hermaphrodite. In a young adult, oocytes mature every 23 min and are fertilized in a sperm storage organ known as the spermatheca, which triggers the development of embryos (Detwiler et al., 2001; McCarter et al., 1999; Miller et al., 1999). After fertilization, the oocyte completes meiosis and a protective egg covering is made.

C. elegans embryogenesis can be divided into three major periods (Sulston et al., 1983). The first period occurs in the uterus, including zygote formation and early cleavage, establishment of the embryonic axes, and determination of the somatic and germ-line founder cell fates, and takes place during the first two hours after fertilization. The five initial divisions result in 28 cells including six 'founder' cells called AB, MS, E, P4, D, and C that go on to generate distinct sets of tissues (Figure 3a-h and Figure 4), and most of the early embryonic patterning events are completed by this 28-cell stage. The second period, including gastrulation (Figure 3i), completion of most cell proliferation, and the beginning of cell differentiation and organogenesis, continues until about halfway through embryogenesis. In third period, terminal differentiation and morphogenesis occur, with only a very few additional cell divisions (Figure 3j-l). The first period will be described in detail in this introduction since our study focuses on early embryogenesis.

Mature oocytes pass from the oviduct into the spermatheca and become fertilized by fusion with sperm. At this time, the anterior-posterior polarity of the embryo is established, with the sperm pronucleus at the posterior pole. At first cleavage, the 1-cell stage embryo, called P0, divides asymmetrically along its A/P axis to produce the larger anterior ectodermal founder cell AB and the smaller posterior germ-line cell P1. Like first cleavage, the next three P-cell divisions

are also unequal, each division gives rise to a larger somatic founder cell and a smaller germ-line (P-cell) daughter, producing the somatic founder cells C and D, and the germ-line founder cell P4. At 2-cell stage, the larger AB blastomere divides symmetrically to produce ABa and ABp, whereas P1 divides unequally to yield the EMS and P2 cells. At the next division at 4-cell stage, EMS divides to produce the endodermal founder cell E and the mesodermal founder cell MS, while the AB daughters divide symmetrically. The descendants of each founder cell divide in an invariant pattern and 558 cells are generated by the time of hatching (Figure 5).

During the first period, proteins or RNAs produced maternally during oogenesis specify body axes. Thus, maternal genes specify the fates of early blastomeres, and maternal-effect mutations have been the entry point for analysis of early pattern formation. The first asymmetric division and early A/P axis formation depend on six *par* genes (**par**titioning defective) (Kemphues et al., 1988; Morton et al., 1992; Watts et al., 1996), *pkc-3* (**p**rotein **k**inase **C**) (Tabuse et al., 1998; Wu et al., 1998), *mex-1* (**m**uscled in **ex**cess), *mex-3* (Schnabel et al., 1996), and *mes-1* (**m**aternal-**e**ffect **s**terile) (Strome et al., 1995; Tenenhaus et al., 1998). These initial asymmetries set up the unequal distribution of a number of developmental fate determinants such as SKN-1 (**skin** in excess), PIE-1 (**p**harynx and **i**ntestine in **e**xcess), and PAL-1 (**p**osterior **al**ae in males) to specific cells of the early embryo (Figure 6). SKN-1 is a composite bZIP/homeodomain

transcription factor required for EMS fate (Blackwell et al., 1994; Bowerman et al., 1993). In *skn-1* mutants the muscle, pharynx, and intestine normally produced by MS and E are absent. PIE-1 is a zinc finger protein required to specify the P2 fate (Mello et al., 1992). Mutations in *pie-1* produce a phenotype that is the converse of SKN-1 phenotype, with germ-line cells adopting somatic fates. The fate of the C and D blastomeres is dependent on the PAL-1 protein (Hunter and Kenyon, 1996). PAL-1 is a homeodomain protein of the caudal family and is thus predicted to be a transcriptional regulator (Waring and Kenyon, 1990). In embryos depleted for maternal PAL-1, C and D no longer produce body muscle and hypodermis, but the MS and E lineages are normal.

Specifying cell fates

The first AB cleavage generates developmentally equivalent daughter cells, ABa and ABp. During AB cleavage, the spindle slides one way or the other so that one of the two daughters, designated ABp, becomes located posterior to and to one side of the other. This defines the dorsal side of the embryo and also establishes the future left-right axis. The symmetry of this cleavage and the apparently random nature of the change in spindle orientation that defines which daughter will become ABa and which will become ABp suggest that these two

cells are equivalent at the 4-cell stage (Priess and Thomson, 1987), and studies have shown that their different fates are determined by subsequent cell-cell interactions (Wood, 1991).

In contrast to AB, the division of P1 is asymmetric in terms of cell size and cytoplasmic inheritance and the resulting asymmetries are responsible for the differences in fates of the EMS and P2 blastomeres. Further restrictions in cell fates then occur via both cell-autonomous and cell-cell signaling mechanisms to give rise to the MS, E, C, D, and P4 unique fates as described above.

The EMS cell divides to produce an anterior daughter MS, which will produce mainly body muscle and pharynx, and a posterior daughter E, which is the clonal precursor to the intestine. This polarized division requires an interaction between P2 and EMS (Goldstein, 1992; Schierenberg, 1987). EMS isolated early in its cell cycle and cultured alone produces two MS-like daughters that make only mesodermal tissue consisting of body wall muscle and pharyngeal muscle. Contact with P2 appears to polarize EMS so that its division is asymmetric and the daughter born adjacent to P2 becomes E (Goldstein, 1995a, b). The molecular mechanisms underlying polarized EMS cell division will be discussed in greater detail later in this Chapter.

In summary, the fates of early blastomeres in *C. elegans* are specified by mechanisms including cell-cell interactions as well as the asymmetric expression of maternally provided transcriptional activators and repressors.

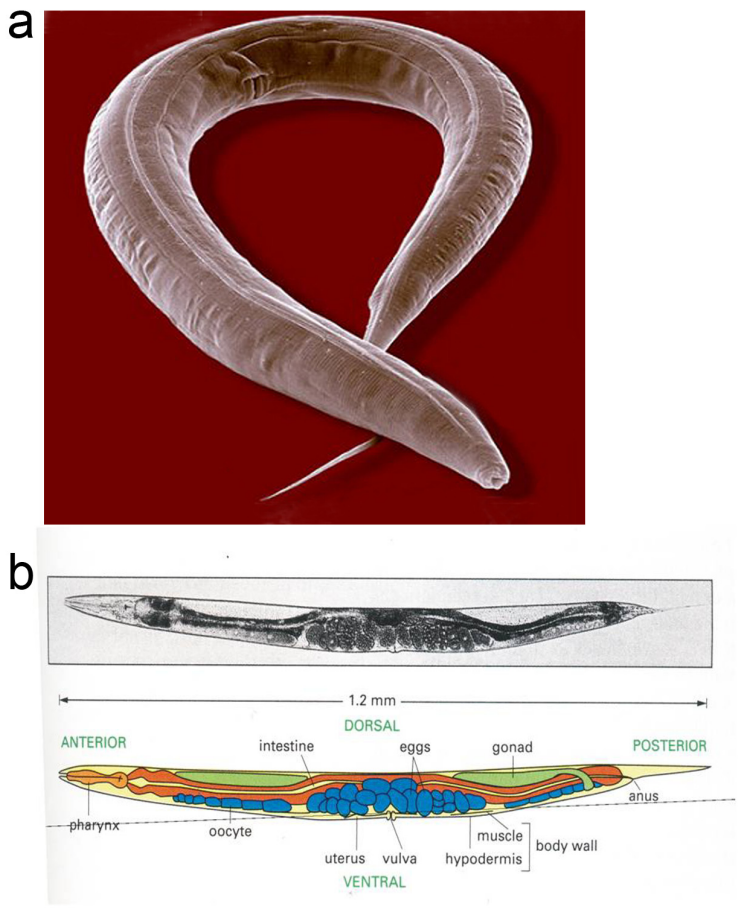

Figure 1. The Worm !!!

The nematode *Caenorhabditis elegans* has a simple cylindrical body plan which is typical of many nematodes species. **a**, scanning electron micrograph of an adult hermaphrodite. **b**, at the anterior end of this simple elongated tube-like body, the two-bulbed pharynx opens with six lips, while the tail ends in a tapering whip-like structure and accommodates an anal opening. Midbody is marked by vulval opening that is used to lay fertilized eggs generated by a two-armed gonad.

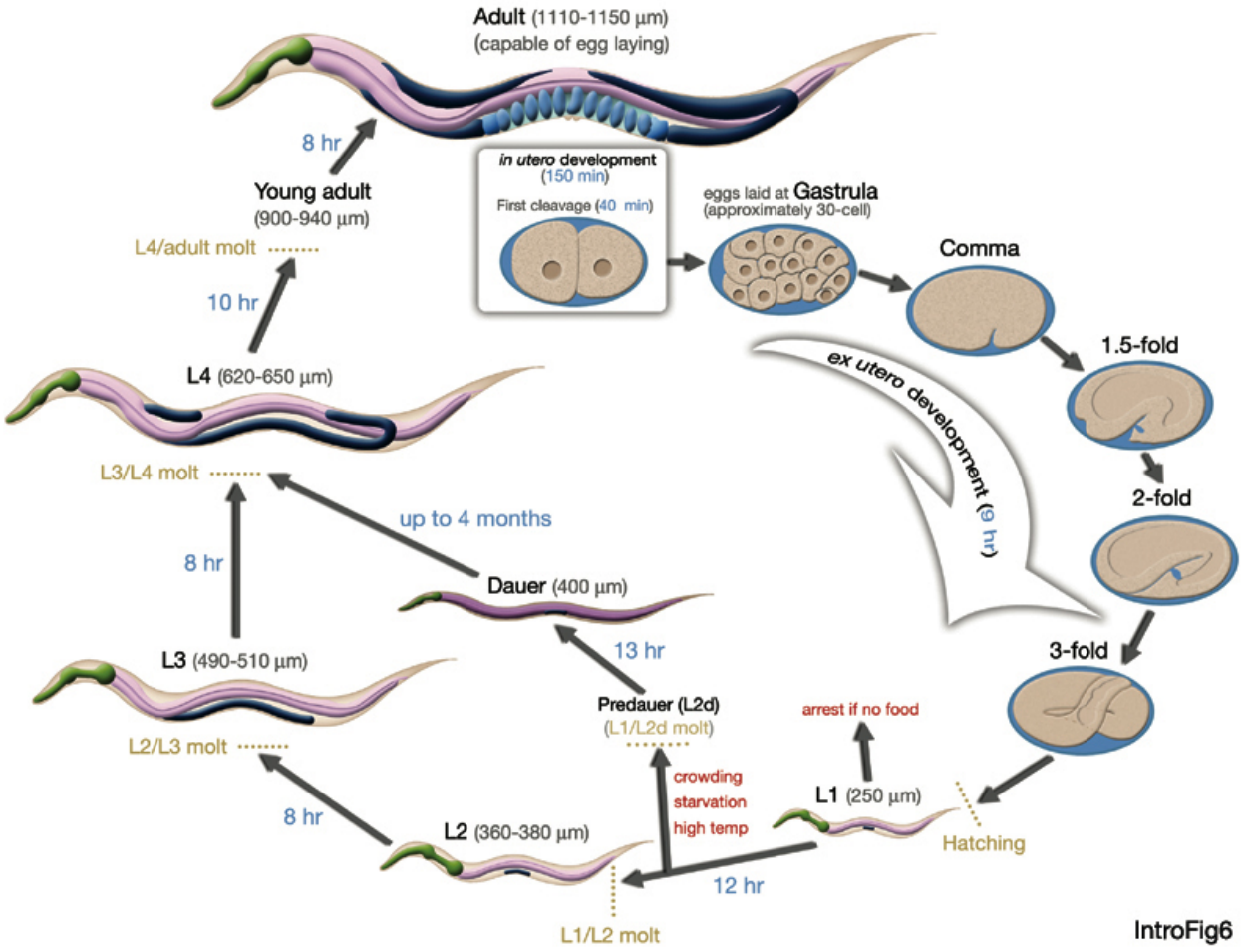

Figure 2. Life cycle of *C. elegans* at 22°C.

0 min is fertilization. Numbers in blue along the arrows indicate the length of time the animal spends at a certain stage. First cleavage occurs at about 40 min. post-fertilization. Eggs are laid outside at about 150 min. post-fertilization and during the gastrula stage. The length of the animal at each stage is marked next to the stage name in micrometers (www.wormatlas.org).

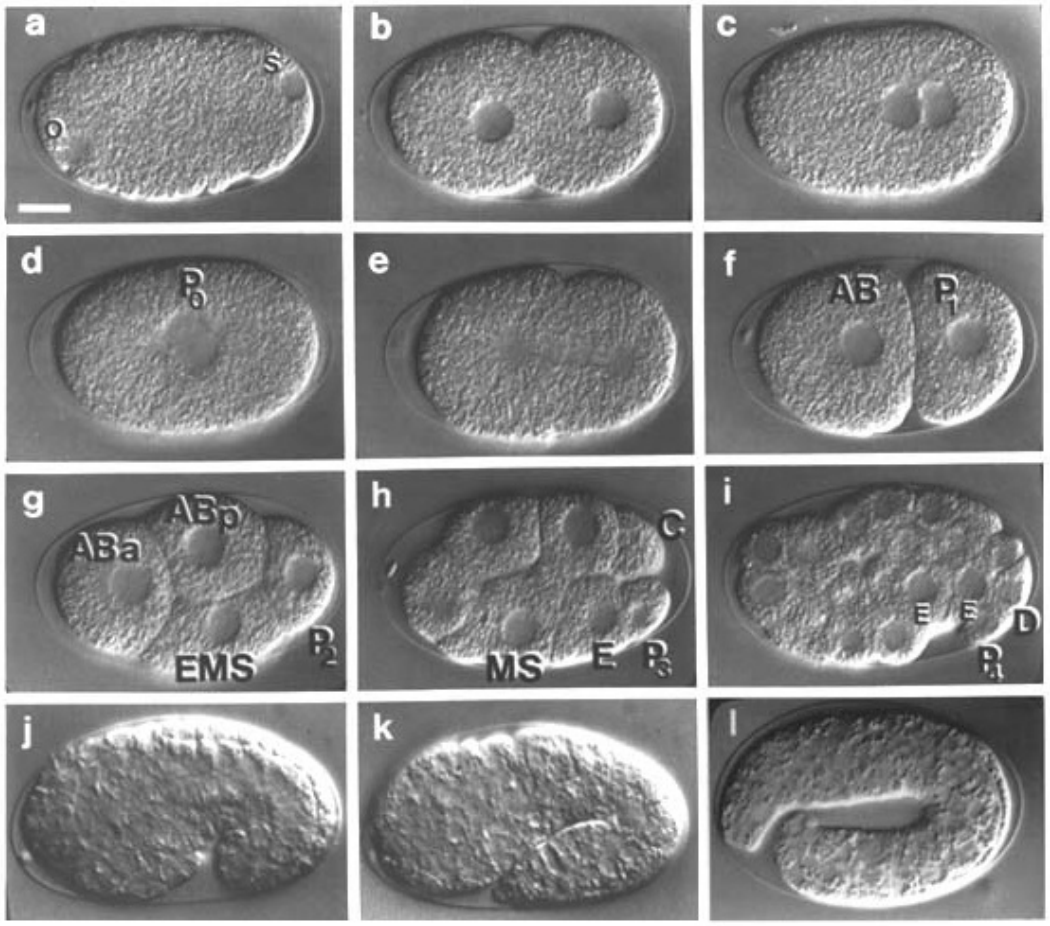

Figure 3. Images of early *C. elegans* embryos.

a-d: migration and fusion of pronuclei; zygote formation. **e-i**: early cleavage divisions. **f**: 2-cell stage. **g**: 4-cell stage. **h**: 8-cell stage. Formation of germ-line cells P1-P4 (P4=primodial germ cell). **i**: beginning of gastrulation with immigration of 2 gut precursor cells, E. **j-k**: different morphogenesis stages. **j**: lima bean stage. **l**: 2-fold stage (Nematode and Neglected Genomics at www.nematodes.org).

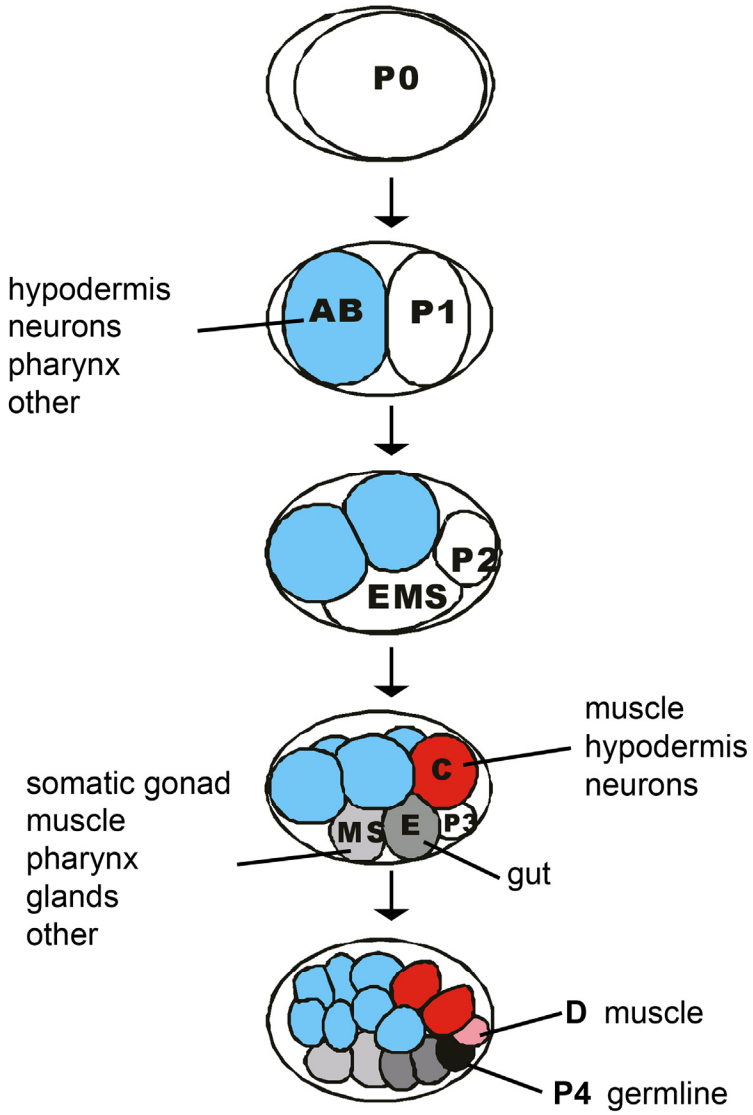

Figure 4. Formation of the founder cells.

Anterior is to the left and dorsal is up. The founder cell names and their contributions to the embryo are indicated. Each founder cell with its lineage is shown in different colors.

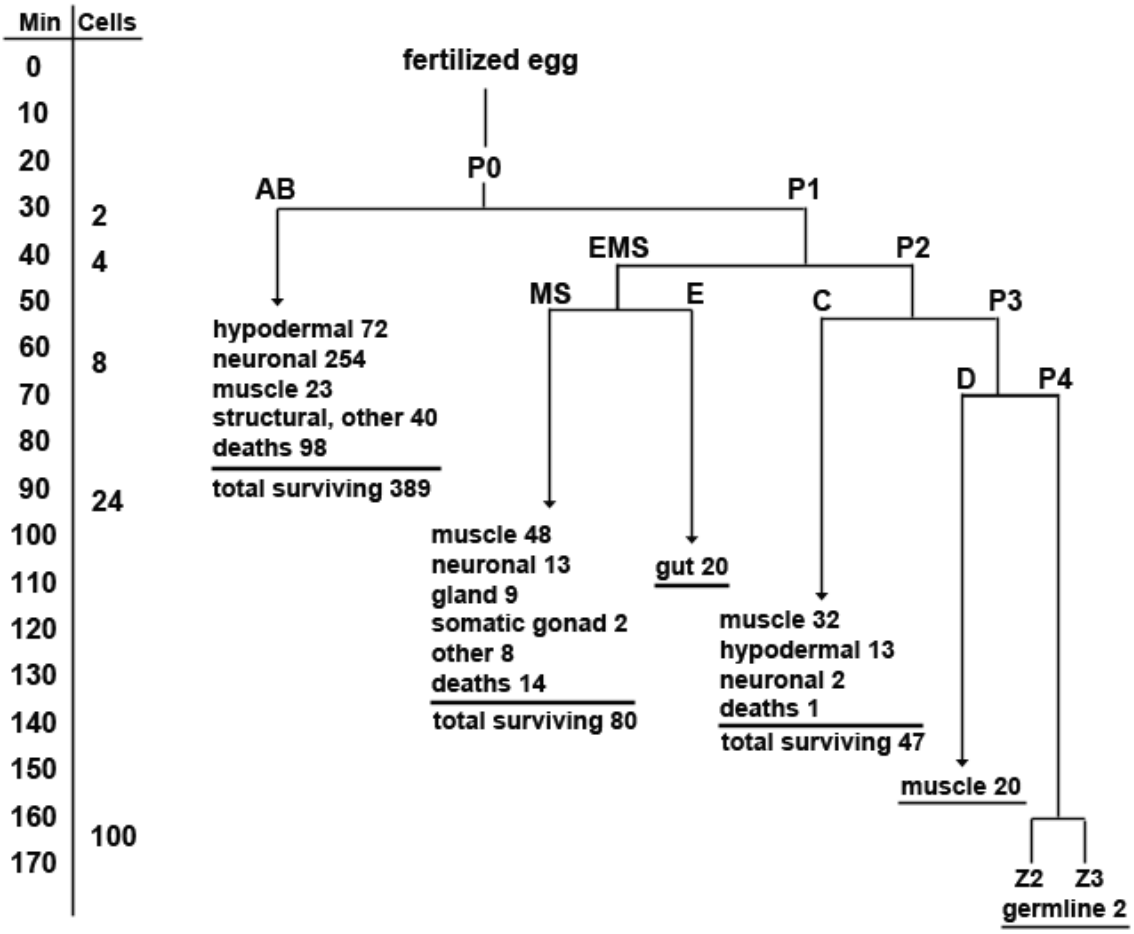

Figure 5. Lineage pattern of early cleavages in the *C elegans* embryo.

Scale indicates minutes after fertilization at 25°C. Horizontal lines connecting sister cells indicate approximate times of cleavages. Second scale shows number of cells in the embryo with time. Below each founder cell are indicated the type and number of cells (at hatching) that derive from it (Sulston et al. 1983).

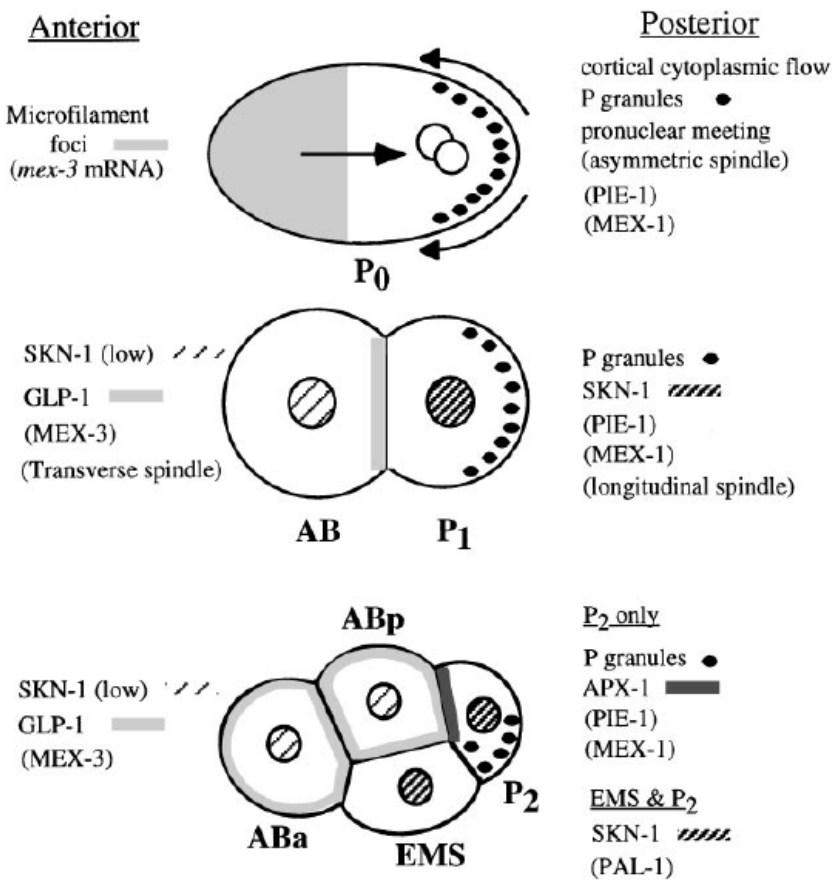

Figure 6. Summary of known asymmetries in 1-cell (top), 2-cell (middle) and 4-cell (bottom) ***C. elegans*** **embryos (Rose and Kemphues, 1998).**

II) Specification of gut cells in *C. elegans* early embryos

P2/EMS signaling polarizes the EMS cell, resulting in 20 endoderm cells from the E blastomere only. In the absence of P2 signaling, EMS produces two MS-like daughters, which produce more mesoderm (mom) tissue such as pharyngeal tissue but no endoderm cells (Figure 7). Understanding the nature of P2/EMS signaling has started from the isolation of *mom* mutants functioning in gut specification, some of which encode homologs of the highly conserved canonical Wnt/Wg signaling pathway.

In the overview given here, the canonical Wnt/Wingless pathway will be discussed, followed by P2/EMS signaling involving the Wnt pathway in *C. elegans*.

Wnt/Wingless signaling

The Wnt/Wingless signaling pathways are highly conserved among species and play fundamental roles in multiple biological processes during development and disease. Genetic studies in *Drosophila, C. elegans* and humans, biochemistry in cell culture, and ectopic gene expression in *Xenopus* have revealed insights into the mechanisms of Wnt signaling. Many of the Wnt genes in the mouse have been mutated, leading to highly specific developmental defects. Mis-regulation of the Wnt pathway is implicated in driving the formation of various human

cancers in self-renewing tissues (Barker and Clevers, 2006). Moreover, the canonical Wnt cascade has emerged as a critical regulator of stem cells (Bhardwaj et al., 2001; Reya et al., 2001; Taipale and Beachy, 2001; Varnum-Finney et al., 2000). These studies suggest that Wnt signaling not only function in the development, but also maintains a variety of systems and regulate stem cell/progenitor cell renewal. Thus, the ability to modulate the Wnt pathway either positively or negatively may be of therapeutic relevance.

The binding of Wnt to its receptor (Frizzled/LRP complex) triggers a complex signal transduction cascade. In the well-characterized canonical Wnt pathway involving β-catenin (Figure 8), this binding leads to the activation of Dishevelled family proteins, and results in stabilization of β-catenin by blocking its degradation by a complex of proteins that includes Axin, GSK3 (**G**lycogen **S**ynthase **K**inase), and APC (**A**denomatous **P**olyposis **C**oli). In the absence of Wnt, β-catenin is in a cytoplasmic complex where it is phosphorylated sequentially by CK1 (**C**asein **K**inase I), and then by GSK3. Phosphorylation targets β-catenin for ubiquitination and degradation via the proteasome complex (Giarre *et al.*, 1998; Miller *et al.*, 1999). β-catenin stabilized by Wnt signaling enters the nucleus and interacts with TCF (**T c**ell **f**actors)/LEF (**L**ymphoid **e**nhanced **f**actor) family transcription factors and the co-activators p300 and creb-binding protein (CBP) to activate specific gene expression (Bienz, 1998; Brantjes et al., 2002). In

the absence of the Wnt signal, TCF/LEF functions as a transcriptional repressor through its interaction with the corepressor Groucho (Cavallo et al., 1998). The repressing effect of Groucho is mediated by interactions with histone deacetylases (HDAC), which are thought to make DNA refractive to transcriptional activation (Chen et al., 1999).

The signal: Wnt proteins

Wnt proteins form a family of highly conserved secreted signaling molecules that bind the Frizzled (Fz) receptors. Since the first Wnt gene, mouse Wnt-1, was discovered in 1982 as a proto-oncogene activated by integration of mouse mammary tumor virus in mammary tumors (Nusse and Varmus, 1982; van Ooyen and Nusse, 1984), approximately 100 Wnt genes including *wingless* (*wg*) in *Drosophila* (Cabrera et al., 1987; Rijsewijk et al., 1987), have been isolated and studied. All encode proteins with 350-400 amino acids in length and are characterized by a high number of conserved cysteine residues, a nearly invariant pattern of 23 cysteines.

Wnt proteins are relatively insoluble due to a particular protein modification, cysteine palmitoylation (Willert *et al.*, 2003). A *Drosophila* gene named *porcupine* and its worm homolog *mom-1* required in Wnt secretion appear to be responsible for Wnt palmitoylation as they encode

homologs of acyl-transferases enzymes that acylate a variety of substrates in the endoplasmic reticulum (Hofmann, 2000; Zhai *et al.*, 2004).

Signal relay at the membrane

Wnts signal across the plasma membrane by interacting with serpentine receptors of Frizzled (Fz) family (Bhanot *et al.*, 1996) and the LRP family proteins known as Arrow in *Drosophila* (Wehrli *et al.*, 2000) and LRP5 and -6 in vertebrates (Pinson *et al.*, 2000; Tamai *et al.*, 2000). Binding of Wnt ligands to these receptors triggers a series of events that ultimately disrupts the APC/Axin/GSK-3β and stabilizes the cytosolic key signal transducer β-catenin.

Upon signaling, Fz activates Dishevelled (Dsh), a cytoplasmic protein that functions upstream of β-catenin and the kinase GSK3. This might involve phosphorylation of Dsh, but the mechanism of activation or how Dsh proteins work as Wnt signal-transducing components is unknown (Wallingford and Habas, 2005). One intriguing possibility is that it involves G-protein signaling. Studies suggest that trimeric G proteins are essential in transmitting the Wnt signal (Ahumada *et al.*, 2002; Katanaev *et al.*, 2005; Liu *et al.*, 2005), a possibility first indicated by the serpentine topology of Fz receptors, which is shared with all G-protein-coupled receptors (GPCRs). Recent cell culture experiments further support the role of G proteins in the

transduction of the Wnt signal from Fz to β-catenin (Liu *et al.*, 2005), although direct evidences are necessary.

Activated Dsh inhibits GSK3β in the cytoplasm, possibly by interacting with the Axin/Conductin complex and relocate it to the plasma membrane, which results in titrating away Axin that functions as a negative regulator of Wnt signaling (Cliffe *et al.*, 2003; Li *et al.*, 1999; Mao *et al.*, 2001; Tolwinski *et al.*, 2003). Recent studies suggest that LRP5/6 interacts with Axin through phosphorylated cytoplasmic tail of LRP (Davidson *et al.*, 2005; Zeng *et al.*, 2005). Wnts are thought to induce this phosphorylation of LRP by Casein Kinase-1γ and GSK3, thus regulating the docking of Axin. It remains presently debated whether Wnt controls GSK-3 (Zeng *et al.*, 2005) or CK1γ (Davidson *et al.*, 2005) - mediated phosphorylation of LRP5/6 (Figure 9).

Cytoplasmic destruction complex

At the heart of the canonical Wnt signaling pathway is the β-catenin destruction complex, which functions in the absence of Wnt signaling to keep the cytosolic and nuclear levels of β-catenin very low by promoting the phosphorylation and ubiquitination of β-catenin. Axin acts as a scaffold of this complex since it directly interacts with all other components – β-catenin, the tumor suppressor protein APC, protein phosphatase 2A, and the two kinase families (CK1 and

GSK3) (Price, 2006). In the absence of Wnt ligands, CK1 and GSK3 sequentially phosphorylate β-catenin, which results in its ubiquitination and rapid proteasomal degradation by βTrcP (an F-box containing E3 ubiquitin ligase) (Aberle *et al.*, 1997; Amit *et al.*, 2002; Hart *et al.*, 1999; Rubinfeld *et al.*, 1996).

It is unclear how receptor activation by Wnt ligands inhibits these kinase activities, but it likely involves the Wnt-induced recruitment of Axin to the phosphorylated tail of LRP and/or to Fz-bound Dsh. As a consequence, stable, nonphosphorylated β-catenin accumulates and translocates into the nucleus, where it binds to the N terminus of LEF/TCF transcription factors. Thus, the stabilization of β-catenin by Wnt signaling is accomplished through sequestration of scaffolding proteins, rather than by direct inhibition of GSK3β activity.

Phosphorylation of the APC tumor suppressor appears to trigger the release of ubiquitinated β-catenin from the Axin/APC/GSK3β complex (Ha et al., 2004; Xing et al., 2003; Xing et al., 2004). Unphosphorylated β-catenin and APC bind to separate sites on Axin, and both proteins are targets for phosphorylation by CK1 and GSK3β, which changes their affinity for other components of the destruction complex. However, the relevance of these phosphorylation events in the regulation of Wnt signaling remains incomplete.

Nuclear events

Upon stabilization by Wnt signals, the cytosolic β-catenin enters the nucleus by a constitutive shuttling mechanism that is independent of classical nuclear localization sequences (Fagotto et al., 1998; Krieghoff et al., 2006). Since the armadillo repeat region of β-catenin resembles the HEAT repeats found in the nuclear import factor importin-β, it is postulated that β-catenin can mediate its own nuclear import through direct interactions with nucleoporins (Suh and Gumbiner, 2003). Thus β-catenin is thought to continually shuttle in/out of the nucleus, and interactions with either cytosolic or nuclear proteins ultimately influence β-catenin's distribution.

In the absence of Wnt signals, TCF/LEF-1 in the nucleus acts as a transcriptional repressor by forming a complex with Groucho/Grg/TLE proteins (Cavallo et al., 1998; Roose et al., 1998). The TCF proteins were originally identified in the immune system, but clearly play important roles in embryonic development (Clevers and van de Wetering, 1997). TCFs bind to specific sites in promoters of target genes via an HMG box. The interaction of β-catenin with the N terminus of TCF (Behrens et al., 1996; Molenaar et al., 1996; van de Wetering et al., 1997) transiently converts it into an activator by displacing Groucho from TCF (Daniels and Weis, 2005), translating the Wnt signal into the transient transcription of TCF target genes.

Once β-catenin binds to TCF in the nucleus, β-catenin functions as a scaffold by linking the TCF proteins to specific chromatin remodeling complexes and the Wnt coactivators. The COOH-terminal region binds proteins involved in chromatic remodeling, such as CBP/p300 histone acetylases (Hecht et al., 1999), Brg-1(Barker et al., 2001), and TTRAP/TIP60 and mixed-lineage-leukemia (MLL1/MLL2) SET1-type complexes (Sierra et al., 2006), as well as components that influence transcription initiation by RNA polymerase II, such as parafibromin/hyrax of the histone ubiquitination polymerase associated factor-1 (PAF1) complex (Mosimann et al., 2006), the helicase pontin52 (Bauer et al., 2000), and TATA binding protein (Hecht et al., 1999). The NH_2 terminus of β-catenin binds to a complex consisting of the adaptor legless/Bcl9 and pygopus, which promote transcriptional activation in a manner that is not fully understood (de la Roche and Bienz, 2007; Hoffmans et al., 2005) (Figure 10).

The non-canonical Wnt pathways

Within the past decade, a β-catenin-independent Wnt signaling pathway has been identified that primarily modulates cell movements, as first observed during embryonic gastrulation. The signaling events of the β-catenin-independent pathway are relatively poorly defined, partly because there are at least three mechanisms, which also overlap with other

signaling pathways. First, specific Wnt and Frizzled homologs can activate calcium/calmodulin-dependent kinase II (CamKII) and protein kinase C (PKC) in a Wnt/calcium pathway (Kuhl et al., 2001; Wallingford et al., 2001). This pathway has so far been only reported in vertebrates. It is implicated in *Xenopus* ventralization and in the regulation of convergent extension movements. Second, some frizzled receptors, like other seven transmembrane receptors, act through heterotrimeric GTP-binding proteins to activate phospholipase C (PLC) (Slusarski et al., 1997) and phosphodiesterase (PDE) (Ahumada et al., 2002). Lastly, the planar cell polarity (PCP) pathway in *Drosophila* is mediated by Frizzled which activates the Jun-N-terminal kinase (JNK) and perhaps small GTP-binding proteins to control the orientation of hairs, bristles and ommatidia (Fanto and McNeill, 2004).

P2/EMS signaling that specifies gut cells in *C. elegans*

At 4-cell stage embryos in *C. elegans*, the posteriormost blastomere, called P2, polarizes a neighboring cell, EMS, to specify endoderm tissue. P2/EMS signaling involves multiple inputs, including the Wnt (Rocheleau et al., 1997; Thorpe et al., 1997), MAPK-like (Ishitani et al., 1999; Meneghini et al., 1999; Shin et al., 1999), and Src-mediated receptor tyrosine kinase (Bei et al., 2002) signaling pathways (Figure 11).

The Wnt signaling pathway

Genetic screens have identified several maternally expressed loci that are required to specify the gut tissues. These include five *mom* genes, *lit-1*(**l**oss of **i**ntes**t**ine) and *pop-1*(**po**sterior **p**harynx-defective) (Kaletta et al., 1997; Lin et al., 1995; Meneghini et al., 1999; Rocheleau et al., 1997; Thorpe et al., 1997). Some *mom*s encode homologs of Wnt pathway components: *mom-1*, *mom-2*, and *mom-5* correspond to *porcupine*, *wingless* and *frizzled*, respectively. The *mom-3/mig-14* gene encodes a homolog of the Wnt-secretion factor Wntless, a conserved membrane protein that promotes the secretion of Wnt to extracellular milieu (Banziger *et al.*, 2006). The genes *mom-4* and *lit-1* are the homologs of a mitogen-activated protein kinase (MAPK)-related pathway that converges with Wnt signaling to downregulate POP-1/TCF (Ishitani et al., 1999; Meneghini et al., 1999; Rocheleau et al., 1999). The *pop-1* gene encodes the *C. elegans* homolog of Drosophila dTCF/Pangolin and mammalian TCF/LEF family members. Using RNA-mediated genetic interference (RNAi) (Fire et al., 1998; Rocheleau et al., 1997), other Wnt pathway components required for endoderm induction in *C. elegans* have been identified: a β-catenin homolog called *wrm-1*(**wo**r**m**adillo), an APC tumor suppressor-related gene *apr-1*(**AP**C-**r**elated), a GSK-3 homolog *sgg-1*(for ***sha*gg*y-like***) or *gsk-3* (Schlesinger et al., 1999), an Axin homolog *pry-1*, two dishevelled homologs *dsh-2* and *mig-5* (Table 1).

The Wnt pathway that induces gut tissue in *C. elegans* differs from the canonical Wnt signaling pathway in several steps (Figure 12). First, both *apr-1*/APC and *sgg-1*/GSK-3 are required positively for endoderm induction in *C. elegans* (Schlesinger et al., 1999), while the fly and mammalian counterparts of APC and GSK-3 appear to act negatively by promoting the degradation of β-catenin in the absence of Wnt signals. Second, TCF/LEFs become activated by β-catenin in vertebrates but are inactivated in *C. elegans*. Canonical Wnt signaling converts the TCF/LEF factor from repressor to activator by increasing the nuclear level of its coactivator, β-catenin. However, in *C. elegans*, the TCF/LEF homolog *pop-1* represses endoderm fate in MS since in *pop-1* mutant embryos the MS blastomere adopts the fate of E and produces endoderm (Lin et al., 1998). Third, instead of associating with TCF/LEF and activating Wnt-responsive gene transcription, WRM-1/β-catenin functions to export POP-1 out of the nucleus in E (Rocheleau *et al.*, 1997). Fourth, unlike the canonical Wnt signaling pathway, WRM-1 does not appear to be regulated by proteasomal-dependent degradation. Recent study suggests that Wnt signaling promotes the nuclear retention of WRM-1 by antagonizing IMB-4 (CRM-1/exportin) – dependent nuclear export of WRM-1 (Nakamura *et al.*, 2005) . Furthermore, the sequence similarity shared by the vertebrates and *C. elegans* homologs of APC and β-catenin is very low (~20%). There are also differences in the molecular interactions of the proteins. WRM-1 does not

interact efficiently with POP-1, and APR-1 appear to lack the 15- and 20-residue repeats present in APC that mediate binding to β-catenin (Rocheleau et al., 1997).

Apparently, the biochemical and functional characteristics of these Wnt signaling components have diverged considerably during evolution.

The MAPK-like pathway

Mitogen-activated protein kinases (MAPKs) play fundamental roles in various receptor-mediated signaling pathways. In the classical Ras/Raf pathway, which transmits signals from growth factor receptors, Ras activate the MAP kinase kinase kinase (MAPKKK) Raf, which through phosphorylation stimulates the MAP kinase kinase MEK1. Finally, the MAPK kinase ERK is activated by MEK1 and modifies the function of various substrates by phosphorylation.

Studies in *C. elegans* and mammalian tissue culture suggest that a conserved MAPK-related pathway, encoded in part by the genes *mom-4* and *lit-1*, converges with Wnt signaling to downregulate the TCF/LEF homolog, POP-1 (Ishitani et al., 1999; Meneghini et al., 1999; Rocheleau et al., 1999; Shin et al., 1999). MOM-4 is the homolog of a MAPK kinase kinase related to vertebrate TAK-1, whereas LIT-1 is highly homologous to nemo and to the mammalian nemo-like kinase (NLK) in its kinase and C-terminal domains.

In cell culture assays, WRM-1 and LIT-1 form a kinase complex that can directly phosphorylate POP-1, suggesting that the WRM-1/LIT-1 kinase may directly downregulate POP-1 (Shin et al., 1999). Consistent with observation, recent *in vivo* study shows that WRM-1 promotes the phosphorylation of POP-1 by LIT-1, which results in the nuclear export of POP-1 via a 14-3-3 protein, PAR-5 (Lo et al., 2004).

It is not understood how MOM-4 is activated and how MOM-4 in turn activates LIT-1. It will be interesting to determine whether MOM-4 and LIT-1 are directly regulated by Wnt signaling and/or whether they represent entry points by which other signal transduction pathways become connected to the Wnt pathway.

The Src pathway

C. elegans endoderm induction also provides one of the best-studied examples of a cell division that is oriented in response to extrinsic signals. After replication of the EMS centriole, the two centrosomes migrate to align initially along the left/right (L/R) axis. Shortly before mitosis, the EMS nucleus and centrosomes rotate 90° together with mitotic spindle, and EMS divides along the anterior/posterior (A/P) axis (Hyman and White, 1987; Sulston et al., 1983). Studies using the isolation of blastomeres and their reassembly into chimeric embryos *in vitro*

revealed that if EMS is cultured alone, its mitotic spindle elongates along the axis established by centrosome migration, without any rotation. Contact with P2 early in the EMS cell cycle induces rotation of the EMS nucleus and centrosomes, orienting the mitotic spindle along the A/P axis (Goldstein, 1995a, b). Therefore P2 signaling not only induces the endoderm fate but can also direct the cleavage orientation of the EMS blastomere.

Although Wnt signaling contributes to this polarizing interaction, no mutants identified in this pathway to date abolish P2/EMS signaling. For example, no single or multiple mutant combinations completely prevent the A/P orientation of the EMS division axis (Rocheleau et al., 1997; Schlesinger et al., 1999; Thorpe et al., 1997), suggesting the involvement of unidentified factors for endoderm specification and spindle orientation during P2/EMS signaling. The finding of Src pathway answered this question. Two tyrosine kinase-related genes, *src-1* and *mes-1*, strongly enhance endoderm and EMS spindle rotation defects associated with Wnt pathway mutants since the double mutants between either *src-1* or *mes-1* and any of Wnt signaling components exhibit a complete loss of P2/EMS signaling (Bei et al., 2002). MES-1 protein, localized at the P2/EMS cell junction in a 4-cell stage embryo, is an atypical receptor tyrosine kinase that is not believed to have a functional kinase domain (Berkowitz and Strome, 2000). *C. elegans* SRC-1 is homologous to the proto-oncogene product, c-Src. SRC-1 functions

downstream of MES-1 to form an enhanced phospho-tyrosine accumulation at the P2/EMS junction which directs EMS spindle orientation (Bei et al., 2002).

These results suggest that the Wnt and Src pathways function in parallel to control the fate of endoderm and the spindle orientation (Figure 11). Although the molecular aspects of this collaboration are still not clear, the literature on Src and Wnt signaling suggests they may converge on the multiple points, for example, WRM-1 (Hinck et al., 1994; Papkoff, 1997), GSK-3 (Hughes et al., 1993; Kim et al., 1999; Wang et al., 1994) or G-protein of the Rho family (Arthur et al., 2000; Billuart et al., 2001; Crespo et al., 1997; Habas et al., 2001; Winter et al., 2001).

Functions and regulation of WRM-1/β-catenin

β-catenin, a multi-functional protein involved in cell adhesion as well as in signal transduction (Figure 13), plays a central role in the Wnt signaling pathway in animal development, and its mis-regulation leads to numerous forms of cancer in humans. It activates the transcription of target genes through interactions with members of the TCF/LEF transcription factor family (Inoue et al., 2004; Lu et al., 2004; Yoshikawa et al., 2003). There are two pools of

β-catenin, one associated with cadherins at the cell surface and the other soluble one in the cytoplasm, whose state and concentration are critical for Wnt signaling.

The β-catenin protein was initially discovered for its role in cell adhesion (Kemler, 1993). As a component of adherens junctions, it promotes cell adhesion by binding to the intracellular domain of the transmembrane protein cadherin, a Ca^{2+}-dependent homotypic adhesion molecule, and linking cadherin to the actin cytoskeleton through the adaptor protein α-catenin. This adhesion function is based on a subcellular pool of β-catenin that is membrane-associated and stable. In contrast, the signaling function of β-catenin is conferred by a soluble cytoplasmic pool that is highly unstable in the absence of Wnt signal as a result of multiple phosphorylations in the protein's amino terminus that earmark it for proteasome-mediated degradation. These phosphorylations depend on the combined actions of the APC tumor suppressor, the Axin scaffolding protein and two serine/threonine protein kinases: GSK3β and its priming kinase, CK1.

Upon Wnt signaling, GSK3 is inhibited, leading to accumulation of unphosphorylated ('activated') β-catenin, thus increasing the levels of β-catenin available for nuclear translocation and transcriptional activation (Bullions and Levine, 1998; Polakis, 2000; Willert and Nusse, 1998). These transcriptional changes are the key outputs of canonical Wnt signaling, and are the

basis for Wnt-induced changes in normal and malignant development (Nusse, 1997; Sancho et al., 2003).

In most invertebrates and vertebrates, including *Drosophila* and mammals, a single β-catenin regulates both cell adhesion and Wnt signaling (Bienz, 2005; Schneider et al., 2003). In contrast, *C. elegans* carries four β-catenin homologs, BAR-1, HMP-2, WRM-1, and SYS-1, which appear to have distinct functions. BAR-1 is the only canonical β-catenin homolog and transcriptional coactivator that functions in the canonical Wnt signaling pathway and interacts directly with POP-1, while only HMP-2 interacts with the single cadherin of *C. elegans*, HMR-1 (Costa et al., 1998; Korswagen et al., 2000; Natarajan et al., 2001). WRM-1 is part of a divergent Wnt pathway that, in collaboration with a MAP kinase pathway, mediates the asymmetric distribution of POP-1 between daughter cells of many anterior/posterior cell divisions (Lin et al., 1998; Meneghini et al., 1999; Rocheleau et al., 1999; Shin et al., 1999). SYS-1 functions as a limiting coactivator of POP-1 in regulating asymmetric cell division, although it does not have clear homology with β-catenin (Kidd et al., 2005).

In a 4-cell-stage *C. elegans* embryo, Wnt signaling specifies endoderm by controlling the fate of EMS blastomere daughters through WRM-1. Unlike in the canonical Wnt signaling pathway, WRM-1 appears to be regulated by nuclear transport, instead of proteasome-dependent

degradation (Nakamura et al., 2005). During polarized EMS cell division, P2/EMS signaling involving the Wnt, MAPK, Src pathways promotes the nuclear retention of WRM-1 in the signal-responding cell by antagonizing IMB-4/CRM-1 dependent nuclear export, leading to asymmetrical nuclear localization in its daughter cells.

Cortical WRM-1 has also been shown to be regulated in a developing larva in *C. elegans*. Wnt signals release cortical WRM-1 from the posterior cortex to generate cortical asymmetry that may control WRM-1 asymmetric nuclear localization (Takeshita and Sawa, 2005). WRM-1 localizes at the anterior cortex during cell division that this cortical localization generates its nuclear asymmetry, such that WRM-1 is localized to the nucleus of the opposite side (posterior) to regulate the fate of the posterior daughter. However, the mechanism by which signaling events at the cell cortex are translated to asymmetric nuclear accumulation of WRM-1 is not well understood. One study showed that cortical WRM-1 has an active role in regulating the nuclear localization of WRM-1 in seam cells in *C.elegans* (Mizumoto and Sawa, 2007a). When membrane-tethered WRM-1 (WRM-1::CAAX) that localizes symmetrically in the cortex is expressed in wild-type animals, WRM-1 is localized in both nuclei symmetrically, and affects the fate of the posterior daughter. This result suggests that WRM-1 has two antagonistic functions: a negative function in the cortex, and a positive function in the nucleus.

Though β-catenin localizes to the cortex in a variety cells and plays dual functions in cell adhesion and signaling, physiological aspect of these pivotal roles still remain elusive. Recent studies suggest that Lgs/BCL9-2 and APC might mediate dual functions by regulating β-catenin (Bienz and Hamada, 2004; Kramps et al., 2002). Lgs/BCL9-2 preferentially binds to phosphorylated β-catenin on the pivotal tyrosine residue Y142, and switches the function of β-catenin from cell adhesion to Wnt signaling (Brembeck et al., 2004). APC may also have a role in the choice of β-catenin between cell adhesion and Wnt signaling (Bienz and Hamada, 2004) since it forms interaction with β-catenin similar to those formed by E-cadherin and TCF (Graham et al., 2000; Ha et al., 2004; Huber and Weis, 2001; Xing et al., 2004) and competes with these proteins for binding to β-catenin (Hulsken et al., 1994; Xing et al., 2004). It is interesting to note that WRM-1 regulates the cortical localization of APR-1/APC, which in turn regulates the nuclear localization of WRM-1 in *C. elegans* seam cells (Mizumoto and Sawa, 2007a), though currently there is no evidence of direct binding between WRM-1 and APR-1 (Natarajan et al., 2001).

C. elegans provides a unique system that has a polarized cell division regulated by the Wnt, MAPK-like and Src pathways involving cortical and nuclear regulation of WRM-1, which can shed light on how these two types of WRM-1 are regulated and linked. Further, study of this

process may provide insights into the mechanism by which β-catenin shifts between cell adhesion and Wnt signaling, a switch associated with epithelial-mesenchymal transitions and cancer.

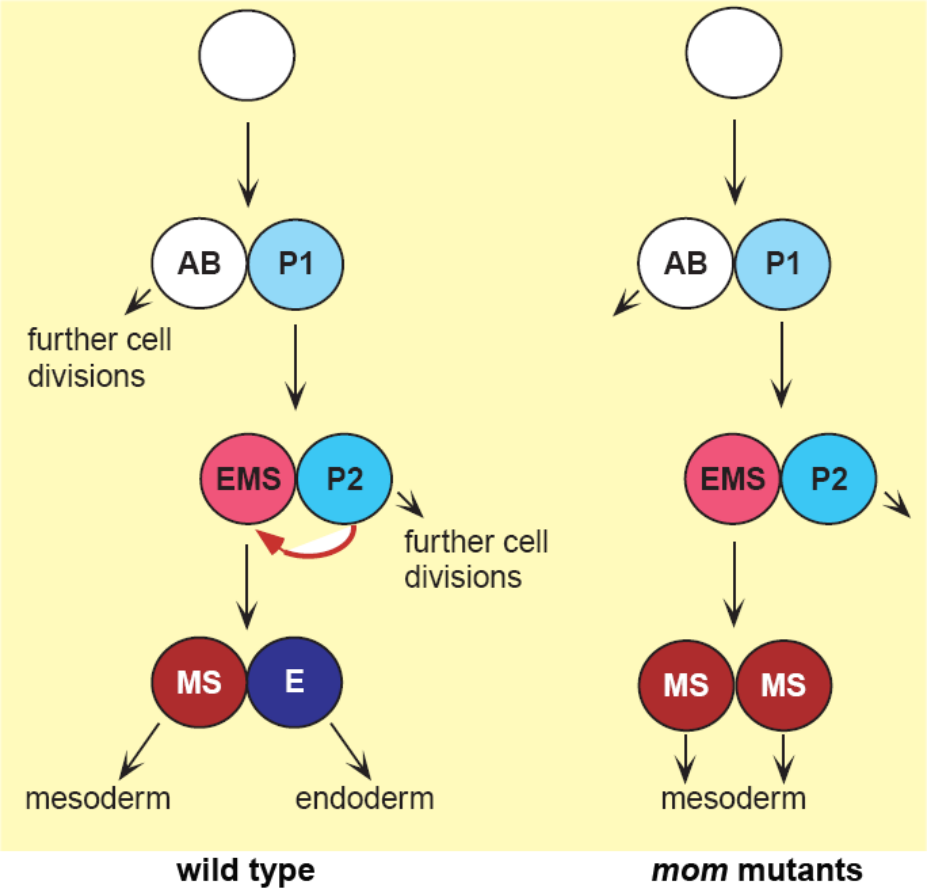

Figure 7. Early development of the *C. elegans* embryo and phenotype after mutation or disturbance of P2/EMS signaling.

In wild type *C. elegans* the daughters of the EMS cell become committed to the mesodermal or endodermal cell fate by a signal from P2 to EMS (Left). Disturbance in P2/EMS signaling results in formation of mesoderm by both daughter cells of the EMS cell (Right). Red arrow indicates P2/EMS signaling.

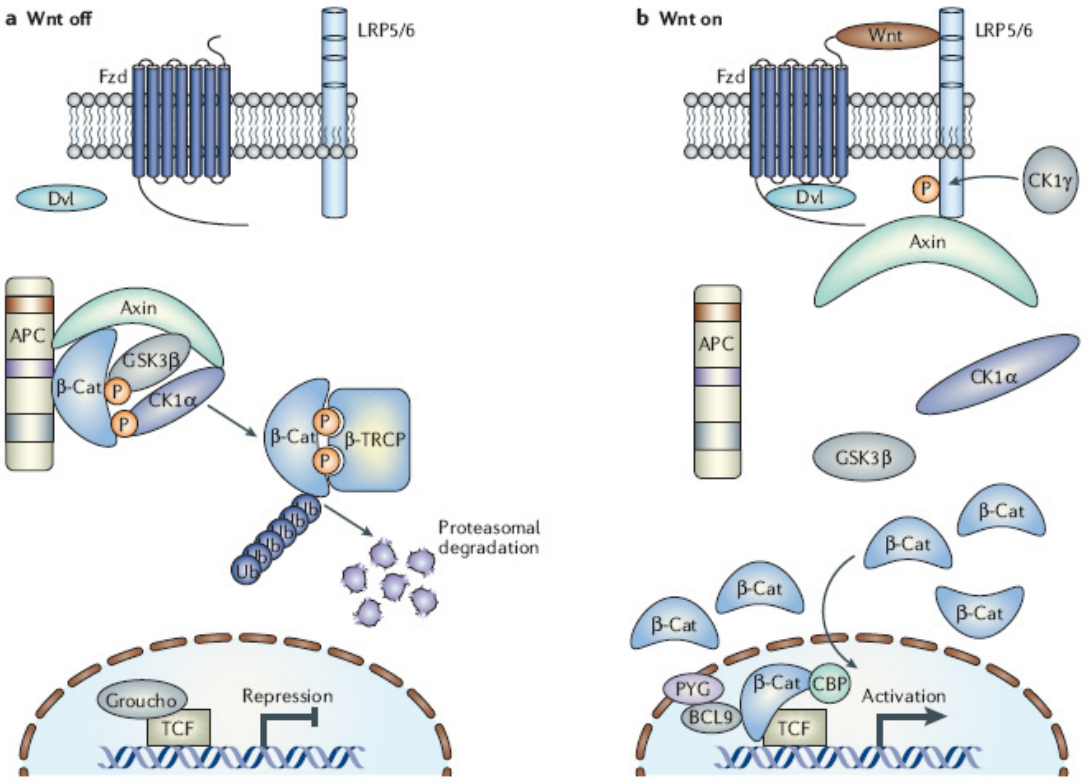

Figure 8. Canonical Wnt signaling.

a, In the absence of a Wnt signal, β-catenin is captured by APC and Axin within the destruction complex, facilitating its phosphorylation by the kinases CK1α and GSK3β. CK1α and GSK3β then sequentially phosphorylate a conserved set of serine and theronine residues at the amino terminus of β-catenin. This facilitates binding of the β-TRCP, which subsequently mediates the ubiquitinylation and efficient proteasomal degradation of β-catenin. The resulting β-catenin 'drought' ensures that nuclear DNA-binding proteins of the TCF/LEF transcription factor family actively repress target genes by recruiting transcriptional co-repressors (Groucho/TLE) to their

promoters and/or enhancers. **b**, Interactions of a Wnt ligand with its specific receptor complex containing a Frizzled family member and LRP5 or LRP6 trigger the formation of Dsh-Fz complexes and the phosphorylation of LRP by Ck1γ, facilitating relocation of Axin to the membrane and inactivation of the destruction box. This allows β-catenin to accumulate and enter the nucleus, where it interacts with members of the TCF/LEF family. In the nucleus, β-catenin converts the TCF proteins into potent transcriptional activators by displacing Groucho/TLE proteins and recruiting an array of coactivator proteins (Barker and Clevers, 2006).

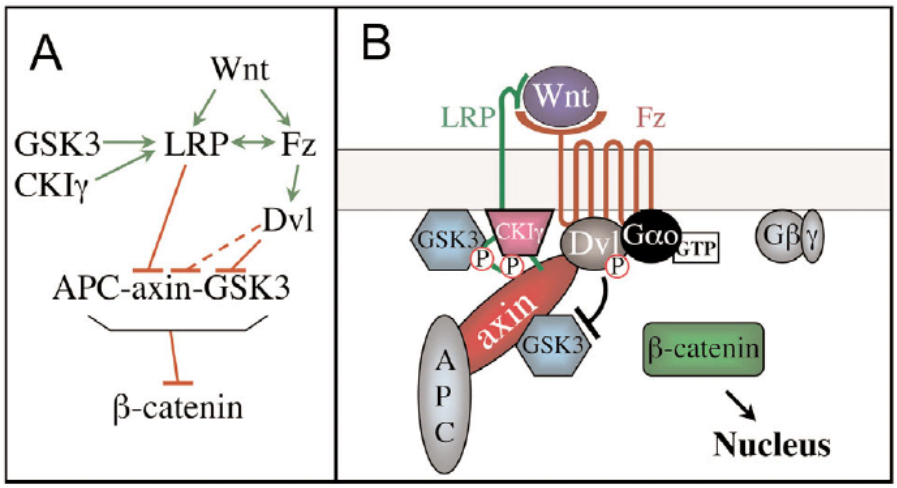

Figure 9. Model for signal relay at the membrane upon Wnt binding.

The two-signal model of Fz-LRP signaling to β-catenin showing the regulatory relationships between each component (A) and summarizing the probable physical interactions (B). In this model, Wnt stimulation promotes Fz-LRP oligomerization, which transduces two separate signals to cytoplasm. The first signal is LRP phosphorylation, mediated by membrane-localized GSK3 and LRP-bound CK1γ. Phosphorylated LRP promotes the recruitment of Axin to the plasma membrane, leading to its inactivation and/or degradation. The second signal is Fz-dependent Dsh phosphorylation, which may involve trimeric G proteins. Activated Dsh then inhibits the APC-Axin-GSK3 complex by a poorly understood mechanism. The dashed line in panel A reflects the fact that Dsh also participates in recruitment of Axin to the plasma membrane (Cadigan and Liu, 2006).

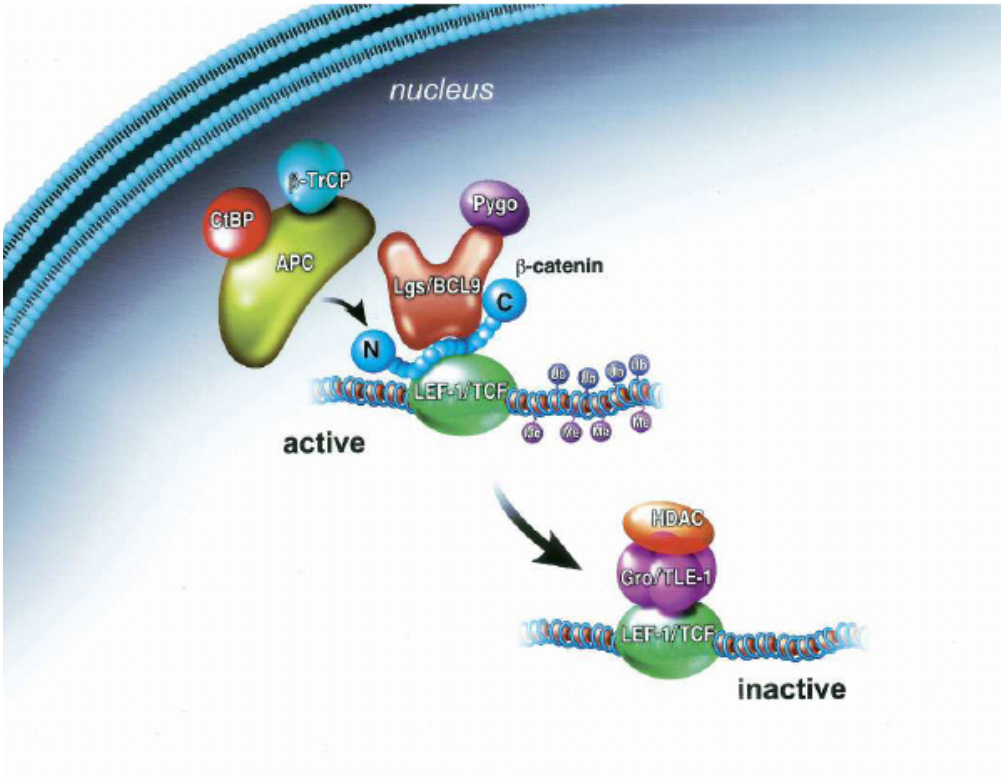

Figure 10. Model for transcriptional regulation of Wnt target genes.

In the nucleus, β-catenin assembles a coactivator complex containing Bcl-9/Lgs, Pygopus, and specific chromatic remodeling complexes that are needed to establish the various chromatic modifications commonly found at active genes, including histone H3K4 trimethylation (Willert and Jones, 2006). See page 20 for details.

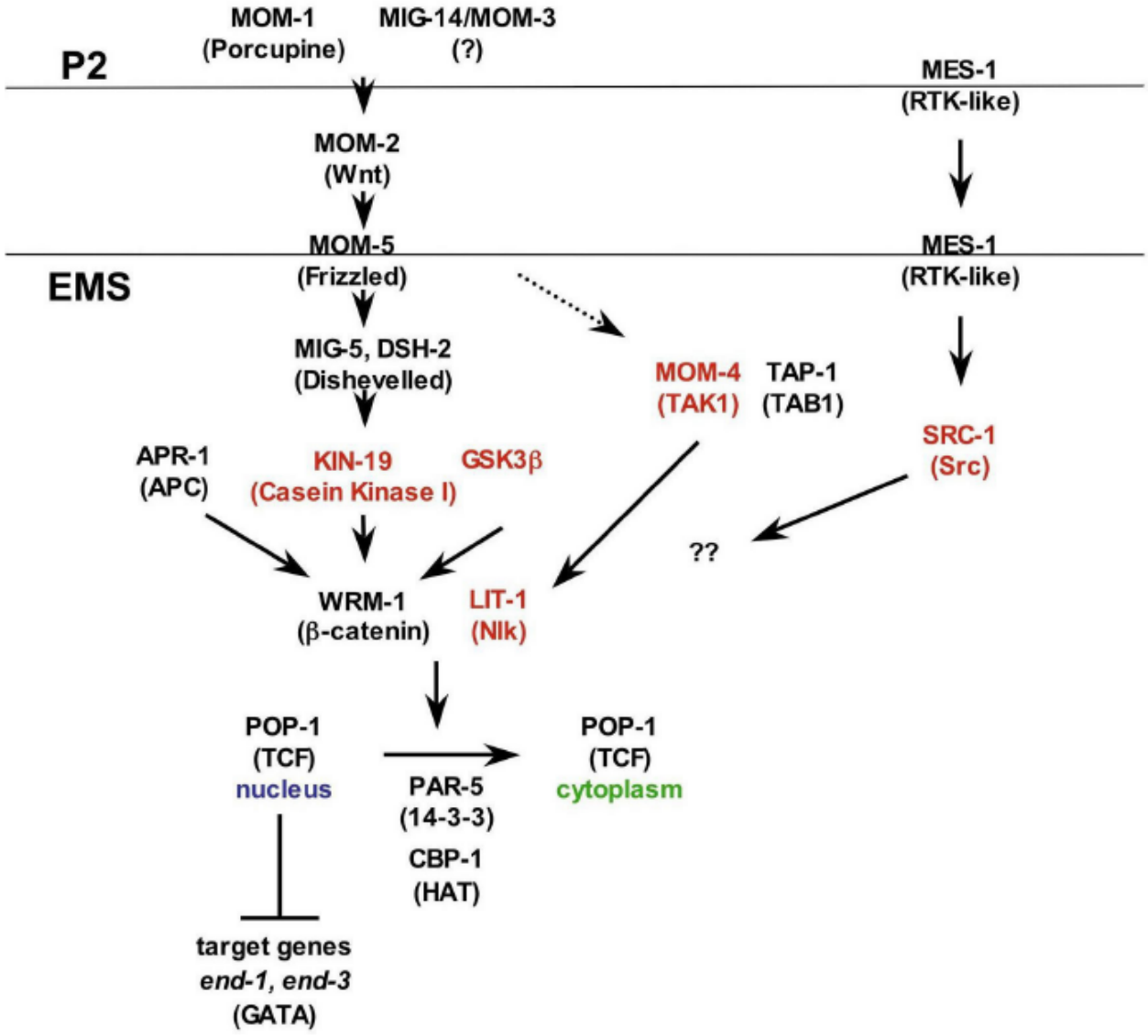

Figure 11. Model for induction of endoderm and cell division axis in EMS .

Active kinases are shown in red. See text for details.

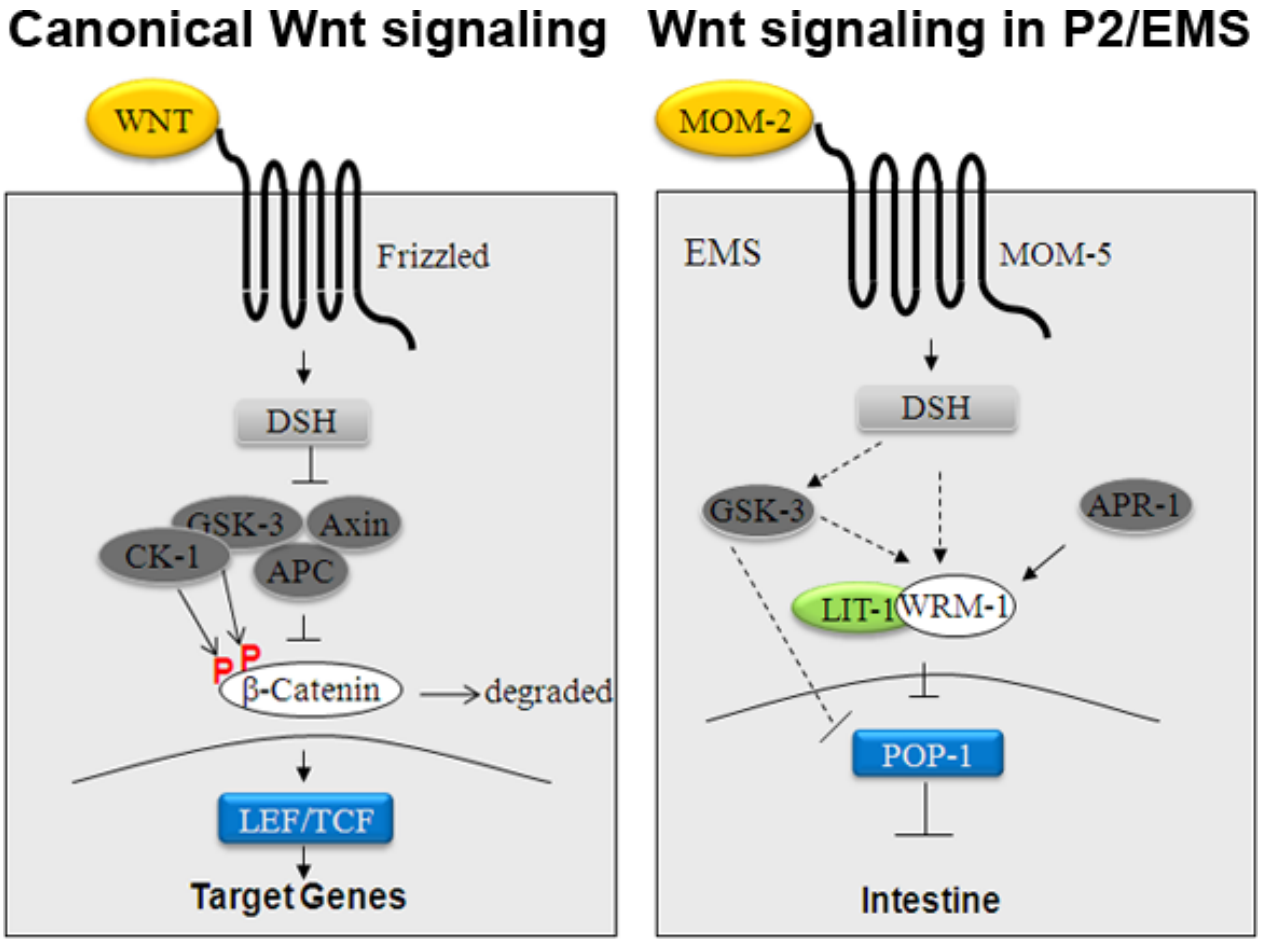

Figure 12. Comparison between canonical Wnt signaling and Wnt signaling in 4-cell stage *C. elegans* embryos.

See page 24 for details.

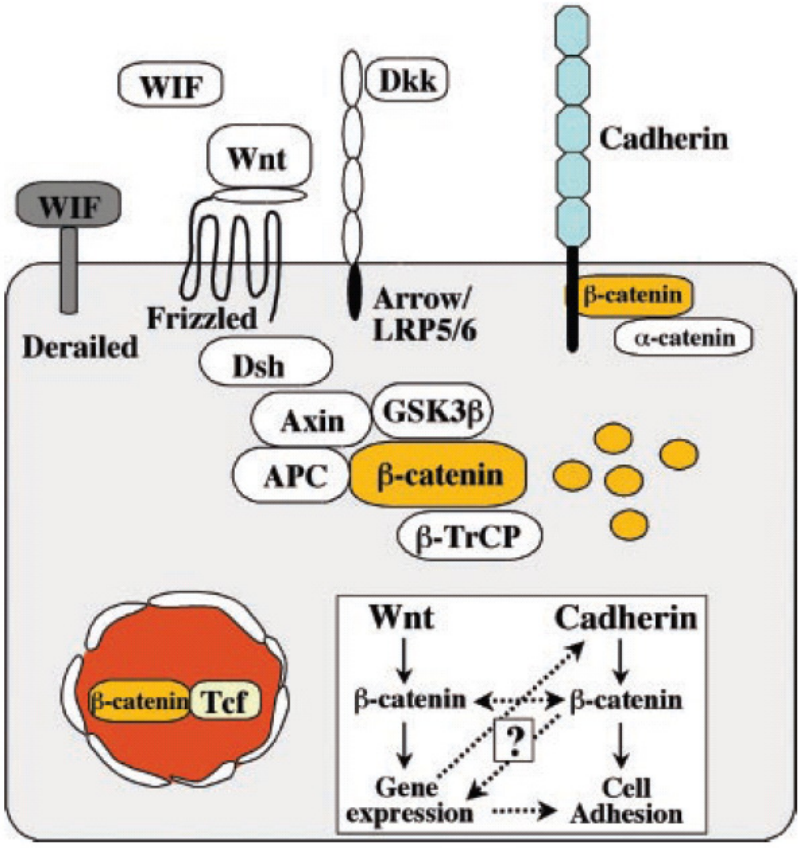

Figure 13. The central role of β-catenin in Wnt signaling and the cadherin complex.

β-catenin exists as a cadherin-bound form that regulates adhesion; in a complex with Axin, APC, and GSK3β, where it is phosphorylated and targeted for degradation; or in the nucleus with TCF/LEF transcription factors (Nelson and Nusse, 2004). See page 29 for details.

Canonical Wnt components	Wnt components in EMS blastomere
Wnt	MOM-2 (Korswagen, 2002)
Frizzled	MOM-5 (Korswagen, 2002)
Dishevelled	DSH-2, MIG-5 (Walston et al., 2004)
GSK3β	GSK-3 (Schlesinger et al., 1999)
CK1	KIN-19 (Korswagen, 2002)
APC	APR-1 (Korswagen, 2002)
Axin	PRY-1 (Korswagen, 2002; Nakamura et al., 2005)
β-catenin	WRM-1 (Korswagen, 2002)
TAK1 (MAPKKK)	MOM-4 (Korswagen, 2002)
NLK (MAPK)	LIT-1 (Korswagen, 2002)
TCF/LEF	POP-1 (Korswagen, 2002)

Table 1. Components of the Wnt pathway in P2/EMS signaling in *C. elegans*.

III) Extra-gut mutants and regulation of OMA-1

Previous large scale genetic screens identified mutants that have excessive endoderm tissue and a suite of other defects in cell polarity and cell fate specification. These mutants were very similar to the phenotype caused by depletion of the conserved protein kinase GSK-3 (Shirayama et al., 2006). These mutants were also similar phenotypically to a gain-of-function allele of the oocyte maturation factor, *oma-1* (Lin, 2003). For example, all of these mutants exhibit mislocalization of cell-fate determinants such as PIE-1 and SKN-1.

These new mutants include one allele of the Dyrk family kinase homolog *mbk-2(ne3442)*, two alleles of the cyclin-dependent protein kinase *cdk-1(ne236, ne2257)*, one allele of the CDK-1 partner, *cks-1(ne549),* and two new gain-of-function alleles of *oma-1 (ne411, ne3800)* (Shirayama et al., 2006) (Figure 14). All these mutants are nonnull alleles. Null alleles of each of these mutants show additional phenotypes, including sterility and cell-division defects (in the case of *cdk-1* and *cks-1* mutants) and polarity and spindle-positioning defects (in the case of *mbk-2* null mutants) (Pang et al., 2004; Pellettieri et al., 2003; Quintin et al., 2003).

OMA-1 is an oocyte maturation factor that exists only in oocytes and 1-cell embryos, and need to be degraded rapidly after the first mitotic division for embryogenesis to proceed normally. Genetic and molecular analyses indicate that OMA-1 level remains high after the 1-cell

stage in *gsk-3*, *cdk-1*, *cks-1* and *mbk-2* mutant embryos (Shirayama et al., 2006) (Figure 15), which suggests these molecules are involved in the proteolysis of OMA-1. Further analyses revealed that OMA-1 is regulated by a series of precisely-timed phosphorylation events by MBK-2 and GSK-3, ensuring a normal oocyte-embryo transition in *C. elegans* (Nishi and Lin, 2005; Shirayama et al., 2006) (Figure 16).

GSK-3

The serine/theronine protein kinase GSK3 was discovered over 20 years ago as one of several protin kinases that phosphorylated and inactivated glycogen synthase (Embi *et al.*, 1980), and is now a well-established component of the Wnt signaling pathway, which is essential for setting up the entire body pattern during embryonic development (see Wnt/Wingless signaling earlier in this Chapter). It may also play important roles in protein synthesis, cell proliferation, microtubule dynamics and cell mobility by phosphorylating initiation factors, components of the cell-division cycle, transcription factors and proteins involved in microbubule function and cell adhesion (Figure 17).

It has been shown that GSK-3 promotes OMA-1 degradation in *C. elegans* early embryos, most likely by direct phoshorylation (Nishi and Lin, 2005; Shirayama *et al.*, 2006). Interestingly,

previous genetic studies have suggested that GSK-3 has direct functions in the Wnt/Wingless pathway for endoderm specification and spindle orientation in *C.elegans* (Peters *et al.*, 1999; Schlesinger *et al.*, 1999; Walston *et al.*, 2004). However, it is not clear by which mechanism GSK-3 functions in P2/EMS signaling. The finding that GSK-3 is required for OMA-1 proteolysis and that the cell fate and spindle-orientation defects of *gsk-3* mutant are suppressed by lowering OMA-1 levels suggests that it may indirectly regulate P2/EMS signaling by lowering OMA protein levels in early embryos (Shirayama et al., 2006).

MBK-2

mbk-2 encodes a serine/threonine kinase of the Dryk family required for microtubule-based processes in the 1-cell *C. elegans* embryo (Pang *et al.*, 2004; Pellettieri *et al.*, 2003; Quintin *et al.*, 2003). The microtubule-related defects are due to the postmeiotic persistence of MEI-1, a homolog of the microtubule-severing protein katanin, which may be a direct target of the kinase MBK-2. Depletion of *mbk-2* also affects the degradation of many maternal proteins (Pang *et al.*, 2004; Pellettieri *et al.*, 2003; Quintin *et al.*, 2003).

MBK-2 regulates the degradation of OMA-1 by direct phosphorylation *in vivo* (Nishi and Lin, 2005; Shirayama *et al.*, 2006). The *mbk-2(ne3442)* allele has a mutation in a conserved

amino acid residue just two amino acids away from an arginine required for substrate recognition in proline-directed kinases (Himpel et al., 2000). This mutation abolishes the phosphorylation of OMA-1 *in vitro*, but exhibits no apparent defects in other MBK-2 functions required for microtubule stability and spindle positioning (Shirayama *et al.*, 2006).

CDK-1 and CKS-1

The highly conserved proteins cyclin-dependent kinases (CDKs) regulate the cell division cycle. CDKs are serine/threonin kinases and composed of a catalytic CDK subunit and a regulatory cyclin subunit; certain CDKs, including CDK-1 and CDK-2, form tight complexes with a small (9-18 kDa) protein known generically as the CDC kinase subunit (CKS) which was originally identified as suppressors of mutations in the fission and budding yeast Cdk-1 genes (Hadwiger et al., 1989; Hayles et al., 1986). The CKS proteins are essential components of the CDKs that regulate mitosis in all eukaryotes. These proteins are sufficiently conserved at the structural and functional level that both human CKS orthologs can functionally substitute for CKS-1 in yeast (Richardson et al., 1990).

Surprisingly, the alleles of *cdk-1(ne236)*, *cdk-1(ne2257)*, and *cks-1(ne549)* show defects in OMA-1 degradation, however, produce well-differentiated mutant embryos with no cell-cycle

related defects (Boxem et al., 1999; Polinko and Strome, 2000). Both CDK-1 mutations alter residues within the T loop (or activation loop) of CDK-1, a region implicated in cyclin binding (Jeffrey et al., 1995). The CKS-1 lesion is predicted to disrupt a single intramolecular hydrogen bond based on the crystal structure of CKS-1 (Bourne et al., 1996).

How CDK-1/CKS-1 function in the regulation of OMA-1 is still not clear. CDK-1 does not appear to phosphorylate OMA-1, suggesting its indirect involvement (Shirayama et al., 2006). There are precedents for CDK-1/CDC2 as a regulator of cell polarity. For example, a mutation that reduces *Drosophila* CDK1 activity results in a loss of polarity in neuroblasts, supporting a model in which different thresholds of CDK1 kinase activity are required for the cell cycle and polarity functions of CDK1 (Tio et al., 2001). However, *cdk-1(ne2257)* has normal kinase activity toward histone H1 and may thus perturb the recognition of only a subset of CDK-1 substrates, or may perturb kinase-independent activities of the CKS-1 and CDK-1 proteins (Yu et al., 2005). How cell fate specification and polarity signaling mechanisms are linked to the cell cycle remains entirely unknown at present, and these special alleles of *cdk-1* and *cks-1* provide a unique opportunity to investigate these fundamental mechanisms.

OMA-1

OMA-1 and OMA-2, two closely related CCCH zinc finger proteins that function redundantly in oocyte maturation, are expressed only in oocytes and the 1-cell embryo, and are rapidly degraded soon after the first mitotic division by the ubiquitination machinery, in a CUL-2/E3 complex-dependent manner (Detwiler et al., 2001; Lin, 2003; Shirayama et al., 2006). Intriguingly, OMA-1 degradation requires multiple conserved protein kinases in addition to MBK-2, including GSK-3, KIN-19/CK1α, and CDK-1/CYB-3 (Nishi and Lin, 2005; Shirayama *et al.*, 2006) (Figure 16). Phosphorylation of OMA-1 by MBK-2 may prime OMA-1 for phosphorylation by GSK-3 and CK1α. This mechanism, involving many kinases, may serve to coordinate meiotic progression with the generation of embryonic polarity.

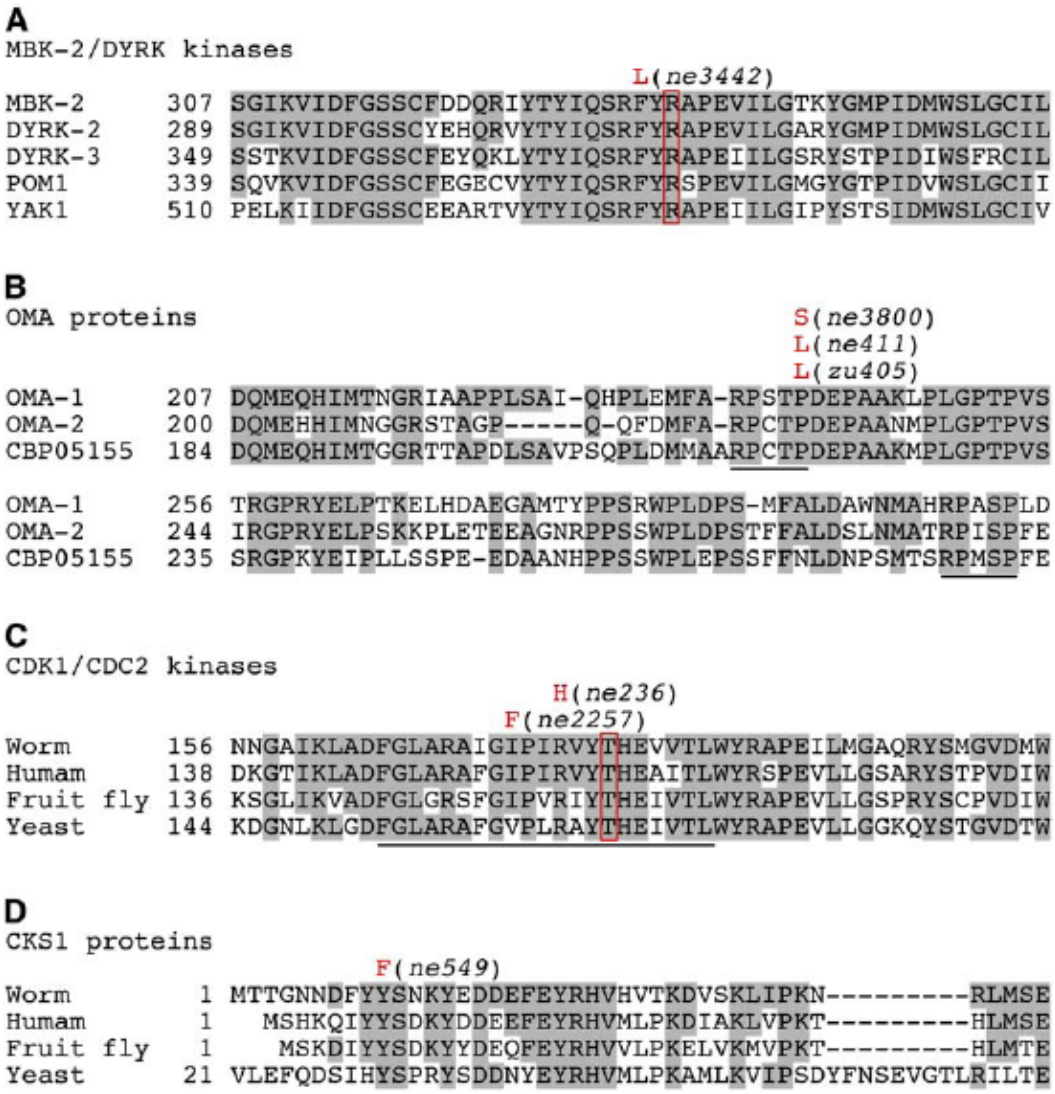

Figure 14. Identification of extra-gut mutants.

Partial amino acid sequence alignments for the MBK-2 protein and other Dyrk-family kinases including human Dyrk2 and 3, fission yeast Pom1, and budding yeast Yak1 (A), for the OMA-1 protein and its *C. elegans* and *C. Briggsae* homologs (OMA-2 and CBP05155, respectively) (B), for the CDK-1 protein and its human, fruitfly, and budding yeast homologs (D). The amino acid

substitutions found in temperature-sensitive or maternal-effect lethal alleles of each protein are indicated in red above the corresponding residue in each alignment. In (A), an arginine residue that is required in proline-directed kinases for P+1specificity is boxed in red. Potential MBK-2 phosphorylation sites in OMA-1 and its homologs are underlined in (B). In (C), a threonine residue that is phosphorylated by CAK kinase is boxed in red. The T loop/activation domain is underlined (Shirayama et al., 2006).

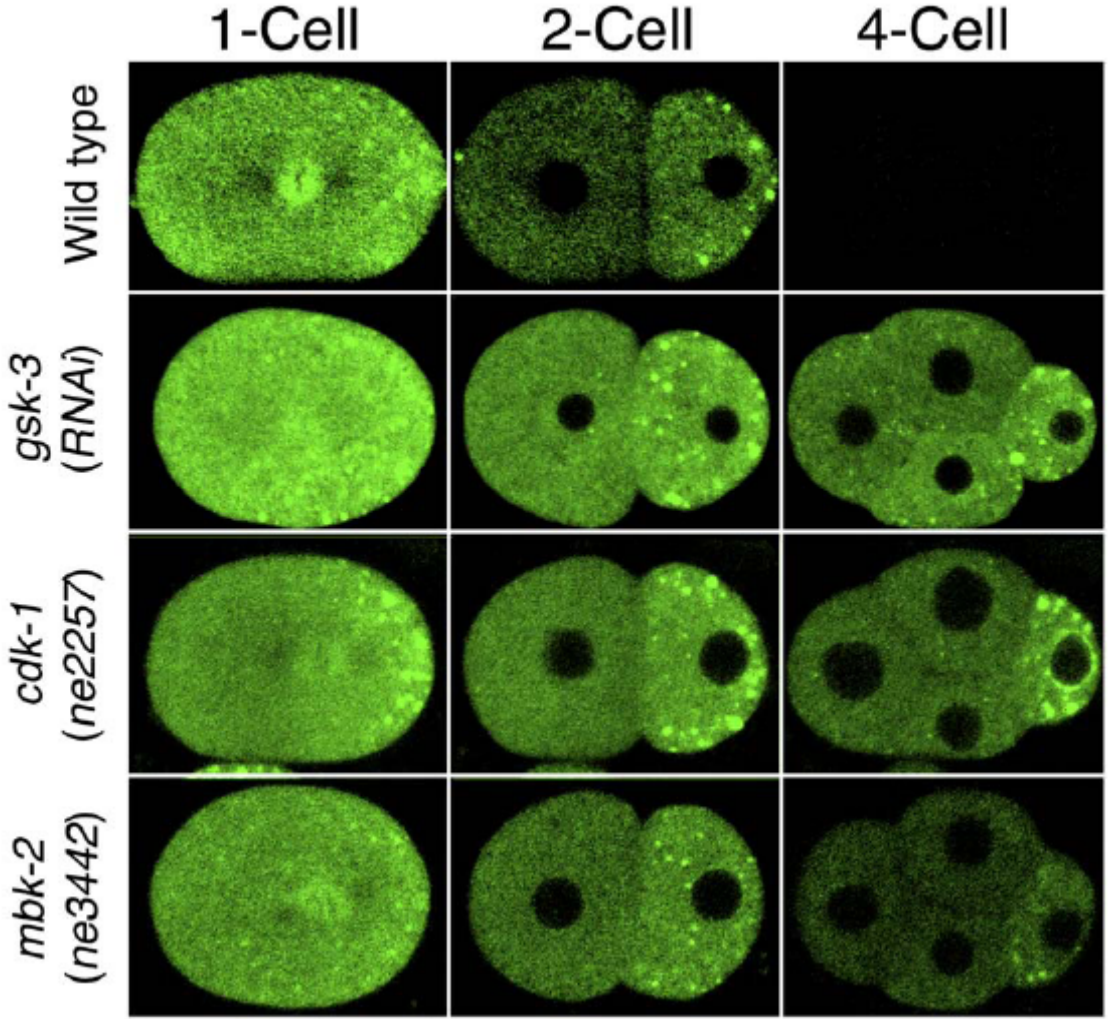

Figure 15. *mbk-2*, *gsk-3*, and *cdk-1* are defective in OMA-1 proteolysis.

Fluorescence micrographs showing OMA-1::GFP in wild-type and mutant embryos at three time points (as indicated) (Shirayama et al., 2006).

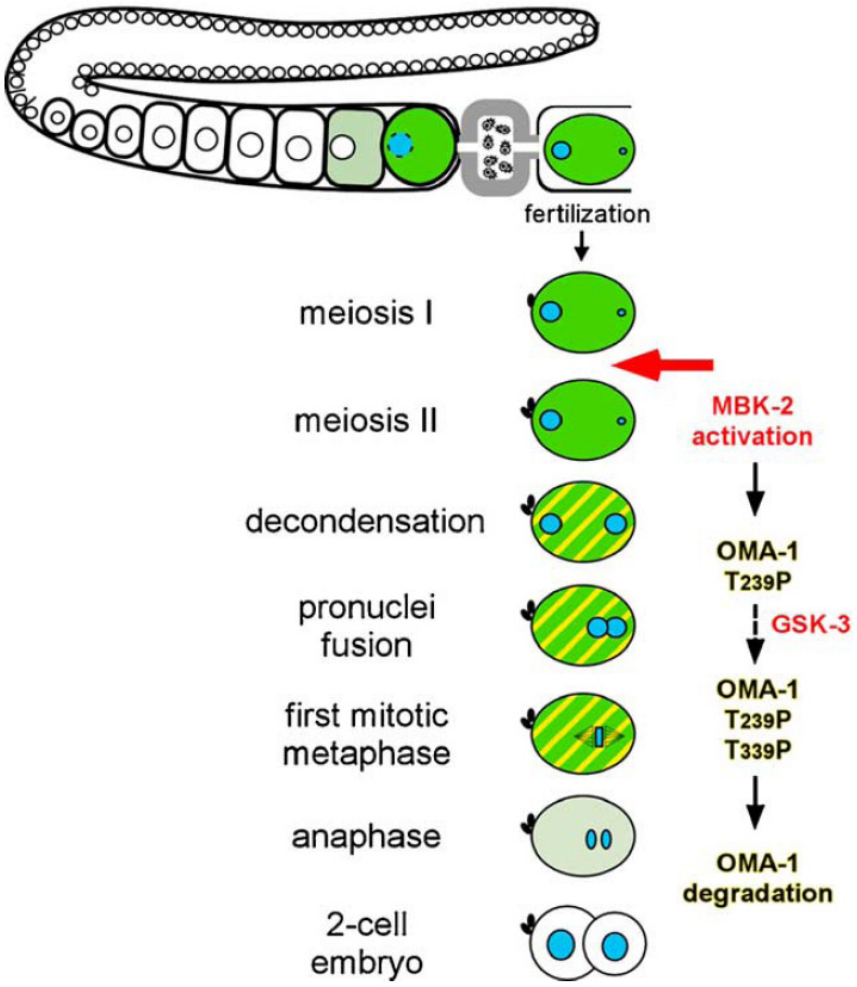

Figure 16. Model for regulation of OMA-1 degradation in early embryos.

The picture shows a schematic diagram of a wild type *C .elegans* hermaphrodite gonad, oocytes, and the first mitotic cycle. OMA-1 expression (green) is highest from oocyte maturation to the first mitotic division, following which it is rapidly degraded by MBK-2 and GSK-3 (Nishi and Lin, 2005; Shirayama *et al.*, 2006).

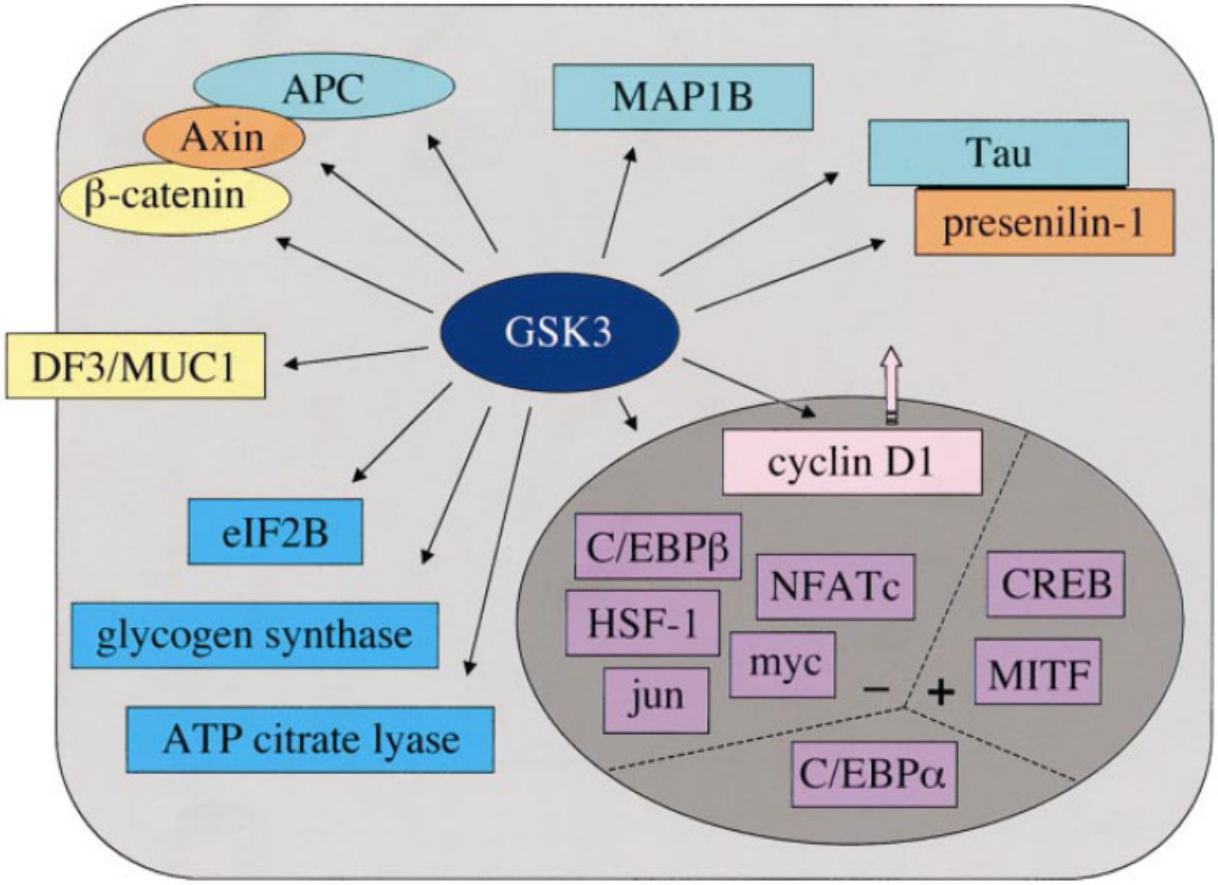

Figure 17. Proposed substrates of GSK3.

Putative substrates are color-coded according to their proposed function in the cell; transcription factors (mauve), enzymes that regulate metabolism (blue), protein bound to microtubules (turquoise), scaffold proteins (orange), or components of the cell division cycle machinery (pink) or involved in cell adhesion (yellow) (Frame and Cohen, 2001).

IV) Overview of this study

Two categories of mutants that display defective specification of gut cells, gutless and extra-gut mutants, have been isolated in the several large genetic screens (Nakamura et al., 2005; Shirayama et al., 2006). Although genetic and molecular studies using these mutants further revealed the pathways and mechanisms governing the fate of gut tissue, there are still many questions remaining. In this work, we present two approaches to understand better how the intestinal cells are specified during early *C. elegans* embryogenesis. First, to learn more about molecular mechanisms by which the gut cells are specified, we examine the key mediator WRM-1/β-catenin during polarized EMS cell division that generates the precursor of gut cells. Second, we utilized suppressor genetic screens using the temperature-sensitive mutants to identify additional components in the pathways defining the fate of gut cells.

Cell-cycle dependent regulation of WRM-1/β-catenin during EMS cell division

Canonical Wnt signaling operates through regulating the phosphorylation and degradation of the transcription co-activator β-catenin (He et al., 2004; Logan and Nusse, 2004). In P2/EMS signaling directing polarized EMS cell division to specify endoderm cells, the β-catenin homolog

WRM-1 functions as a key effector and regulates the transcription of endoderm gene (Rocheleau et al., 1999). Although it has been shown that WRM-1 accumulates highly in the posterior nucleus during EMS cell division (Nakamura et al., 2005), little is known about how WRM-1 is regulated during the signaling process.

In Chapter II, we demonstrate that WRM-1 is regulated by a series of phosphorylation events to mediate signals from the cortex to the nucleus in a cell-cycle dependent manner. Our results show a novel function for MOM-4 and LIT-1, MAPK-like components, that maintains WRM-1 in the cortex throughout the early embryogenesis. During EMS cell division, WRM-1 is released from the posterior cortex in a Wnt, Src, and cell-cycle dependent manner. Furthermore, the major cell-cycle regulator CDK-1 and membrane-bound GSK-3 sequentially phosphorylate WRM-1 to regulate its release from the cortex and subsequent nuclear translocation. By making GSK-3 phosphorylation dependent on prior phosphorylation by CDK-1, the inductive signal and mitosis are tightly coupled so that asymmetric segregation of the signal transducer WRM-1 is achieved at high fidelity. Our findings give novel insights into how cortical WRM-1 integrates Wnt, MAPK-like, and Src signals at the cortex, and links asymmetric cell division with cell cycle cues to specify endoderm tissue.

A suppressor screen of *mom-2*/Wnt

Extensive genetic and biochemical approaches have identified many of the genes that regulate the Wnt pathway in *C. elegans* and other model organisms. However, many components may remain unidentified if mutants do not display a distinguishable "Wnt phenotype". The availability of temperature-sensitive alleles and the complete genome sequence of *C. elegans* provided us with an opportunity to find additional components in endoderm specification by performing a genetic suppressor screen. In Chapter III, a suppressor screen using two temperature-sensitive alleles of *mom-2(ne834, ne874)* was carried out, and an allele of major translational machinery component *eIF4G* was identified for suppression of the *mom-2* phenotype. Although it is not understood how *ifg-1* functions in Wnt signaling during EMS cell division, it implies a novel connection between Wnt signaling and translational machinery.

A suppressor screen of extra-gut mutant *cks-1(ne549)*

A number of mutants with excessive endoderm tissue were isolated in several large genetic screens (Shirayama et al., 2006). Genetic and molecular studies show that they were the Dyrk family kinase homolog *mbk-2(ne3442)*, two alleles of CCCH zinc finger protein *oma-1(ne411, ne3800)*, two alleles of the cyclin-dependent protein kinase *cdk-1(ne236, ne2257)*, and

the CDK-1-interacting protein *cks-1(ne549)*. It has been shown that the extra-gut phenotype is caused by persistent level of the EMS cell fate determinant SKN-1 that results from mis-regulation of OMA-1 (Lin, 2003). Further studies revealed that GSK-3 and MBK-2 phosphorylate OMA-1 for its rapid degradation after the 1-cell stage (Nishi and Lin, 2005; Shirayama et al., 2006). However, the role of CDK-1/CKS-1 in OMA-1 regulation is still elusive. To elucidate the function of the CDK-1/CKS-1 complex and find additional components in this pathway, we conducted a suppressor screen using the temperature-sensitive allele of *cks-1(ne549)*. The molecular identification of one of the suppressor genes revealed it as *npp-10*, a self-cleaving nucleopore protein. Our study shows that *npp-10(ne3744)* suppresses *cks-1* and other extra-gut mutants by reducing the SKN-1 level, implying that nuclear transport of SKN-1 may be regulated by a NPP-10-dependent mechanism. This work is presented in Chapter IV.

In summary, studies shown in this thesis give us a better knowledge of P2/EMS signaling by providing molecular understanding of the signal relay process and identifying potential components in the pathways governing the fate of gut tissue.

CHAPTER II

CDK-1 couples polarity signaling to the cell cycle through WRM-1/β-catenin in early *C. elegans* embryos

Contributors to the work presented in Chapter II:

The author of this thesis, Soyoung Kim, took all the microscopic images of GFP::WRM-1 and GFP::GSK-3 related strains.

Masaki Shirayama and Takao Ishidate performed all the biochemical-related experiments.

Yanxia Bei made the rescuing GFP::GSK-3 transgenic strain.

Rita Sharma helped constructing genetic strains and sequencing experiments related to the work in this Chapter.

Abstract

Asymmetric cell division plays a fundamental role in both development and the homeostasis of tissues. Many forms of asymmetric cell division appear to involve precise coordination between the cell-division cycle and the signaling mechanisms that define the polarized axis of a cell. However, with few exceptions, the molecular intersections between cell-cycle and polarity-signaling pathways have yet to be defined. In early *C. elegans* embryos a polarizing signal induces the EMS cell to divide asymmetrically along the anterior/posterior axis, generating a posterior daughter called E, that produces endoderm. Wnt-signaling and the ß-catenin-related protein WRM-1 play central roles in endoderm specification. In this study we show that during interphase of the cell cycle WRM-1 localizes to the cortex at all cell-contact sites in EMS. However, during mitosis WRM-1 is released specifically from the cortex proximal to a Wnt signaling cell. We show that a mitotic CDK-1-cyclin B complex phosphorylates WRM-1 directly, priming WRM-1 for subsequent phosphorylation by GSK-3. These phosphorylations appear to promote the Wnt-signal-dependent release of WRM-1 from the cortex, making WRM-1 available for transport into the nascent nucleus most proximal to the signaling cell, the nucleus of

the future E cell. These findings identify WRM-1/ß-catenin as a direct developmental target of CDK-1, and as a molecular link that coordinates polarity-signaling with the cell-division cycle.

Introduction

In 4-cell stage *C. elegans* embryos a polarizing signal from the posteriormost blastomere, P2, induces the neighboring cell, called EMS, to divide asymmetrically producing daughter cells committed to mesodermal and endodermal development (Thorpe et al., 2000). This signaling interaction, first identified in a series of elegant classical embryological studies (Goldstein, 1992, 1993, 1995a, b), has been the subject of numerous genetic and molecular studies (Bei et al., 2002; Ishitani et al., 1999; Lo et al., 2004; Meneghini et al., 1999; Rocheleau et al., 1997; Rocheleau et al., 1999; Shin et al., 1999; Thorpe et al., 1997) and provides an ideal opportunity to determine the molecular events that couple cell-polarity signals to cell cycle regulation. P2/EMS signaling integrates multiple inputs from the Wnt, MAPK-like, and Src pathways (Bei et al., 2002; Ishitani et al., 1999; Lo et al., 2004; Meneghini et al., 1999; Rocheleau et al., 1997; Rocheleau et al., 1999; Shin et al., 1999; Thorpe et al., 1997) to modulate transcriptional outputs that are dependent upon a homolog of ß-catenin, WRM-1 (Mizumoto and Sawa, 2007b; Rocheleau et al.,

1999). Recent studies revealed that P2/EMS signaling during the EMS cell division is required for the accumulation of GFP::WRM-1 in the nucleus of the posterior daughter of EMS, the E blastomere (Nakamura et al., 2005; Takeshita and Sawa, 2005).

However, these earlier studies did not address whether or how inductive signals from the membrane are coordinated with the cell-cycle so as to drive the asymmetric nuclear accumulation of WRM-1. In this work, we examine WRM-1 *in vivo* and reveal its novel regulation mechanism to transfer the multiple signaling inputs in the cortex to the nucleus during polarized EMS cell division.

Results and Discussions

To ask whether WRM-1, itself, might integrate signaling and cell-cycle cues we decided to examine WRM-1 localization throughout the EMS cell cycle. In addition to localizing in all nuclei in the early embryo, a rescuing GFP::WRM-1 fusion protein also localized to all cell contact sites during early embryogenesis (Figure 18a). This cortical pattern was maintained throughout the cell cycle in non-signaling cells. However, during mitosis in the Wnt-responsive EMS blastomere, a dramatic loss of GFP::WRM-1 was observed at the cortex adjacent to the

signaling cell P2 (Nakamura et al., 2005) (Figure 18a). In EMS, signaling directs the orientation of the mitotic apparatus, such that both the cortex and cytoplasm adjacent to the signaling cell is only partitioned into the E daughter cell. Interestingly, release of WRM-1 from the cortex proximal to the signaling cell was coincident with cytokinesis. This timing may serve to restrict P2/EMS signaling such that only the daughter most proximal to the signaling cell accumulates high levels of nuclear and cytoplasmic WRM-1 (Figure 18a).

We next turned to genetic studies in order to investigate the cortical localization of WRM-1 and to ask whether its cortical and nuclear distributions are co-regulated. Several factors that comprise MAP-kinase-like and Wnt-signaling-related pathways are required for the asymmetric nuclear accumulation of WRM-1 (Mizumoto and Sawa, 2007a; Nakamura et al., 2005; Takeshita and Sawa, 2005). Mutations in the MAP kinase-like signaling components (Ishitani et al., 1999; Meneghini et al., 1999; Rocheleau et al., 1999; Shin et al., 1999) *mom-4*/MAPKKK and *lit-1*/Nemo completely abolished the cortical localization of WRM-1 in all cells of the early embryo (Figure 19b, Figure 26 and Figure 27), suggesting that the MOM-4 and LIT-1 kinases act constitutively, in all cells to promote WRM-1 cortical association. In contrast, mutants in the Wnt-signaling-related factors (Rocheleau et al., 1997; Schlesinger et al., 1999; Thorpe et al., 1997; Walston et al., 2004) *mom-2*(Wnt), *mom-5*(Frizzled), *dsh-1, dsh-2* and *mig-5*(Dishevelled*)*,

and *sgg-1/gsk-3*(GSK3ß) did not prevent the cortical association of WRM-1, but rather specifically prevented its release from the P2-proximal cortex of EMS and exhibited symmetric accumulation of WRM-1 in the nuclei of MS and E (Figure 19a, Figure 22, Figure 26 and Figure 27). Finally, two other Wnt/ß-catenin-related signaling factors, *pop-1*(TCF/LEF-1) and *apr-1*(APC-related), were not required for release of WRM-1 from the cortex but, as shown previously (Mizumoto and Sawa, 2007a; Nakamura et al., 2005), failed to exhibit WRM-1 nuclear accumulation (Figure 23, Figure 26 and Figure 27), suggesting that these latter two factors promote the nuclear accumulation of WRM-1 downstream of its cortical release.

In the canonical Wnt pathway, sequential phosphorylations of ß-catenin by Casein kinase 1(CK1) and GSK3(GSK3ß) negatively regulate Wnt signal transduction (Amit et al., 2002; Liu et al., 2002; Yanagawa et al., 2002). WRM-1 is quite diverged from ß-catenin and lacks the GSK3 and CK1 sites of ß-catenin that are important for its degradation in other species. However, phosphorylation site prediction software (Scansite 2.0) (Obenauer et al., 2003) identified two potential cyclin-dependent kinase 1 (CDK-1) sites in the N-terminal region of WRM-1 that were conserved between *C. elegans* and the related nematode species *C. briggsae* (Figure 20a). Interestingly, one of these sites is situated such that phosphorylation by CDK-1 could prime WRM-1 for subsequent phosphorylation by GSK-3. Although models for GSK-3 function are

complicated by pleiotropies associated with its mutant phenotype(Nishi and Lin, 2005; Shirayama et al., 2006), the localization studies on WRM-1 described above suggest that, rather than antagonizing Wnt-signaling as it does in the canonical Wnt pathway, GSK-3 may function (directly or indirectly) together with other polarity-signaling factors to promote the cortical release and asymmetric nuclear accumulation of WRM-1 (Schlesinger et al., 1999; Zeng et al., 2005) (Figure 22c, Figure 26 and Figure 27).

Perhaps consistent with a role for GSK-3 in regulating WRM-1 at the cortex, previous studies in vertebrate cells have reported accumulation of GSK3 at cell-contact sites (Bilic et al., 2007; Zeng et al., 2005). We therefore examined the localization of a rescuing *C. elegans* GFP::GSK-3 fusion protein. This analysis revealed a dynamic localization pattern involving cortical accumulation of GSK-3 at all cell contact sites during early embryogenesis (Figure 18b). In addition, GSK-3 was localized to the centrosomes and spindles during mitosis and to nuclei at the end of mitosis. GSK-3 localization was not visibly asymmetric, even in cells undergoing asymmetric cell divisions, nor was GSK-3 mis-localized in embryos with polarity-signaling defects, including *mom-2*(*RNAi*), *mom-5*(*RNAi*), *dishevelled*(*RNAi*), *lit-1*(*RNAi*), or *src-1*(*RNAi*) (data not shown). Thus the cortical localization of GSK-3 occurs via a mechanism that is genetically distinct from the mechanism underlying WRM-1 cortical localization.

We reasoned that CDK-1 and GSK-3 might function together to directly phosphorylate WRM-1, promoting its release from the cell cortex in response to Wnt signaling. Consistent with this idea, an N-terminal peptide of WRM-1 (amino acids 1-140) was robustly phosphorylated *in vitro* by CDK-1/CYB-1 (Cyclin B1) and CDK-1/CYB-3 (Cyclin B3) complexes, recovered by immunoprecipitation from worm embryonic extracts (Figure 20b). A mutation in either of the potential CDK-1 sites (T30A or S46A) reduced the phosphorylation by about 50%, while mutations in both CDK-1 sites completely abolished phosphorylation of the WRM-1 peptide, suggesting that both T30 and S46 are phosphorylated equally *in vitro* (Figure 20c). To determine if CDK-1 phosphorylation of WRM-1 promotes subsequent phosphorylation by GSK-3, GST-WRM-1(1-140) protein was pre-incubated with non-radio labeled ATP and a commercially available CDK/Cyclin complex (CDC2/cyclin B) and after extensive washing, was then incubated with vertebrate GSK3ß and γ-^{32}P-ATP. Strikingly, WRM-1 pretreated with CDC2/Cyclin B was robustly phosphorylated by GSK3ß (Figure 20d). The ability of GSK3ß to phosphorylate WRM-1 was absolutely dependent on both preincubation with CDC2/Cyclin B and the CDK-1 sites (T30 and S46) (Figure 20d), demonstrating that CDK phosphorylation can prime for GSK-3 phosphorylation *in vitro*. Thus, phosphorylation of WRM-1 by CDK-1 may serve as a cue that couples WRM-1 cortical release to the onset of M phase.

The physiological relevance of sequential phosphorylation of WRM-1 by CDK-1 and GSK-3 was confirmed *in vivo*. A GFP::WRM-1 fusion protein with mutations in both CDK-1 sites not only failed to dissociate from the P2-proximal cortex during the EMS cell division, but also failed to exhibit asymmetric accumulation in the nuclei of EMS daughter cells (Figure 21a, c). WRM-1 bearing a mutation in a single GSK-3 site (S26A) exhibited similar, albeit less prominent, defects (Figure 21b, c). Taken together, these results suggest that phosphorylation of WRM-1 by CDK-1 and GSK-3 promotes WRM-1 release from the cortex during the EMS cell cycle.

Previous work has shown that LIT-1 binds to and phosphorylates WRM-1 (Rocheleau et al., 1999). A kinase-dead LIT-1 protein failed to form a stable complex with WRM-1 (Fig. 3e), suggesting that a stable and active WRM-1/LIT-1 kinase complex may be required for WRM-1 cortical localization, possibly through phosphorylation of WRM-1. Recombinant WRM-1 proteins with mutations in the CDK-1 or GSK-3 phosphorylation sites formed stable and active WRM-1/LIT-1 kinase complexes *in vitro* (Figure 28). Furthermore, prior phosphorylation of WRM-1 with CDK-1 and GSK-3 did not alter the subsequent binding or phosphorylation of WRM-1 by LIT-1. Conversely, pre-incubation of WRM-1 with LIT-1 had no effect on the phosphorylation of WRM-1 by CDK-1 and GSK-3. These findings suggest that phosphorylation

by CDK-1 and GSK-3 may promote WRM-1 dissociation from the cortex and nuclear translocation without altering its ability to bind and activate the LIT-1 kinase.

In other systems, the tyrosine phosphorylation of ß-catenin promotes its signaling functions while down-regulating its role in cell adhesion (Brembeck et al., 2006). We found that the cortical and nuclear asymmetry of WRM-1 depended in part on SRC-1 (Figure 25, Figure 26 and Figure 27). A previous study has shown that SRC-1 functions together with the Wnt-signaling pathway to control both endoderm specification and the orientation of the EMS cell-division in *C. elegans* (Bei et al., 2002). Furthermore, SRC-1 is specifically activated on the EMS cell membrane at the P2 contact site (J. Liu and CM, unpublished results), and can phosphorylate WRM-1 *in vitro* (Figure 29), suggesting that the Wnt and Src pathways may converge on WRM-1/ß-catenin directly.

Our data support a model for P2/EMS signaling in which WRM-1/ß-catenin integrates cell cycle cues and polarity signals to control the asymmetric division of EMS (Figure 30). First, a constitutive MAP kinase-like pathway promotes cortical localization of WRM-1 in all embryonic cells. Second, Wnt and Src-dependent signaling mechanisms polarize the EMS cell to prime and/or activate cortical WRM-1 at the P2/EMS junction for endoderm induction, and to direct the rotation of the EMS spindle complex. Simultaneous with the rotation of the EMS

spindle apparatus and the onset of cytokinesis, sequential phosphorylation by CDK-1 and GSK-3 triggers the release of WRM-1 from the P2/EMS junction, such that only the posterior daughter of EMS inherits cytoplasmic WRM-1 that is competent for nuclear translocation and endoderm induction. *wrm-1* mutants are not defective in the orientation of the EMS spindle (Bei et al., 2002; Rocheleau et al., 1999; Schlesinger et al., 1999). Thus, Wnt and Src, and perhaps CDK-1 and GSK-3, must have additional target(s) involved in directing EMS spindle orientation.

The regulation of the cortical release of WRM-1 through sequential CDK-1 and GSK-3 phosphorylations provides a molecular link between P2/EMS polarity signaling and cell cycle regulation. An important question that remains is whether CDK-1 targets WRM-1 in a signaling-dependent manner- for example, by only phosphorylating a subpopulation of WRM-1 on the membrane proximal to the P2/EMS contact site. Recent reports suggest that Wnt induces Frizzled to interact in the membrane with its co-receptor LRP6 (Pinson et al., 2000; Tamai et al., 2000; Wehrli et al., 2000). This complex recruits Dishevelled, which in turn induces GSK3ß and CK1γ-dependent phosphorylation of LRP6 (Bilic et al., 2007; Zeng et al., 2005). Although an LRP6-like co-receptor has not been identified in *C. elegans,* Frizzled and Dishevelled have been reported to accumulate at the Wnt-responsive cortex of EMS (Goldstein et al., 2006; Hawkins et al., 2005; Mizumoto and Sawa, 2007a; Park and Priess, 2003; Takeshita and Sawa, 2005;

Walston et al., 2004; Wu and Herman, 2007). Perhaps a similar signaling-induced complex modifies WRM-1 within this cortical domain, permitting its subsequent recognition, at the appropriate time in the cell cycle, by CDK-1 and GSK-3. Whatever the specific mechanism, it is clear that signaling renders WRM-1 protein sensitive to release from the cortex in response to CDK-1 phosphorylation, thus providing a molecular link between polarity-signaling and the cell-division cycle during endoderm induction in *C. elegans*.

Materials and Methods

Microscopy

Axioplan2 Microscope (Zeiss) equipped with epi-flurorescence and differential interference contrast (DIC) optics was used for light microscopy. GFP::WRM-1 and GFP:: GSK-3 embryos were mounted in dH_2O on RITE-ON glass slides (Beckton Dickinson). ORCA-ER digital camera (Hamamatsu) and OPENLAB software were used to take DIC and GFP images. For GFP::GSK-3 movie, embryos were mounted on a 3% agarose pad in M9 buffer, and DIC and GFP images were captured at 30 sec interval using same equipment and software specified above.

Plasmids and transgenic strains

The translational fusion *gfp::wrm-1* transgenic strain was described previously (Nakamura et al., 2005). The translational fusion *gfp::gsk-3* transgene was constructed in yeast artificial chromosome (YAC) as described (Rocheleau et al., 1999). The *gfp* gene with *sup4*^{o} selection marker embedded within a synthetic *C. elegans* intron was inserted in frame in front of the stop codon of *gsk-3*. The recombinant YAC, Y18D10 (*gsk-3::gfp*) was injected into worm gonads to create transgenic line. After integration, the transgenic line was crossed to the *gsk-3 (nr2047)* strain to obtain rescue line, *gsk-3 (nr2047) I, neIs1 [Y18D10 (gsk-3::gfp); pRF4 (rol-6)] V* . To express *gfp*::*wrm-1* with various mutations *in vivo*, the *Spe*1 and *Bgl*II (5.7 kb) genomic fragment containing the entire *wrm-1* coding sequence was cloned from cosmid T16E10 into the *Xba*I and *Bam*HI sites of Bluescript pKS(+). A *Bgl*II site was created by site directed mutagenesis after the first codon of *wrm-1* coding region and the *gfp* sequence amplified from pPD95-75 by PCR was subcloned. Mutations in CDK-1 sites (T30 and S46) and GSK-3 site (S26A) were introduced in this construct by site direct mutagenesis. Microparticle bombardment (Praitis, 2006) was used to create the transgenic strains, *neIs15* (*gfp*::*wrm-1* $_{T30A\ S46A}$;;*unc-119*) and *neIs16* (*gfp::wrm-1*$_{S26A}$::*unc-119*). For *in vitro* kinase assay, the following plasmids were made to express GST fusion WRM-1 or POP-1 proteins. B1224 to express GST-WRM-1(1-140), B1337; GST-WRM-

1(1-140, T30A), B1338; GST-WRM-1(1-140, S46A), B1339; GST-WRM-1(1-140, T30A; S46A), B1360; GST-POP-1(1-888) (Lo et al., 2004).

Cell culture and transfection

293T cells were grown in Dulbecco's modified Eagle's medium (DMEM) supplemented with 10% fetal bovine serum on 35mm dish. Transient transfections were performed using Effectene reagent (QIAGEN) according to manufacturer's instruction.

Immunoprecipitation and *in vitro* kinase assays

Transfected cells were harvested 24 hrs post transfection and lysed in 750µl of lysis buffer (50mM Tris-HCl [pH 7.4], 150mM NaCl, 1% NP-40, 1mM DTT, 50mM β-glycerophosphate, 1mM sodium orthovanadate, 0.05mM sodium fluoride, 1mM PMSF, supplemented with Complete mini Protease Inhibitors (Roche). Immunoprecipitation of FLAG-tagged proteins from 293T cells was performed using anti-FLAG M2-Agarose (Sigma). Beads were washed three times with the lysis buffer and once with kinase buffer (50mM HEPES [pH7.4], 10mM $MgCl_2$, 10mM DTT, 0.5mM NaF, 0.1mM Sodium orthovanadate, 5µg/ml leupeptin) and then aliquoted for kinase assays. *In vitro* kinase assays were done in 25µl of kinase buffer supplemented with [γ-

^{32}P]ATP [6000 Ci/mmol; Amersham] for 15 min at 25^{o}C. After kinase reaction, supernatants and pellets were separated and subjected to SDS-PAGE followed by autoradiography. In order to remove background, supernatants were transferred to fresh tubes to which 500µl of binding buffer (0.5% NP-40, 50mM Tris-HCl [pH8.5], 100mM NaCl, 1mM EDTA, 1mM DTT, 1mM PMSF supplemented with Phosstop phosphatase inhibitors (Roche) and Complete mini Protease inhibitors (Roche) and glutathione-sepharose (G.E.) beads were added. After rotating at 4°C for 1 hour, the beads were washed three times with the binding buffer and once with water and then subjected to SDS-PAGE. For immunoprecipitation of endogenous CDK-1 complexes, ~3.5 x 10^6 embryos were suspended in 2ml of lysis buffer and homogenized by "One shot" cell disruptor (Cell Disruption Systems). The lysate was cleared by centrifugation and subjected to immunoprecipitation using anti-CYB-1 or anti-CYB-3 antisera (kindly provided by Dr. Sander van den Heuvel) and protein A sepharose beads (Amersham Pharmacia). Beads were washed three times with the lysis buffer and once with the kinase buffer and then subjected for kinase assays. For CDK1/GSK3β sequential kinase assay, the substrate GST-fusion proteins were first incubated with CDK1 (NEB) in the presence of 100µM of non-radiolabeled ATP in the kinase buffer at 25°C for 30 min. After immobilizing the substrates on glutathione-sepharose beads and

washing three times with the binding buffer and once with the kinase buffer, the substrates were incubated with GSK3β (NEB) together with γ-ATP at 25°C for 15 min.

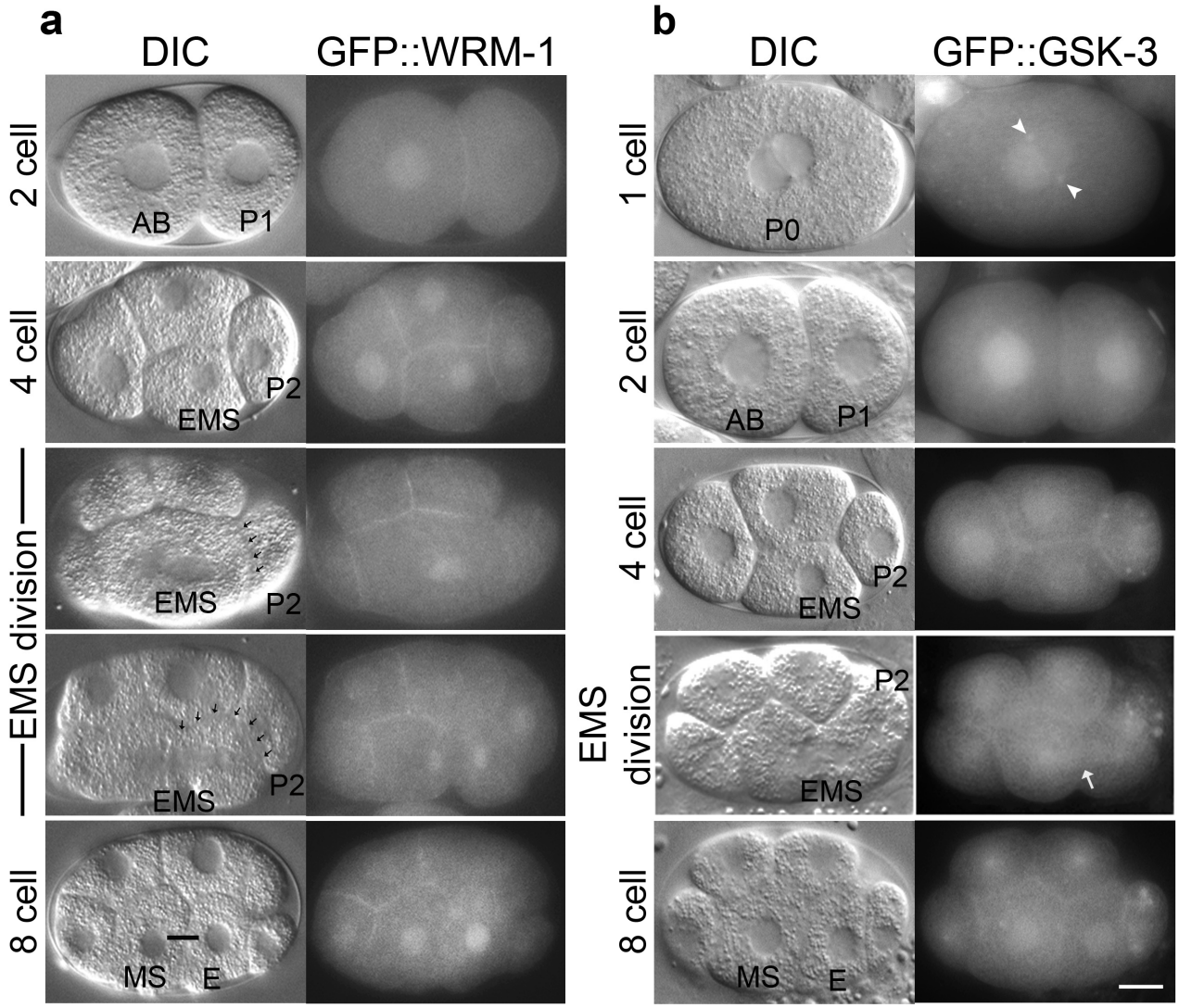

Figure 18. Cell-cycle dependent regulation of WRM-1 and GSK-3 localizations.

(**a, b**) Nomarski (DIC) and fluorescence micrographs of GFP-transgenic embryos at various stages (as indicated). Anterior is to the left and dorsal is up. In (**a**) the black arrows indicate the EMS cortex. In (**b**) white arrowheads indicate the centrosomes, and the white arrow indicates the

spindle in EMS. In this and subsequent figures, the black line in 8-cell stage connects a pair of A-P sister nuclei of EMS daughters, and the white bar indicates 10 μm.

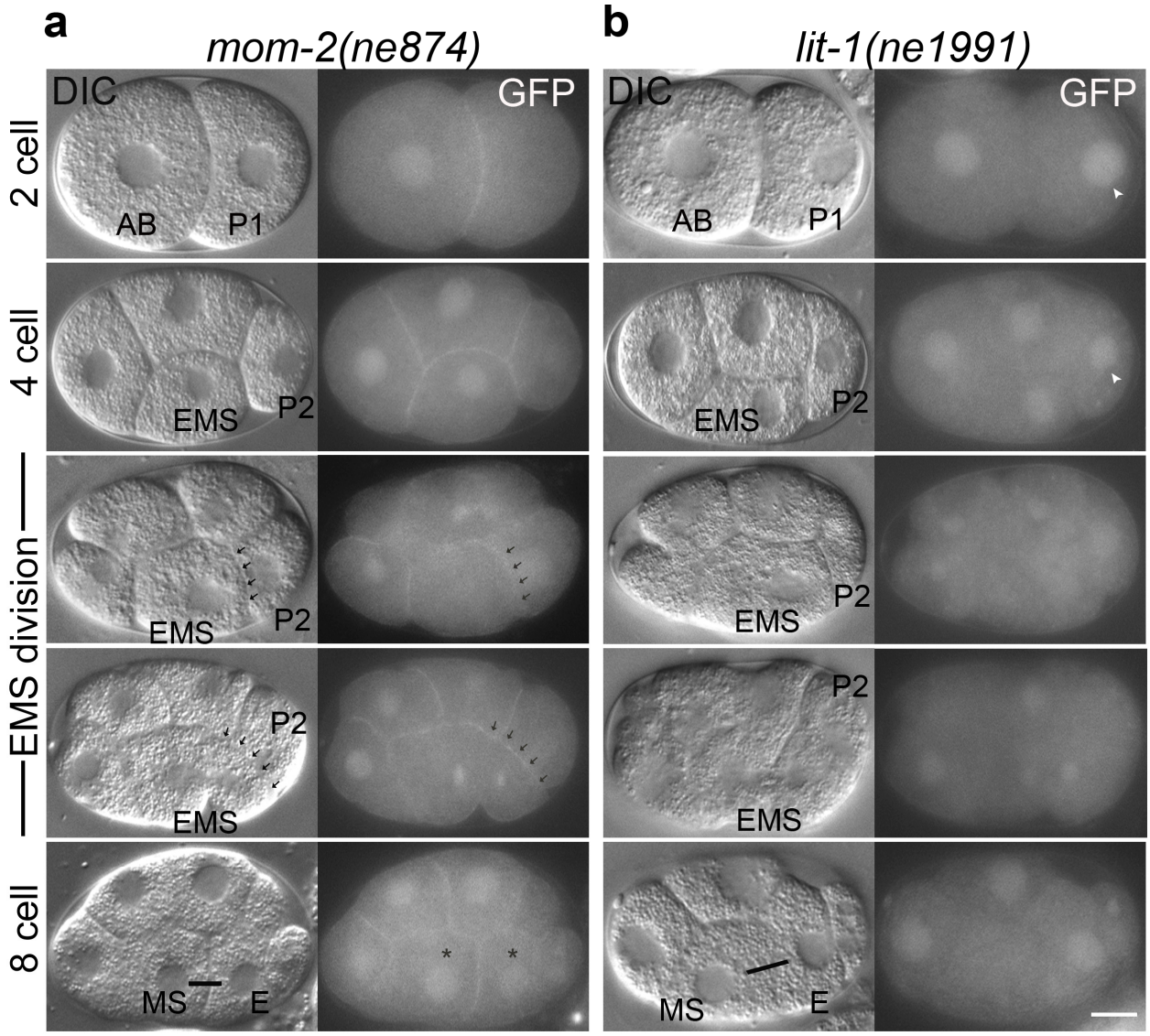

Figure 19. The Wnt and MAPK-like pathways regulate the localization of WRM-1.

(**a, b**) Nomarski (DIC) and fluorescence images of GFP-transgenic embryos at various stages (as indicated). Departures from wild-type localization are indicated as follows, in (**a**) black arrows indicate retention on the EMS cortex, asterisks indicate symmetric nuclear accumulation in MS

and E. White arrow heads indicate higher than wild-type nuclear accumulation in P1 and P2 in *lit-1(ne1991)* embryos.

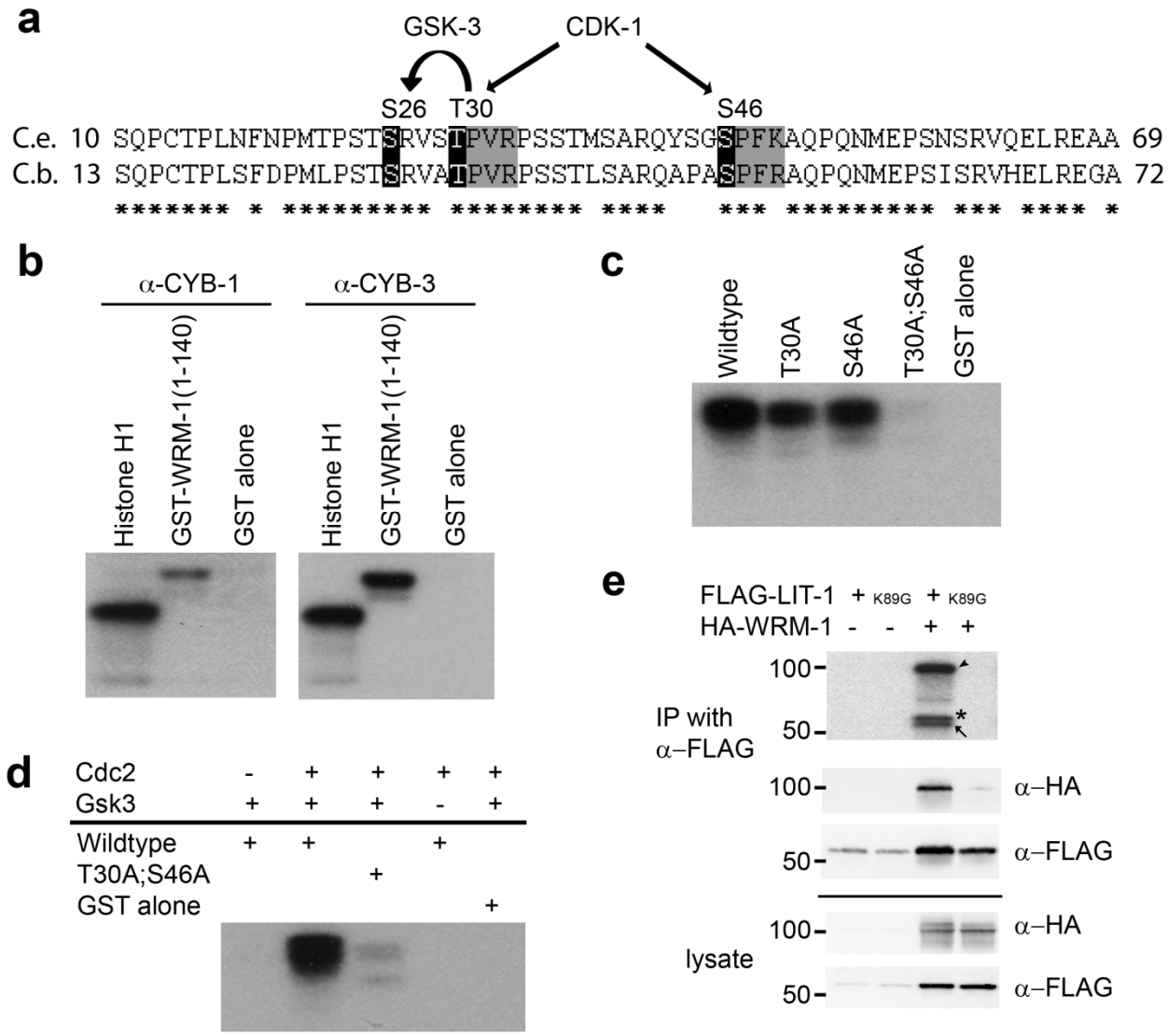

Figure 20. CDK-1 and GSK-3 sequentially phosphorylate WRM-1.

a, Amino acids alignments of the N-terminal domain of WRM-1 in *C. elegans* (C.e.) and *C. briggsae* (C.b.). Conserved CDK-1 and coupled GSK-3 sites are highlighted. Asterisks indicate the conserved amino acid residues. **b**, *In vitro* kinase assay using anti-CYB-1 or anti-CYB-3

immunoprecipitates and indicated substrates. CDK-1/CYB-3 complex is more efficient in phosphorylating GST-WRM-1(1-140) than CDK-1/CYB-1 complex after normalizing their activities toward histone H1. **c**, *In vitro* kinase assay to map phosphorylation sites using human recombinant Cdc2 and indicated substrates. **d**, *In vitro* GSK3 kinase assay. GST-WRM-1(1-140) was first incubated with non-radio-labeled ATP and Cdc2 then after extensive washing incubated with radio-labeled ATP in the presence or absence of GSK3. **e**, *In vitro* LIT-1 kinase assay. 293T cells were transfected with wild type (+) or kinase dead (K89G) FLAG-LIT-1 expression plasmid with or without HA-WRM-1 plasmid. *In vitro* kinase assay using immunoprecipitated HA-WRM-1/FLAG-LIT-1 complex and GST-POP-1(1-188) as the substrate (top panel) and western blot analysis with indicated antibodies (lower panels) were performed. LIT-1 and WRM-1 phosphorylations are indicated by an arrow and an arrowhead, respectively, while GST-POP-1 phosphorylation is indicated by an asterisk.

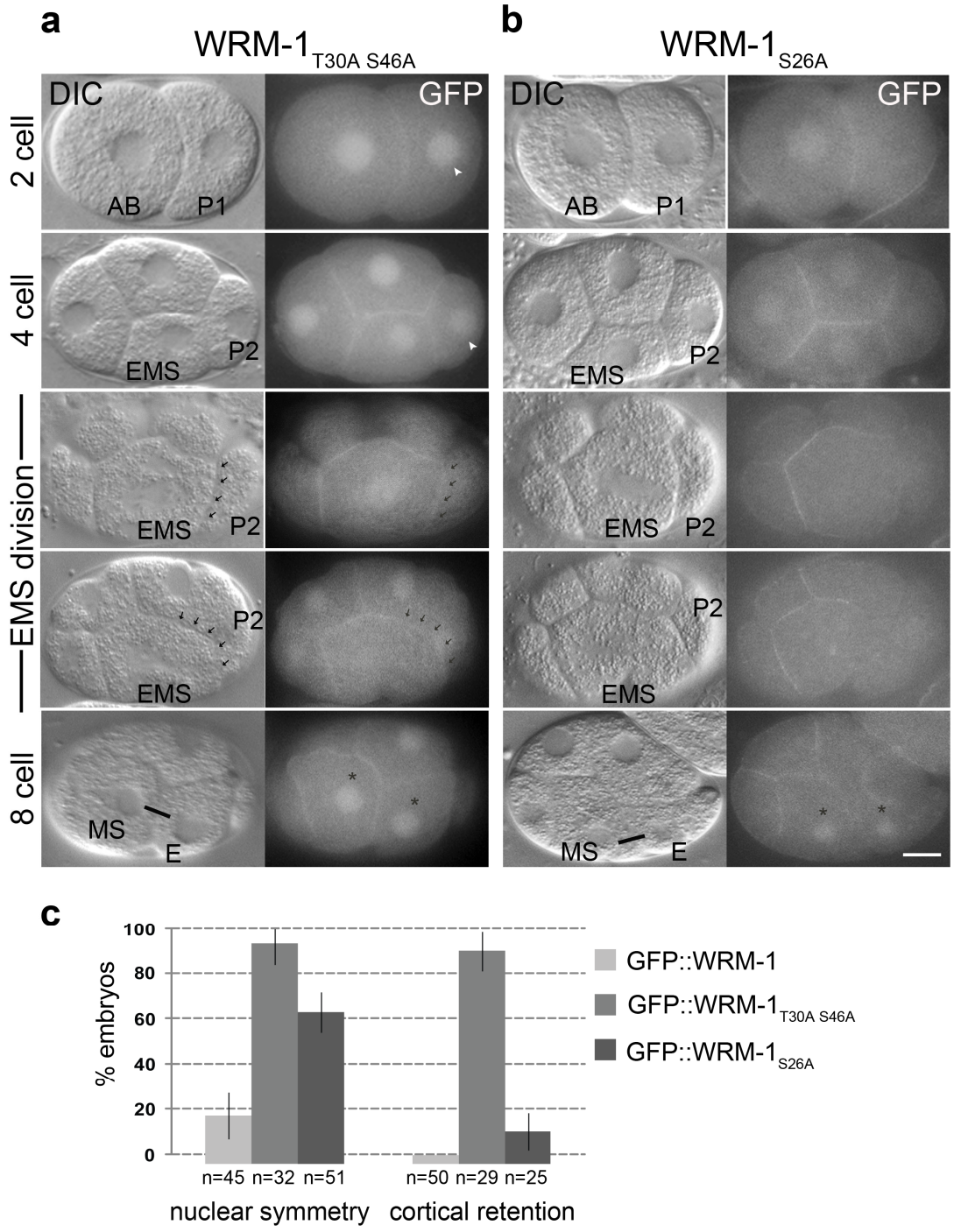

Figure 21. WRM-1 localization requires the CDK-1 and GSK-3 sites.

(**a,b**) Nomarski (DIC) and fluorescence (GFP) micrographs of representative transgenic embryos, as indicated. Departures from wild-type localization are indicated as follows in (**a**) arrowheads indicate higher than wild-type nuclear accumulation in P1 and P2; black arrows indicate retention on the posterior cortex of EMS. In (**a, b**) asterisks indicate symmetric accumulation in MS and E. Only ~5% of GFP::WRM-1_{S26A} embryos exhibited defects in cortical release. In the example shown in (**b**), the cortical localization is wild type. (**c**) Quantification of MS/E nuclear symmetry and cortical retention defects. The error bars indicate standard deviation.

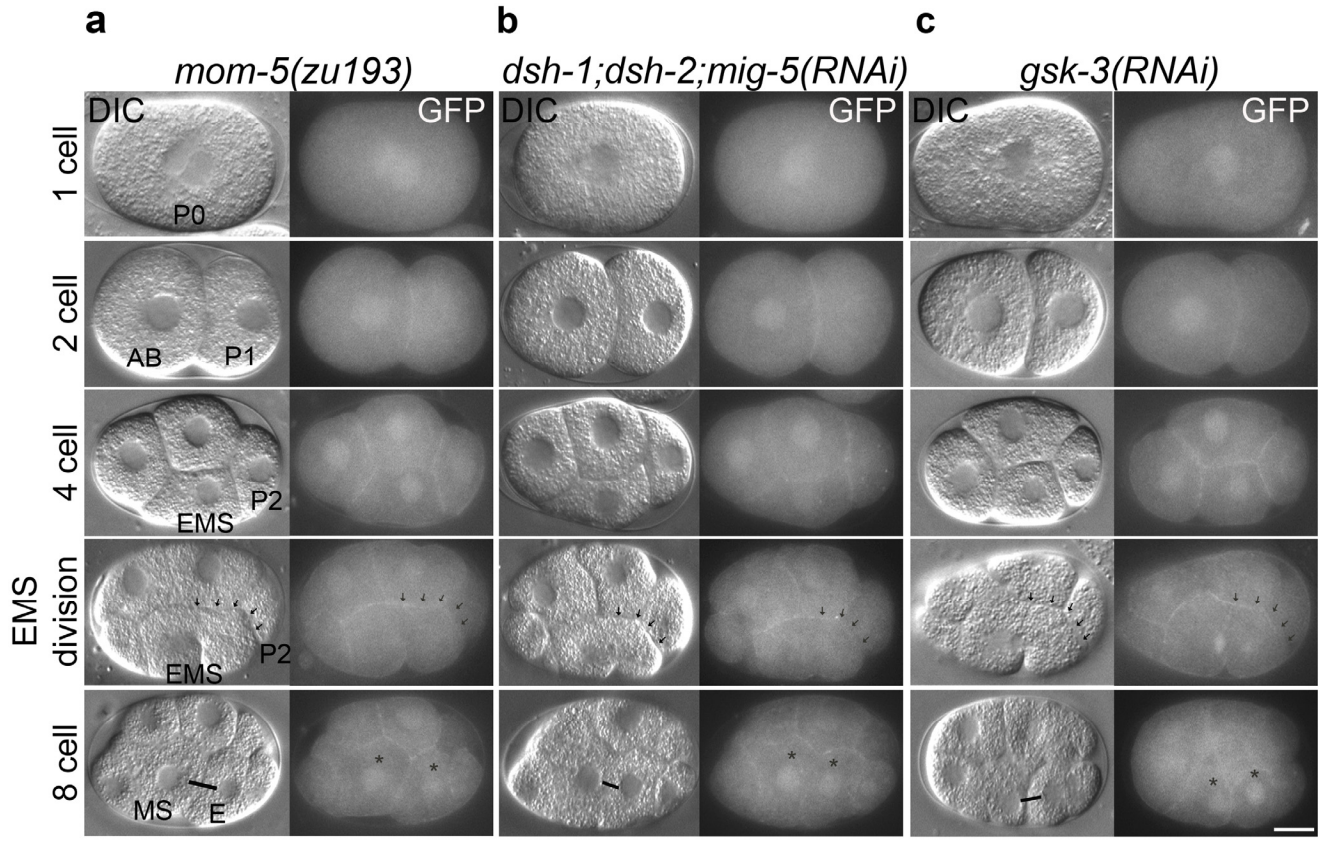

Figure 22. Genetics of the asymmetrical localization of WRM-1.

Nomarski (DIC) and fluorescence micrographs of GFP-transgenic embryos at various stages (as indicated). Departures from wild-type localization are indicated as follows, in (**a**, **b, c**) black arrows indicate retention on the EMS cortex, asterisks indicate symmetric nuclear accumulation in MS and E.

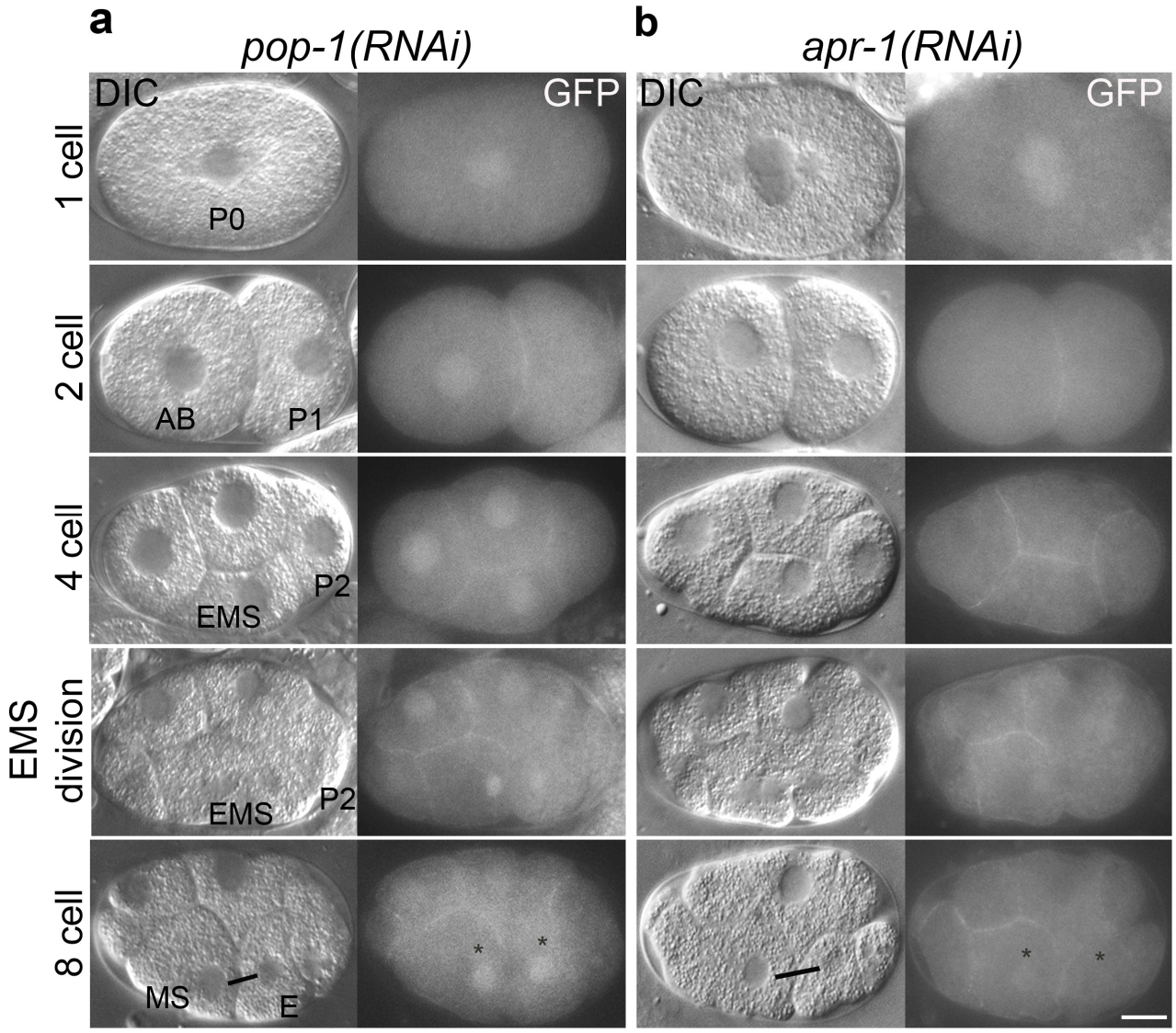

Figure 23. Cortical and nuclear localization of WRM-1 is regulated independently.

In (**a, b**) asterisks indicate symmetric nuclear accumulation in MS and E. *apr-1(RNAi)* embryos exhibit significantly reduced nuclear localization in early blastomeres.

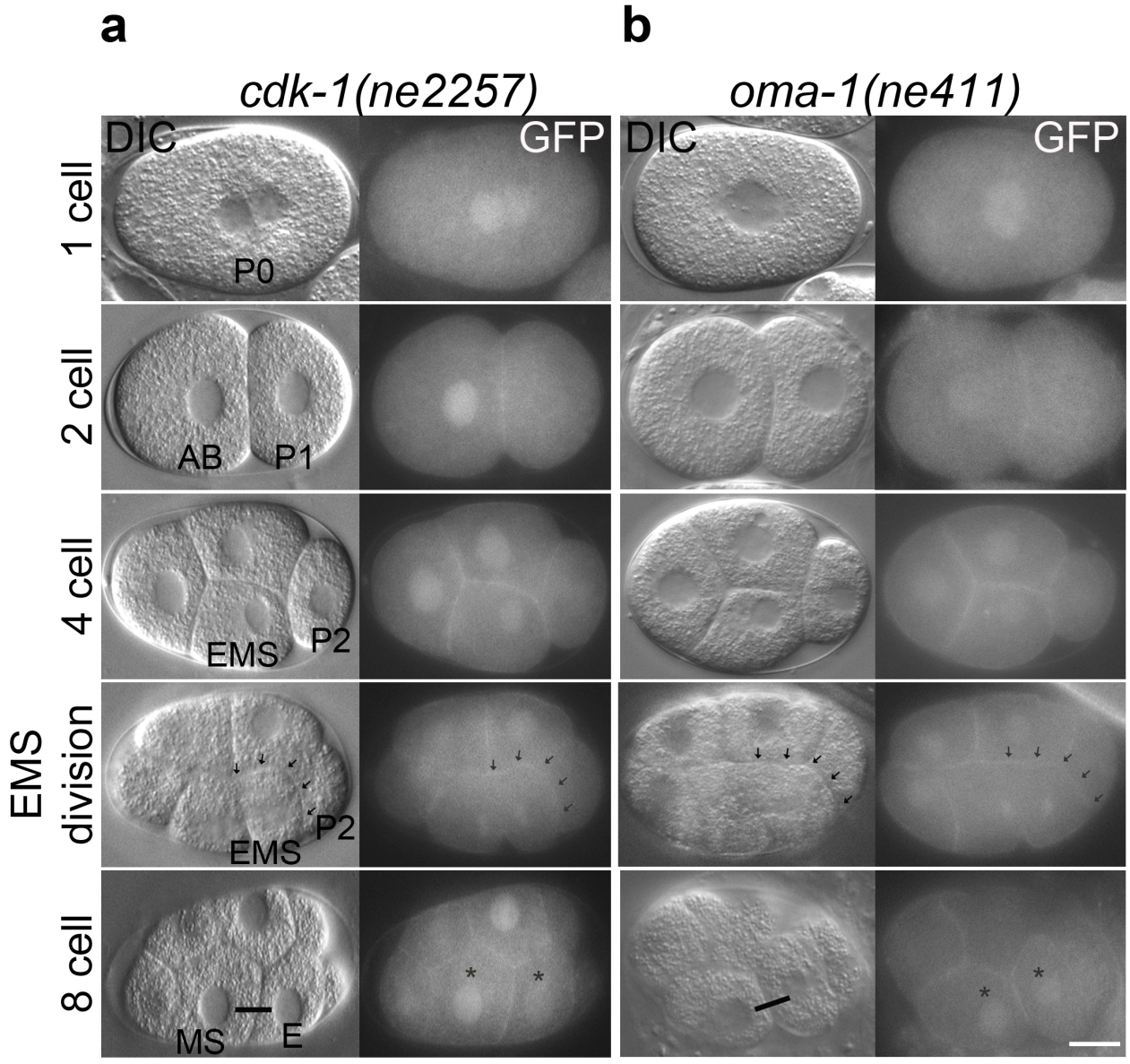

Figure 24. Mis-regulation of OMA-1 affects the localization of WRM-1.

Nomarski (DIC) and fluorescence (GFP) micrographs of representative transgenic embryos, as indicated. Departures from wild-type localization are indicated as follows. In (**a, b**) black arrows indicate retention on the EMS cortex, asterisks indicate symmetric nuclear accumulation in MS and E. The gain-of-function allele *oma-1(ne411)* and hypomorphic allele *cdk-1(ne2257)* have excessive endoderm and a suite of other defects in cell polarity and cell-fate specification that are very similar to the phenotype caused by the deletion allele *gsk-3(nr2047)* (Shirayama et al., 2006). It has been previously shown that the persistence of OMA-1 protein observed in *gsk-3(nr2047), cdk-1(ne2257),* and *oma-1(ne411)* interferes with Wnt signaling in the 4-cell stage embryo through an unknown mechanism (Lin, 2003; Nishi and Lin, 2005; Shirayama et al., 2006).

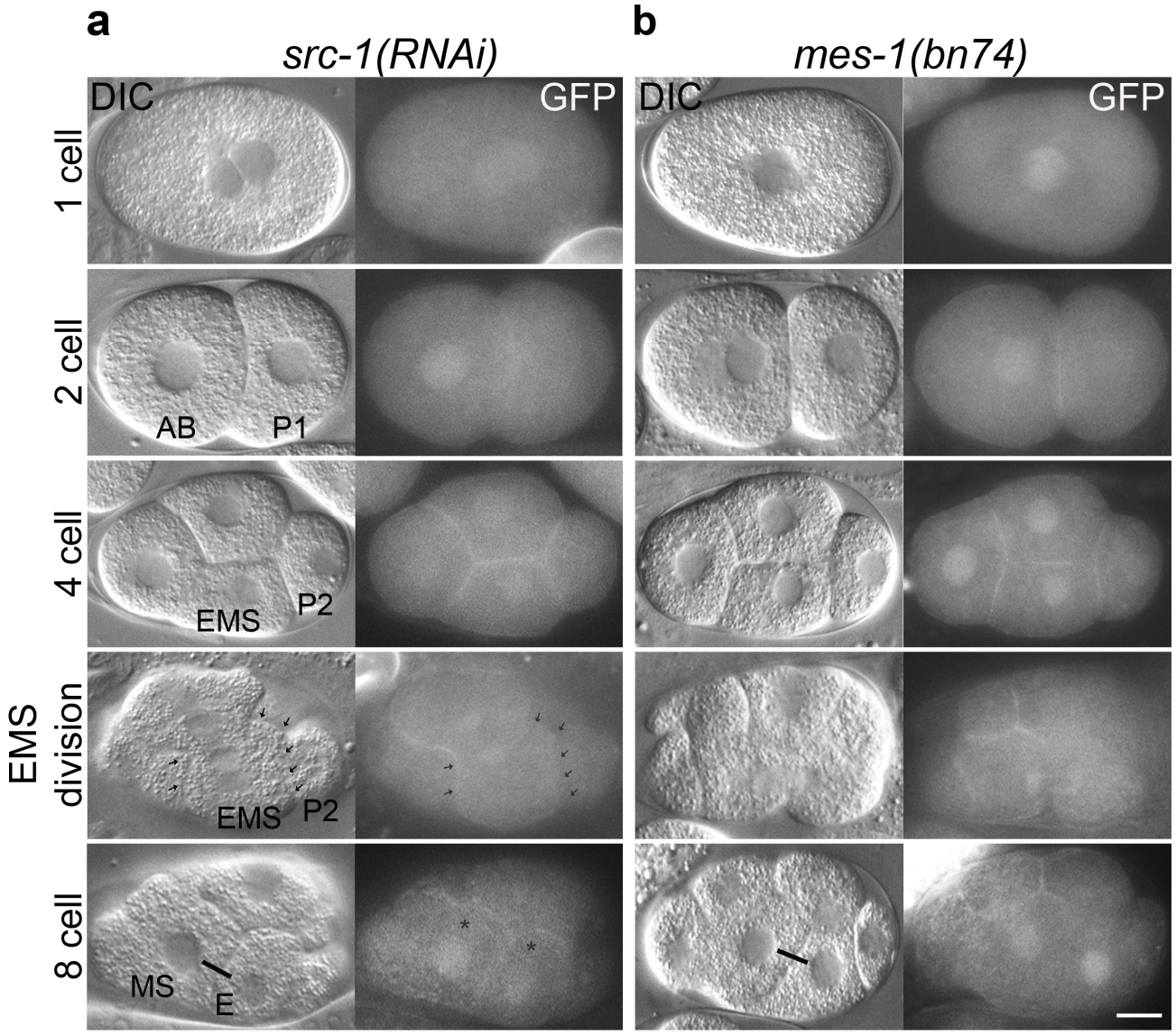

Figure 25. SRC-1 contributes to the localization of WRM-1.

Nomarski (DIC) and fluorescence (GFP) micrographs of representative transgenic embryos, as indicated. In (**a**), black arrows indicate retention on the EMS cortex, asterisks indicate symmetric nuclear accumulation in MS and E. Cortical and nuclear localization of WRM-1 is partially

defective in *src-1(RNAi)* embryos, while *mes-1(bn74)* embryos in (**b**) do not show any defects in WRM-1 localization.

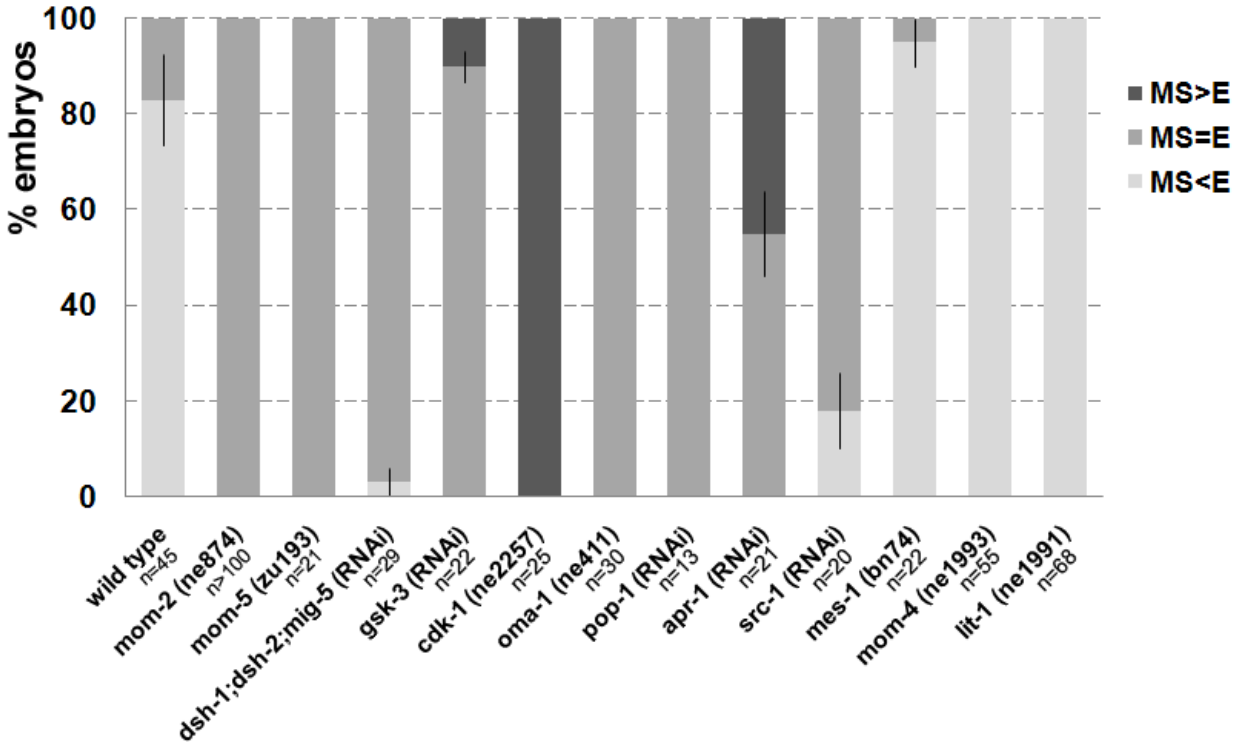

Figure 26. Genetics of the nuclear WRM-1 asymmetry between the E and MS blastomeres in 8-cell embryos.

Graphic representation showing the percentage of embryos in 3 phenotypic categories: nuclear level in MS is higher than that in E (MS>E), nuclear level in MS is equal to that of E (MS=E), nuclear level in MS is lower than that in E (MS<E). Genotypes and the number of embryos scored are indicated at the bottom of each bar graph. The error bars indicate standard deviation.

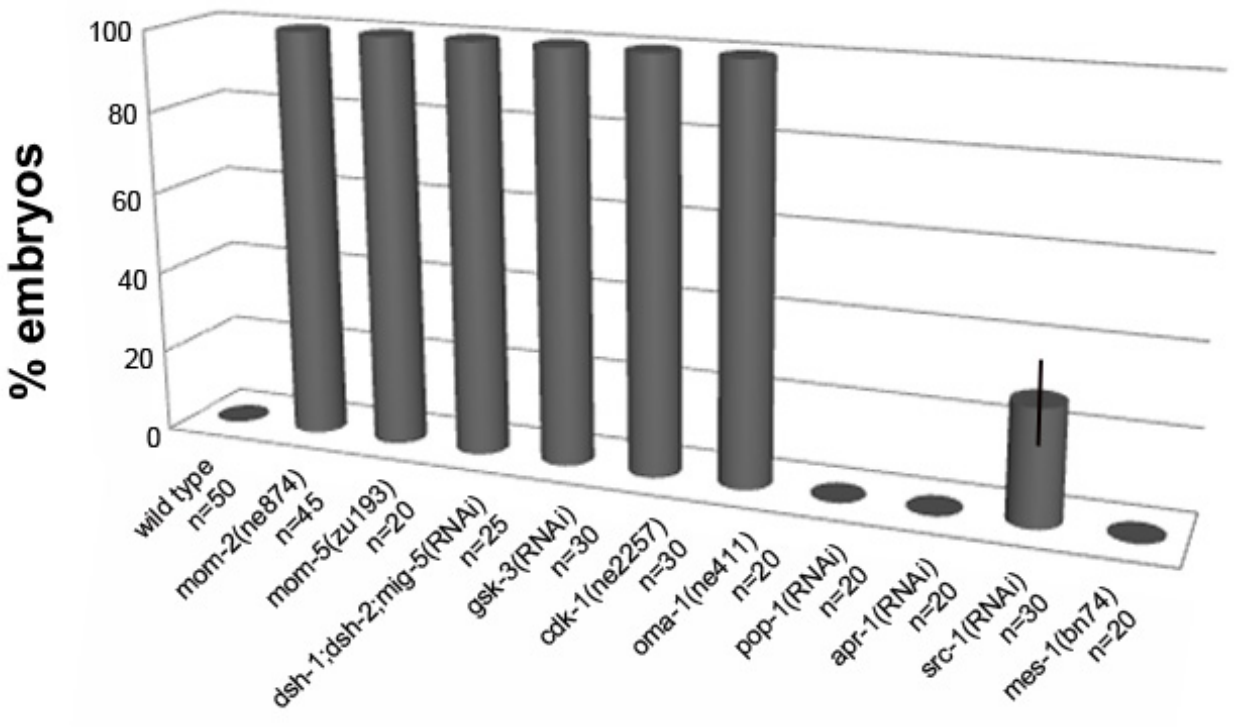

Figure 27. Genetics of the cortical WRM-1 asymmetry during EMS division.

Graphic representation showing the percentage of embryos defective in releasing the cortical WRM-1 from the posterior cortex during EMS cell division. Genotypes and the number of embryos scored are indicated at the bottom of each bar graph. The error bar shows standard deviation.

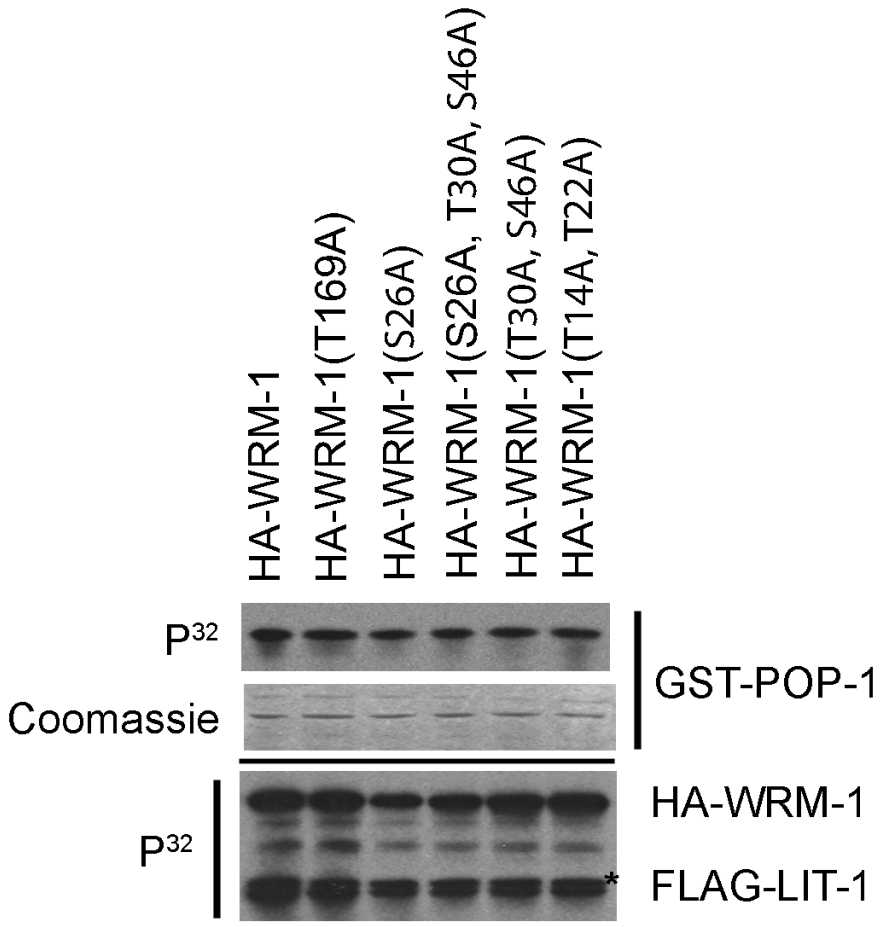

Figure 28. *In vitro* LIT-1 kinase assay using various WRM-1 mutations.

293T cells were transfected with FLAG-LIT-1 expression plasmid and HA-WRM-1 expression plasmids harboring various mutations affecting the phosphorylation sites of GSK-3 (S26), CDK-1 (T30, S46) and potential MAP Kinase sites (T14, T22 and T169) as indicated on top. FLAG-LIT-1/HA-WRM-1 complexes were pulled down from the cell lysate with anti-FLAG antibody conjugated beads and used in kinase assay against GST-POP-1(1-188) protein. Phosphorylated

GST-POP-1 protein is recovered from the kinase reactions and analyzed by SDS-PAGE followed by autoradiography (top panel), while anti-FLAG immunoprecipitates were analyzed for HA-WRM-1 and FLAG-LIT-1 complex formation and autophosphorylation (bottom panel). Asterisk indicates phosphorylated GST-POP-1 protein carried over from the kinase reaction. These kinase sites are neither required for HA-WRM-1 to bind to LIT-1, nor for the kinase activity of the WRM-1/LIT-1 complex.

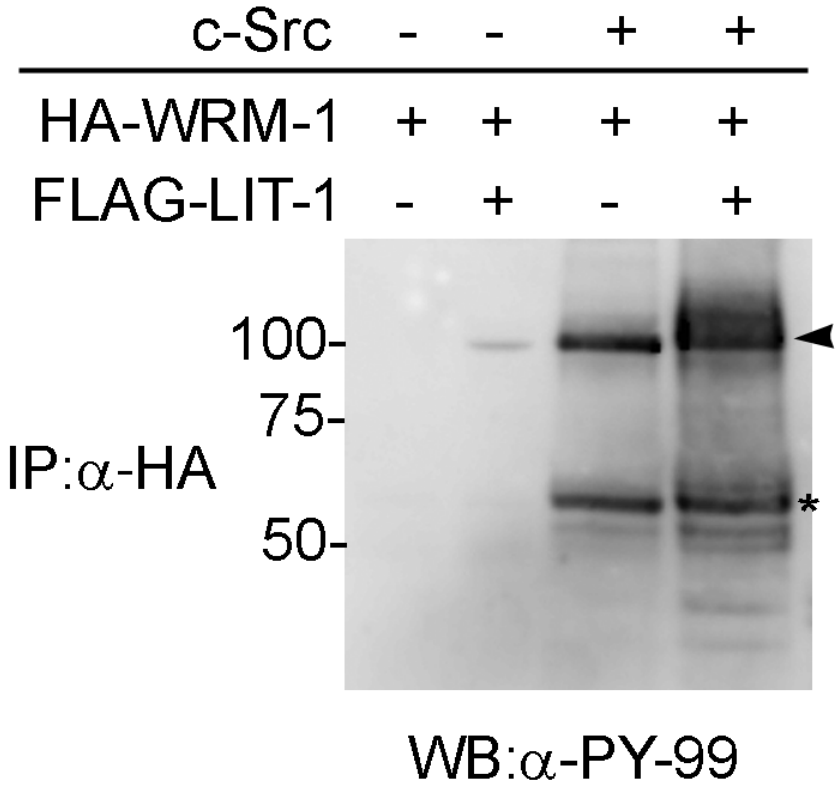

Figure 29. *In vitro* Src kinase assay using HA-WRM-1.

293T cells were transfected with HA-WRM-1 expression plasmid with or without FLAG-LIT-1 expression plasmid. HA-WRM-1 was then immunoprecipitated from the cell lysate and incubated with ATP with or without recombinant Src as indicated. Tyrosine phosphorylation of HA-WRM-1 was detected by western blot analysis using the phospho-tyrosine specific antibody PY99 (Santa Cruz). Arrowhead indicates tyrosine phosphorylated HA-WRM-1 while asterisk indicates autophosphorylated Src.

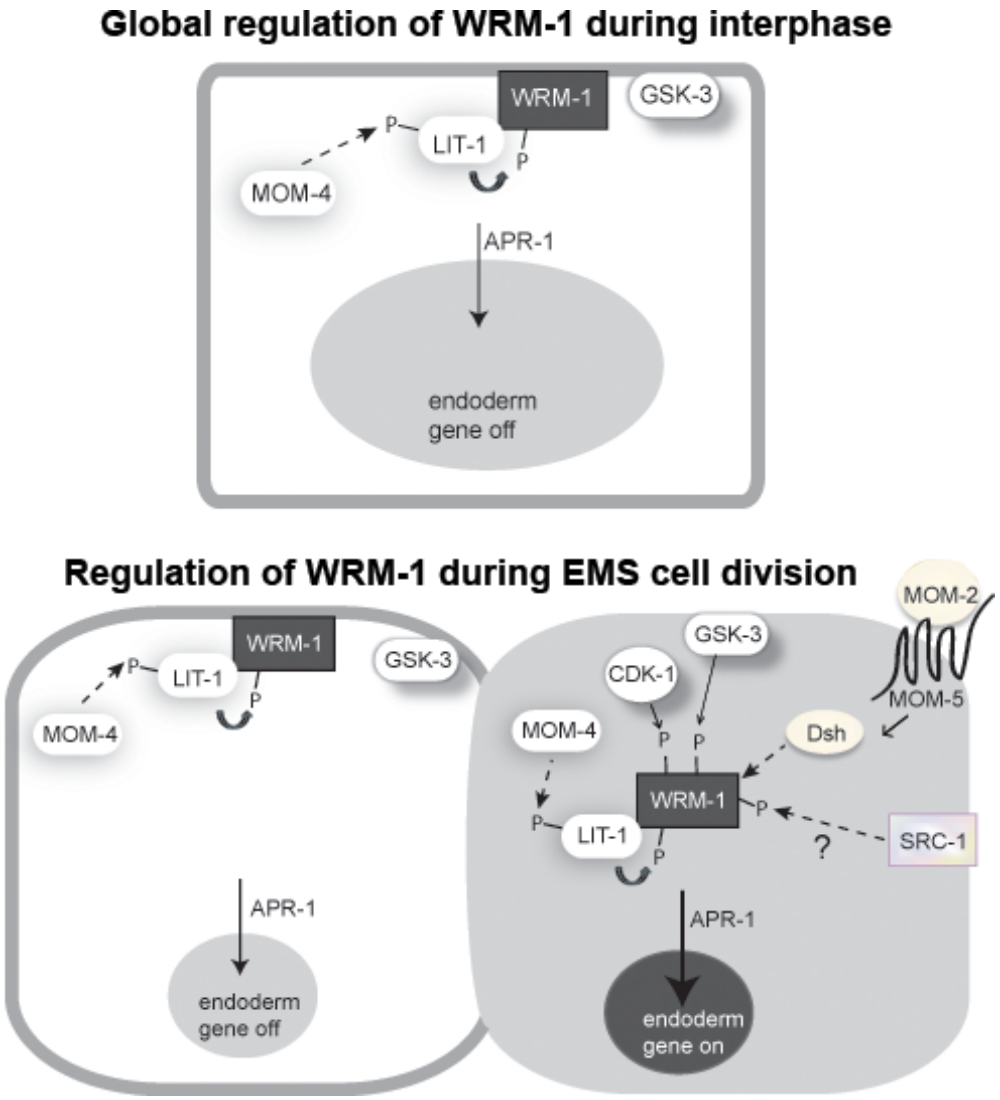

Figure 30. Working model describing how the localization of WRM-1 is regulated by the LIT-1, CDK-1 and GSK-3 kinases.

WRM-1 is localized to the cell cortex and nuclei throughout early embryonic cells. The MAPK-like pathway components MOM-4 and LIT-1 are required for cortical localization of WRM-1 in

all early cells. At the 4-cell stage, the EMS cell receives the inductive signal comprised of Wnt and Src signals from P2. However, WRM-1 remains at the cortex until the EMS cell starts to divide. During EMS cell division, CDK-1 and GSK-3 sequentially phosphorylate WRM-1 to release it from the posterior cortex of the EMS cell and regulate its nuclear localization. A subset of GSK-3 is constitutively localized to the cell cortex at all cell-cell contact sites. Gray shades indicate the level of WRM-1, with darker shades representing higher levels.

CHAPTER III

A potential connection between the Wnt signaling pathway and the translational machinery in *C. elegans*

Contributors to the work presented in Chapter III:

The author of this thesis, Soyoung Kim, mapped and cloned *ifg-1*, one of the extragenic suppressors of *mom-2*/Wnt, and performed its genetic analyses presented in this Chapter.

Tuba Bas and Takao Ishidate conducted suppressor screens of *mom-2*/Wnt, and isolated three extragenic and five intragenic suppressors.

Rita Sharma helped constructing genetic doubles and sequencing experiments.

Abstract

The highly conserved Wnt/Wingless family of secreted proteins regulates many aspects of animal development. In 4-cell stage *Caenorhabditis elegans* embryos Wnt signaling specifies endoderm by controlling the fate of EMS blastomere daughters. To identify additional regulators of the Wnt/Wingless signaling pathway in endoderm specification, suppressor genetic screens utilizing two temperature-sensitive alleles of *mom-2*/Wnt were carried out. Among 20 million chromosomes screened, five intragenic and three semi-dominant extragenic suppressors were isolated. Here we report an identification of one extragenic suppressor as an allele of *ifg-1,* a homolog of eukaryotic translation initiation factor *eIF4G*. The allele *ifg-1(ne4271)* is associated with a substitution, arginine 745 to cysteine, at a highly conserved residue in the middle third domain essential for the translational activity. Genetic analyses using the *ifg-1* deletion allele and *ifg-1*(RNAi) indicate that *ifg-1(ne4271)* acts as loss-of-function for suppressing the *mom-2* phenotype. Furthermore we show that *ifg-1(ne4271)* suppresses other mutants in the pathway such as *wrm-1*/β-catenin, *lit-1*/MAPKKK, NEMO, and *mom-4*/MAPK, suggesting it functions downstream of these molecules. Our result implies a potential connection between the Wnt signaling pathway and the translational machinery.

Introduction

In *C. elegans,* the Wnt signaling pathway acts very early in development to specify endoderm tissue (Rocheleau et al., 1997; Thorpe et al., 1997). In 4-cell stage embryos signaling from the posteriormost P2 blastomere polarizes the EMS cell to produce one of the daughter cell, the endoderm founder cell E. In the absence of P2/Wnt signal, E adopts the fate of the other EMS daughter, the MS blastomere, and develops the mesodermal tissues instead of endoderm.

Genetic screens and studies using RNA-mediated genetics interference (RNAi) have identified genes involved in P2/EMS signaling. Several of these genes define the components of the conserved Wnt/Wg signaling pathway, including *mom-1* (Porcupine), *mom-2* (Wnt/Wg), *mom-5* (Frizzled), *sgg-1 (gsk-3)*, *wrm-1* (β-catenin/Armadillo), *apr-1* (adenomatous polypopsis coli, APC), and *pop-1* (TCF/LEF) (Lin et al., 1995; Rocheleau et al., 1997; Thorpe et al., 1997). Genetic studies also indicate that other signaling mechanisms contribute to the endoderm specification including the MAP kinase signaling factors, *mom-4*(TAK1, MAP kinase kinase related) and *lit-1* (Nemo, MAP kinase related) (Ishitani et al., 1999; Meneghini et al., 1999; Rocheleau et al., 1999; Shin et al., 1999), and the Src-signaling pathway (Bei et al., 2002).

Despite the discovery of these components, how Wnt signaling is precisely regulated is still not completely understood.

To gain further insights into the mechanisms that govern Wnt signaling in the early *C. elegans* embryos to specify endoderm tissue, we searched for more components using a suppressor genetic screening of the temperature-sensitive (Ts) alleles of *mom-2*/Wnt. We designed a genetic suppressor screen for maternal-effect mutations that would rescue embryos of *mom-2(ne874, ne834)* to viability. Suppressors were extremely rare, and we could isolate only five intragenic and three extragenic suppressors among 20 million chromosomes screened. We identified one extragenic suppressor with a point mutation in the gene *ifg-1,* a homolog of eukaryotic translation initiation factor *eIF4G* that plays an important role in translation. We show that the semi-dominant suppressor *ifg-1(ne4271)* is a loss-of-function allele, and functions downstream of *lit-1*/MAPKKK, NEMO and *wrm-1*/β-catenin. Our results have provided new insight into the function of Wnt signaling in endoderm specification, suggesting an involvement of the translational machinery in the biological functions of Wnt signaling in early *C. elegans* embryos.

Results

Isolation of maternal-effect suppressors of *mom-2*/Wnt

To screen for *mom-2* suppressors, we utilized two *mom-2*/Wnt Ts alleles, *ne834* and *ne874*, which were among five alleles of *mom-2* isolated in the previous large scale Ts screening (Figure 31 and Figure 32) (Nakamura et al., 2005). The mechanics of the screen were straightforward, as the assay looked for viable embryos at non-permissive temperature 25°C. After the parent hermaphrodites (P0) of *mom-2(ne834, ne874)* were mutagenized using ENU (N-**E**thyl-N-**N**itroso**u**rea), we looked for suppressors in F1 generation to obtain dominant suppressors, and in F2 generation for recessive ones (Figure 33).

From *ne834* screening, we were unable to find any suppressors in the F1 generation. However, we isolated three suppressors (*TT10, TT11, TT12*) among one million F2 worms. In *ne874* screening, we recovered five independent suppressors (*TT1, TT2, TT3, TT4, TT5*) in F1 screening among five million worms, and none in F2 generation (Table 2). Isolated suppressors showed weak suppression rate at 25 ^{0}C, about 5% in viability, and we did not isolate any stronger

ones in this screening. When we lowered the temperature to 24 or 23 ^{0}C, we saw significant increase in the suppression rate (Table 3).

To determine the chromosomal locations of the suppressors, we used linkage analysis combined with SNP (**S**ingle **N**ucleotide **P**olymorphism) mapping method. The results showed that five suppressor strains from the *ne874* screening contained the mutations that were tightly linked to *mom-2*. We further mapped other suppressors which did not appear to be linked to *mom-2* to determine their approximate chromosomal locations. It appeared that *TT10* is located far from the center of chromosome II, *TT11* is on chromosome X, and *TT12* on the center of chromosome II. Also we were able to determine if the suppressors function in a dominant or recessive manner during these initial mapping procedures. We show that *TT10*, *TT11* and *TT12* are weak dominant suppressors (semi-dominant) (Figure 34).

Identification of intragenic suppressors of *mom-2(ne874)*

When we performed the linkage analysis on chromosome V where *mom-2* is located, we found that five suppressors (*TT1, TT2, TT3, TT4, TT5)* from *ne874* screen were tightly linked to the *mom-2* locus and could not be separated. To see if they were intragenic suppressors, we sequenced the *mom-2* locus in these five strains, and found a second site mutations in all of them

(Figure 35). Interestingly, we found that *TT4* has a substitution in cysteine 167 to tyrosine, which is the same mutation as that of another Ts *mom-2* allele *ne834.* And *TT5* has two amino acid substitutions in methionine 235 and aspartic acid 239.

***TT12* is associated with an R745C substitution in *ifg-1*/eIF4G**

Linkage and SNP analyses showed that *TT12* was located around the center of chromosome II. To perform three-factor SNP mapping, we constructed a strain with *unc-83(e1414*) and *rol-1(e19)* in the *mom-2(ne834)* genetic background, which covers the location on chromosome II from -2.98 to 6.65. After crossing this mapping strain with *TT12* males, we isolated the recombinants in F2 generation, and tested for the suppression of *mom-2(ne834)* and checked SNP loci to narrow down the location of the suppressor. We tested approximately 700 recombinants and were able to locate *TT12* in 9 cosmids interval from T05H10 to Y1E3A on chromosome II which contains approximately 30 genes.

We decided to sequence the candidate genes to find a mutation, and were able to find a point mutation in *ifg-1,* a homolog of eukaryotic translation initiation factor *eIF4G* (Figure 36). The *ifg-1(ne4271*) allele has a substitution in highly conserved arginine 745 to cysteine in the

eIF4A and eIF3 binding domain. This mutation will be further discussed later in this chapter (See Discussion).

ifg-1(ne4271) is a loss-of-function allele

To find out how *ifg-1* functions to suppress the *mom-2* phenotype, we conducted two experiments. First, *ifg-1* dsRNA was injected into *mom-2(ne834)* worms to see if its embryonic lethal phenotype could be rescued. It appears that the injection of diluted dsRNA (1000 fold dilution of 1 ug/ul) rescues *mom-2(ne834)* embryos to viability, suggesting that *ifg-1(ne4271)* is likely to act in a loss-of-function manner in rescuing the *mom-2* phenotype (Table 4). Second, we obtained the deletion allele *ifg-1(ok1211)* from CGC (**C**aenorhabditis **G**enetics **C**enter), and checked if *ifg-1(ok1211) /* + and *ifg-1(ok1211) / ifg-1(ne4271)* would rescue *mom-2(ne834)* embryos. Consistent with the RNAi experiment above, both *ifg-1(ok1211) /* + and *ifg-1(ok1211) / ifg-1(ne4271)* were able to suppress *mom-2(ne834)* embryos to viability (Table 4). These two experiments show that *ifg-1(ne4271)* acts in a loss-of-function manner.

ifg-1(ne4271) suppresses other Wnt signaling pathway mutants

As mentioned above, there are five Ts alleles of *mom-2*, and wanted to see if *ifg-1(ne4271)* rescues other *mom-2* alleles other than *mom-2(ne834)*. A genetic double between *mom-2(ne874)* and *ifg-1(ne4271)* was made and the suppression was scored. We found that *ifg-1(ne4271)* also suppresses *mom-2(ne874),* which implies that it acts as a non-allele specific suppressor (Table 5).

We further tried to determine whether *ifg-1(ne4271)* suppresses other Wnt signaling pathway mutants. Suppression was tested in *wrm-1(ne1982)*, *lit-1(ne1991)*, *mom-4(ne1539)* mutant embryos in the *ifg-1(ne4271)* genetic background. As shown in Table 5, *ifg-1(ne4271)* was able to suppress all of them to viability, suggesting that it is likely to function downstream of these components.

Discussion

Wnt proteins are secreted glycoproteins that play essential roles during embryonic development. Extensive genetic screens in the Wnt pathways of *Drosophila* and *C. elegans* have identified many components of this pathway such as Wnt, Frizzed/LRP, Axin, GSK3, APC, β-

catenin, and TCF/LEF. However, as a result of the complexity of the phenotype and potential crosstalk with other pathways, some pathway regulators will likely not give an obvious *wnt*-related phenotype in the context of the entire organism. In order to identify new Wnt pathway regulators, DasGupta *et al*. used a genome-wide RNAi screening in *Drosophila* to identify 238 candidate regulators of the Wnt signaling pathway, most of which had not been previously connected to Wnt signaling (DasGupta et al., 2005).

In this study, to find additional components of the Wnt/Wingless signaling pathway to specify the endoderm tissue in *C. elegans*, we performed suppressor genetic screens using the Ts alleles of *mom-2*/Wnt, and identified 8 new potential regulators in the Wnt signaling pathway. We molecularly characterized the new loci and found that five of them were intragenic suppressors, and the locus of one extragenic suppressor corresponded to *ifg-1*, which encodes the eukaryotic translation initiation factor eIF4G. We discuss the possible roles of eIF4G and the translational machinery in the Wnt signaling pathway in *C. elegans*.

Intragenic suppressors

Within the same gene, intragenic suppressors have second mutations that restore function of the original mutant gene products. In our suppressor screening using *mom-2(ne874)*, we

identified five intragenic suppressors (*TT1, TT2, TT3, TT4, TT5*). Interestingly *TT4* turned out to have a second site mutation in the residue which is the same mutation of the Ts allele *mom-2(ne834)* (C167Y), suggesting that *mom-2(ne834)* itself acts as a suppressor of *mom-2(ne874)* (C139Y) in an allele specific manner. This implies that the cysteine residues at position 139 and 167 interact with each other.

High proportion of the conserved cysteine residues in Wnt proteins suggests that they may be critical determinants of the final structure of the proteins, most likely through the formation of the intramolecular disulfide bonds. Since Wnt proteins have been shown to be highly hydrophobic and insoluble, making them extremely difficult to isolate and characterize, these intragenic suppressors may help understand their structural aspects *in vivo*.

Identification of the eukaryotic translational initiation factor *eIF4G* as a suppressor of *wnt*

In a suppressor screen using *mom-2(ne834)*, we isolated an allele of gene *eIF4G* as a semi-dominant suppressor of the *wnt* phenotype. The eukaryotic initiation factor eIF4G is a large modular protein which serves as a docking site for the initiation factors and proteins involved in RNA translation. Together with eIF4E and eIF4A, eIF4G constitutes the eIF4F complex which is

a key component in promoting ribosome binding to mRNAs. Thus, the central role of eIF4G in initiation makes it a valid target for events aimed at modulating translation.

eIF4G has been isolated and cloned from many different species including yeasts *S. cerevisiae* and *S. pombe* (Goyer et al., 1993), *Drosophila* (Zapata et al., 1994), wheat (Browning, 1996), and human (Gradi et al., 1998; Yan et al., 1992). In *C. elegans*, two splice-variants of eIF4G, encoded by *ifg-1*, have been identified (Kamath et al., 2003; Long et al., 2002). The eIF4G proteins of *C. elegans* and human exhibit moderate sequence conservation but share similar overall biochemical activities.

The mammalian eIF4GI may be divided into three regions; an amino-terminal one-third, which contains the poly(A) binding protein (PABP) and eIF4E binding sites; a middle third, which binds eIF4A and eIF3; and a carboxy-terminal third, which harbors a second site eIF4A binding site and a docking sequence for the Ser/Thr kinase Mnk1 (Morino et al., 2000) (Figure 36A). The mutation in *ifg-1 (ne4271)* has a substitution of the residue arginine conserved in all species by cysteine at position 745. This point mutation lies in the middle third, eIF4A and eIF3 binding domain, which has been shown to be necessary for the cap-dependent translation (Morino et al., 2000).

A mutational analysis was done in some of the conserved residues in this domain to determine their roles in binding to eIF4A or eIF3 in human eIF4GI (Morino et al., 2000). It has been shown that the residues Q533, K610, and F720 have no effects on binding eIF4A or eIF3, but Y273, F650, and F736 abolishes eIF4A binding but not eIF3. The role of R745 where *ifg-1 (ne4271)* has a mutation has not been addressed yet. Therefore it will be interesting to see if the mutation changes binding to either eIF44A or eIF3, and/or disrupt the function of the translation initiation complex eIF4F.

Novel regulator of the Wnt signaling pathway

The finding of a key protein of a basal cellular mechanism such as the translational machinery component, eIF4G, as a suppressor of *mom-2* mutant was unexpected since the direct relation between the Wnt pathway and the translational machinery has not been reported. However, recently, similar unusual functions of the translational machinery components have been identified in many cellular events. Li *et al* isolated eIF4A, a component of the eIF4F complex as a suppressor of *dpp*, a member of the superfamily of TGFβ (**T**ransforming **G**rowth **F**actor β) in *Drosohpila* (Li et al., 2005). Furthermore, they showed that eIF4A acts as a specific inhibitor of Dpp signaling, and mediates the degradation of Smad homologs for signal activation

(Li and Li, 2006). Both human and *Drosophila* eIF4A-III are a part of the exon-junction complex that is formed during mRNA splicing (Ferraiuolo et al., 2004; Shibuya et al., 2004). In mammals, the resulting complex is essential for nonsense-mediated mRNA decay. Strikingly, eIF4A-III is also essential for the proper localization of oskar mRNA in the *Drosophila* embryos (Palacios et al., 2004).

Although we need to conduct more investigations to elucidate the mechanism underlying the connection between eIF4G and the Wnt signaling pathway, currently several possibilities exist to explain their link. First, negative regulators of Wnt signaling may be more sensitive to the IFG-1 level. For example, it is possible that *ifg-1(ne4271)* may act to reduce the POP-1 level since the heterozygote of hypomorphic *pop-1* allele rescues the *mom-2* phenotype (Table 6). Second, eIF4G itself may have a novel function as a negative regulator of the Wnt signaling pathway. Third, the Wnt signaling pathway may directly regulate the translational machinery, for example, by phosphorylating the components of translational machinery. Finally, eIF4G could function completely independently of the Wnt signaling pathway, yet the two pathways converge on the same targets with the opposing effects.

As a conclusion, we isolated a component of translational machinery *ifg-1* as a suppressor of the Wnt signaling pathway in *C. elegans* gut development. Our data suggests an intriguing

connection between the Wnt signaling pathway and the translational machinery, although more experiments are necessary to elucidate underlying mechanism.

Materials and Methods

Genetics and Strains

All strains were handled and cultured as described previously (Brenner, 1974). Mutant strains used were: *mom-2(ne834)* (V), *mom-2(ne874)* (V), *mom-4(ne1539)* (I), *wrm-1(ne1982)* (III), *lit-1(ne1991)* (III), VC778 *ifg-1(ok1211)/mIn1[mIs14 dpy-10(e128)]* (II).

ENU mutagenesis screen for suppressors of *mom-2(ne834, ne874)*

The Ts alleles of *mom-2(ne834, ne874)* in the background of the Hawaiian CB4856-derived *lin-11(ne832)* egg-laying deficient strain (WM59) were used for the suppressor screens. L4 animals mutagenized with ENU (N-**E**thyl-N-**N**itroso**u**rea) were grown at 15°C. Half of F1 progenies were shifted to 25 °C at the L4 stage to look for the F1 dominant suppressors, and the other half was maintained to produce F2 progenies. F2 animals at the L4 stage were shifted to 25°C for screening the F2 recessive suppressors.

RNAi assays

RNAi was performed as described previously by injecting dsRNA (Bei et al., 2002). The *ifg-1* dsRNA was prepared from a full length genomic DNA. Embryos collected 24 hr after injection were scored for phenotypes at the appropriate temperature.

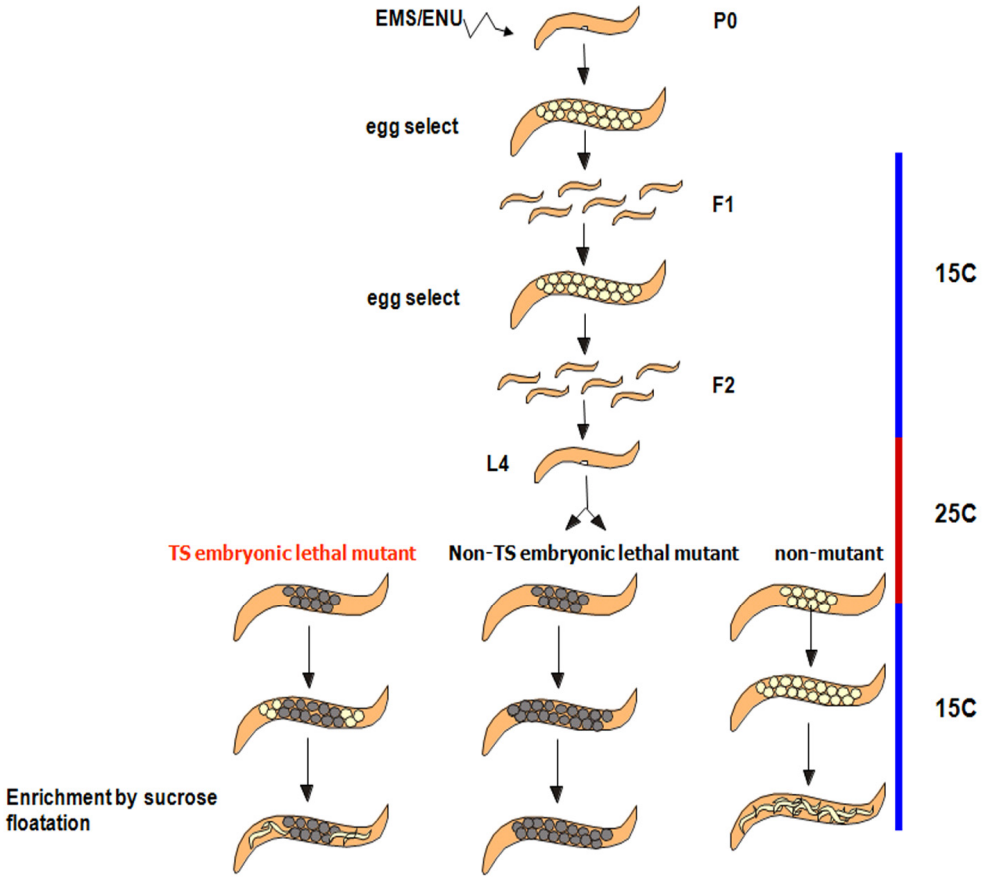

Figure 31. Scheme of temperature-sensitive screening for maternal-effect embryonic lethal mutants.

P0 *lin-11* Hawaiian (CB4856) animals were mutagenized by ENU (N-**E**thyl-N-**N**itroso**u**rea) or EMS (**E**thyl **M**ethane **S**ulfonate). After growing them at permissive temperature (15°C), the F2 L4 stage animals were shifted up to 25°C for 27 hrs then downshifted to 15°C for 18 hrs more. The population is then briefly hypochlorited to kill all hatched larvae and adults so that dead

embryos made at 25°C and viable embryos made after the shift down remain trapped together in the mothers' uterus. The carcasses are then floated in 50% sucrose solution where adults filled with inviable or unhatched eggs remain floating in a band at the top. Candidate Ts mutant were then identified by looking for viable L1 larvae bracketing a collection of dead eggs. Candidate mutants were retested for Ts embryonic lethal and phenotypes analyzed (Pang et al., 2004).

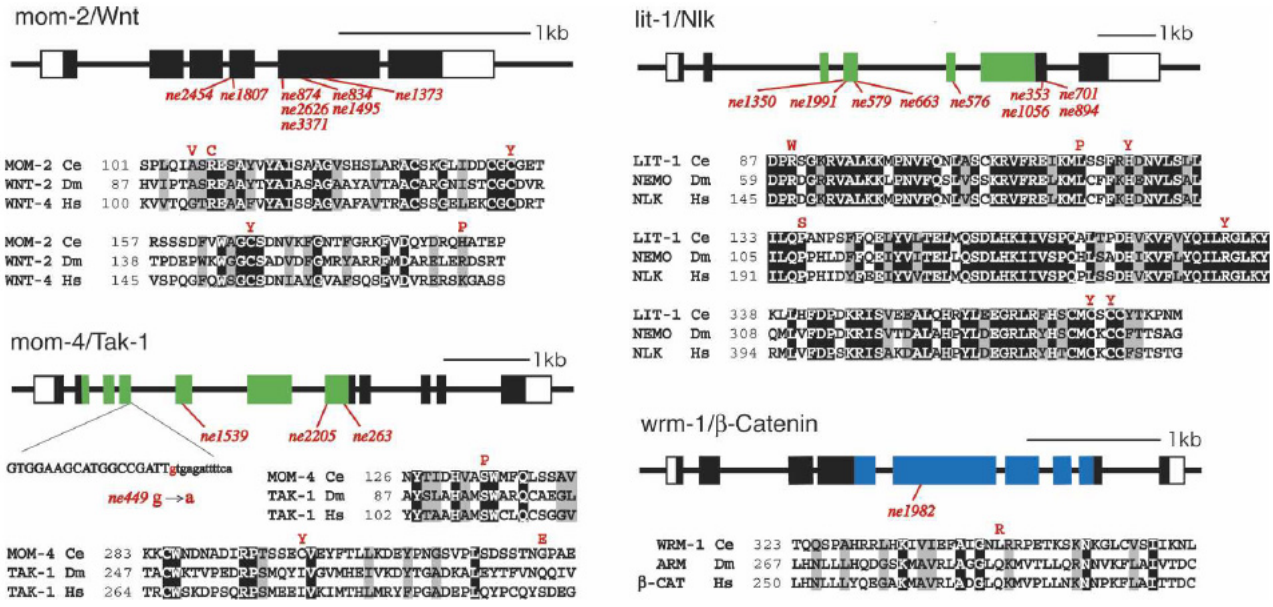

Figure 32. Temperature-sensitive (Ts) mutants defective in P2/EMS signaling.

Schematic diagrams and alignments for 4 P2/EMS signaling genes. Ts-genetic lesions and their allele names are shown below the genomic box/line-exon/intron structures. Alleles with identical lesions are indicated together in columns. In *mom-4* and *lit-1*, the kinase domains are indicated in green; in *wrm-1*, the arm-motif region is indicated in blue. White and black boxes indicate noncoding and coding regions, respectively. A splice donor site lesion is indicated below the structure of *mom-4* with the intron sequence shown in lower case. Amino acids substitutions for each distinct lesion are shown in red type above alignments for the corresponding region in each protein. The alignments compare each *C. elegans* (Ce) protein to *Drosophila melanogaster* (Dm) and *Homo sapiens* (Hs) homologs, as indicated (Nakamura et al., 2005).

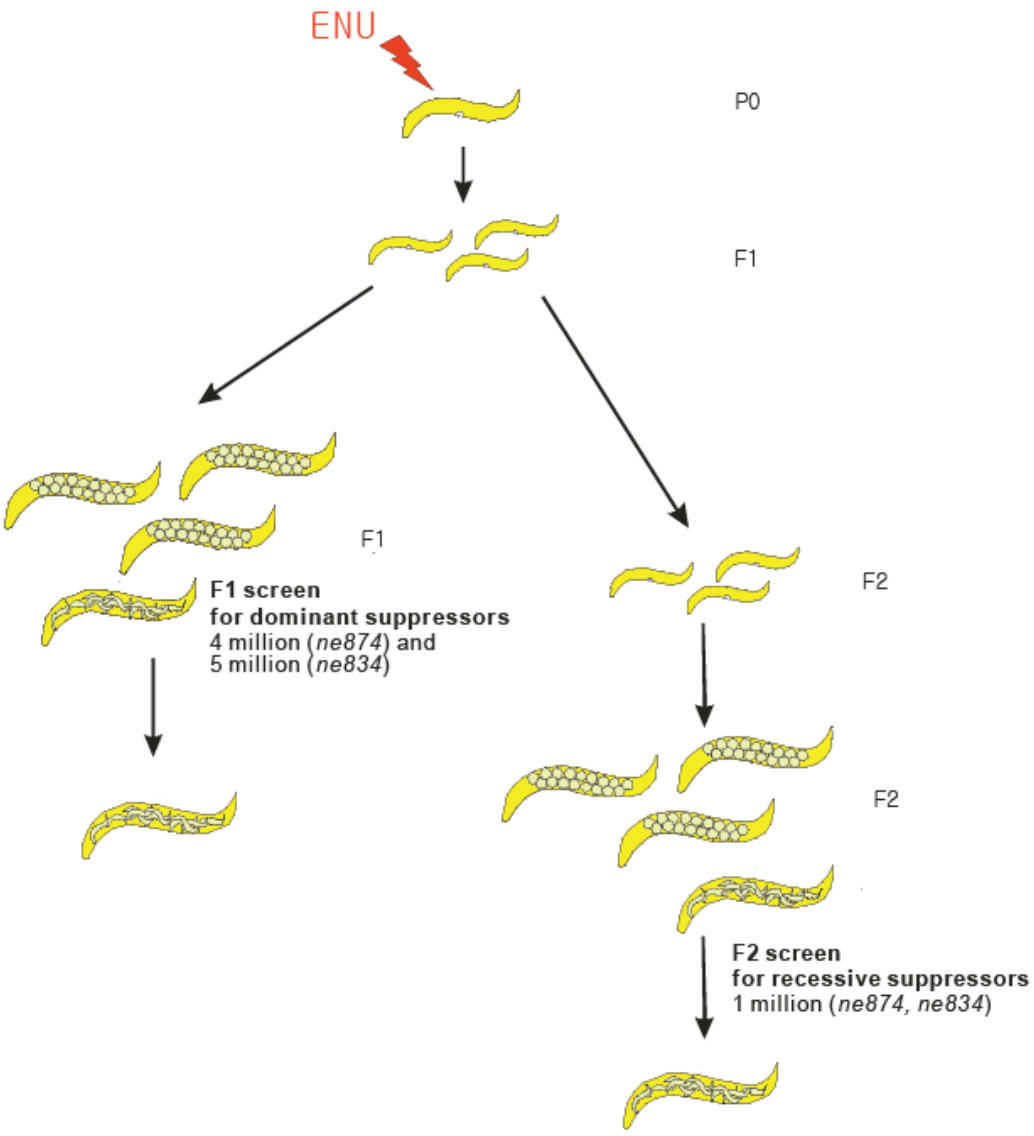

Figure 33. Schematic diagram of the screen for maternal-effect suppressors of *mom-2*/Wnt.

P0 *mom-2(ne834 and ne874)* animals in *lin-11* Hawaiian (CB4856) background were mutagenized by ENU (N-**E**thyl-N-**N**itroso**u**rea). After growing at permissive temperature (15°C), the F1 L4 stage animals were shifted to 25°C for 27 hrs then screened for worms with viable

embryos, F1 suppressors. For F2 suppressors, the F2 L4 stage animals were shifted to 25°C for 27 hrs to look for animals with viable embryos inside the mother worms. See Table 2 for the results of these suppressor screens.

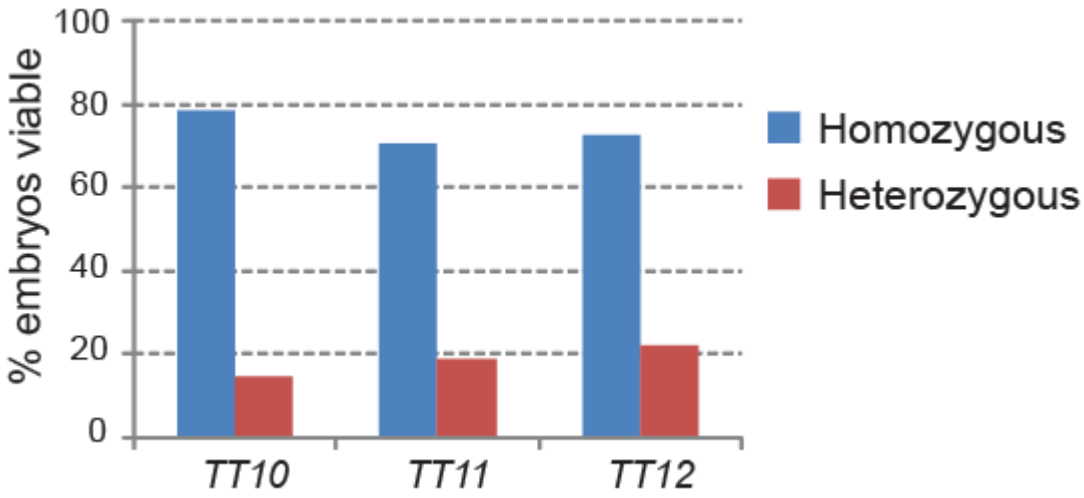

Figure 34. Three extragenic suppressors are weak dominant.

Suppression rate on *mom-2(ne834)* is shown when the suppressors are homozygous or heterozygous for their loci.

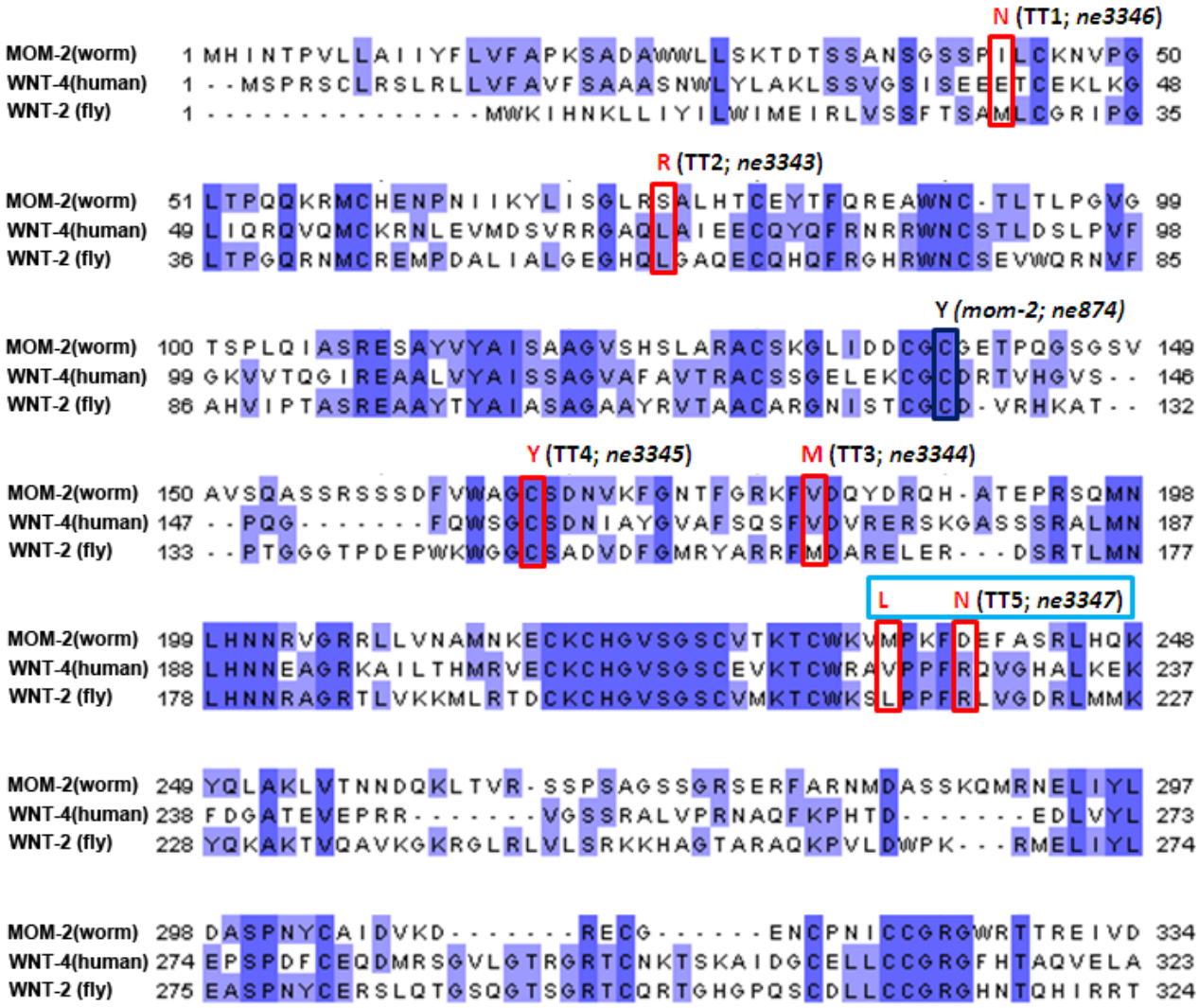

Figure 35. The intragenic suppressors of *mom-2(ne874).*

Partial amino acid alignments of homologs of *mom-2*. Amino acid substitutions for each distinct lesion for intragenic suppressors are shown in red box and characters. The *mom-2(ne874)* mutation is marked in black box and characters. The green box indicates two amino acid

substitutions in *TT5(ne3347)*. Conserved residues are shaded, with the darker shade represents the fully conserved residues.

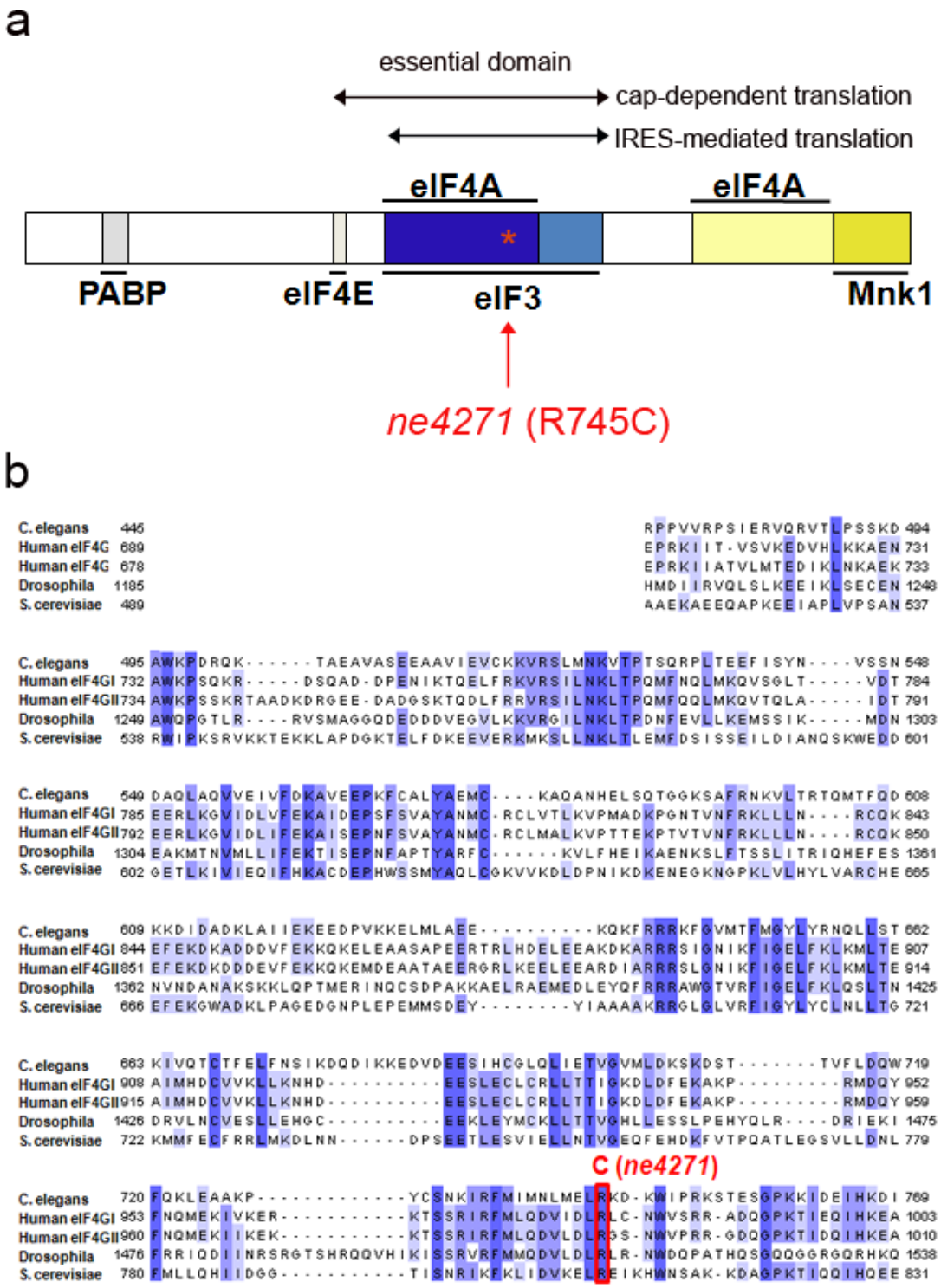

Figure 36. Identification of *ifg-1*, a homolog of *eIF4G* as a suppressor of *mom-2(ne834)*

a, Structure of eIF4G is displayed. Domains of interactions among eIF4GI and eIF4A (Lomakin et al., 2000; Morino et al., 2000), eIF3 (Korneeva et al., 2001), Mnk1 (Morino et al., 2000), and PABP and eIF4E (Gingras et al., 1999) are shown. *TT12 (ne4271)* has a single amino acid change at position 745 from arginine (R) to cysteine (C) in the middle essential domain for translational function and binding eIF4A and eIF3. **b**, Amino acid alignments of the highly conserved region of the middle essential domain. The red box and the characters show the mutation in *ifg-1(ne4271)*.

Suppressor	screen	Number of worms screened	Chromosomal location
TT1(ne3346)	*ne874* F1 screen	4 millions	V
TT2(ne3343)	*ne874* F1 screen	4 millions	V
TT3(ne3344)	*ne874* F1 screen	4 millions	V
TT4(ne3345)	*ne874* F1 screen	4 millions	V
TT5(ne3347)	*ne874* F1 screen	4 millions	V
TT10	*ne834* F2 screen	1 million	V
TT11	*ne834* F2 screen	1 million	X
TT12	*ne834* F2 screen	1 million	II

Table 2. Isolated suppressors from the *ne874* and *ne834* screens.

From the *ne874* F1 screen, we isolated five independent suppressors linked to the chromosome V. From the *ne874* screen, three independent suppressors, *TT10*, *TT11*, and *TT12* were mapped to the chromosomes V, X, and II, respectively.

Allele	Homozygous viability	Suppression at 23°C (%)	Suppression at 24°C (%)	Suppression at 25°C (%)
TT10	viable	70.1 ± 10.2	9.5 ± 5.3	3.5 ± 2.1
TT11	viable	65.3 ± 20.8	7.8 ± 6.5	4.5 ± 3.8
TT12	viable	72.6 ± 15.8	11.9 ± 4.8	3.3 ± 3.1

Table 3. Suppression rate of three extragenic suppressors.

By lowering temperature by 1 or 2°C, the suppression rate on *mom-2(ne834)* increases significantly. Results are presented as the average and standard deviation .

Strain	% Embryos viable (n)
ifg-1(ne4271)/ifg-1(ne4271); mom-2(ne834)/mom-2(ne834)	72.6 ± 15.8 (568)
ifg-1(ne4271)/+; mom-2(ne834)/mom-2(ne834)	21.8 ± 13.8 (550)
ifg-1(ok1211)/+; mom-2(ne834)/mom-2(ne834)	36.0 ± 10.1 (974)
ifg-1(ok1211)/ifg-1(ne4271); mom-2(ne834)/mom-2(ne834)	42.0 ± 4.8 (989)
ifg-1(RNAi) on mom-2(ne834) worms*	10.1 ± 6.0 (396)

Table 4. *ifg-1(ne4271)* functions in a loss-of-function manner.

Heterozygote for the deletion allele *ifg-1(ok1211)* suppresses *mom-2(ne834)*. Also the injection of *ifg-1* dsRNA rescues the *mom-2(ne834)* phenotype. Results are presented as the average and standard deviation .

* 1000 times diluted from standard injection concentration 1ug/ul

Strain	% Embryos viable (n)[a]	% Embryos with gut (n)[b]
mom-2(ne834)	4 (2059)	49 (168)
mom-2(ne834) ifg-1(ne4271)	74 (766)	91 (162)
mom-2(ne874)	6 (1054)	55 (120)
mom-2(ne874) ifg-1(ne4271)	78 (879)	88 (178)
wrm-1(ne1982)	0 (1556)	1 (182)
wrm-1(ne1982) ifg-1(ne4271)	18 (394)	87 (186)
lit-1(ne1991)	0 (1202)	0 (122)
lit-1(ne1991) ifg-1(ne4271)	4 (1505)	28 (80)
mom-4(ne1539)	0 (758)	11 (90)
mom-4(ne1539) ifg-1(ne4271)	32 (956)	86 (218)

Table 5. *ifg-1(ne4271)* suppresses other mutants in the Wnt signaling pathway.

The suppression rate was checked at the temperature indicated.

[a] measured at 23°C

[b] measured at 25°C

Strain	% Embryos viable (n)*
mom-2(ne834)/mom-2(ne834); pop-1(zu189)/+	17± 6 (406)
mom-2(ne834)/mom-2(ne834); +/+	5 ± 3 (978)

Table 6. Reduction of *pop-1* rescues the *wnt* phenotype.

Heterozygote for the hypomorphic allele *pop-1(zu189)* rescues *mom-2(ne834)* embryos to viability. Results are presented as the average and standard deviation .

* measured at 24 °C

Chapter IV

A genetic screen for maternal-effect suppressors of *cks-1* identifies the auto-proteolytic nuclear pore complex protein *npp-10* in *C. elegans*

Contributors to the work presented in Chapter IV:

The author of this thesis, Soyoung Kim, and Kuniaki Nakamura performed the genetic suppressor screen of *cks-1(ne549).*

Soyoung Kim mapped one of the suppressors to the locus *npp-10,* and conducted all the experiments presented in this Chapter.

Masaki Shirayama and Ji Liu helped staining embryos with the SKN-1 antibody.

Abstract

An allele of the cell-cycle regulator *cks-1* with excessive endoderm without cell-cycle related phenotypes was isolated in our maternal-effect temperature-sensitive screening. Interestingly, *cdk-1(ne236, ne2257)*, the CCCH zinc-finger protein *oma-1(zu405, ne411)*, the Dyrk family kinase *mbk-2(ne3442)*, and the deletion allele of *gsk-3* have been shown to be similar to *cks-1(ne549)* phenotypically. These mutants have an elevated level of the EMS fate determinant SKN-1, causing the fate transformation of the C blastomere to EMS-like cell. Recent genetic and molecular studies on these mutants revealed that the oocyte maturation factor OMA-1 is not degraded properly in all these mutants, causing the delayed degradation of several cell fate determinants including SKN-1. It has also been shown that MBK-2 and GSK-3 phosphorylate OMA-1 to regulate its degradation after the 1-cell stage. However, the role of CDK-1/CKS-1 complex in this pathway has not been revealed. To elucidate the function of CDK-1/CKS-1 and possible factors involved in this pathway, we carried out a genetic suppressor screen of *cks-1(ne549)*, and isolated five strong dominant suppressors. One suppressor has a mutation in *npp-10*, a homolog of vertebrate nucleoporin NUP98-NUP96 which has an auto-cleavage activity. The mutation lies in the auto-cleavage domain, resulting in a slightly disrupted auto-proteolytic

activity *in vitro*. The *npp-10(ne3744)* allele acts as loss-of-function to rescue *cks-1(ne549)*, and suppresses other extra-gut mutants. Furthermore we demonstrate that *npp-10(ne3744)* functions to reduce the SKN-1 levels to rescue the extra-gut phenotype. These results suggest that the nuclear transport of SKN-1 may be regulated by NPP-10 mediated mechanism in early *C. elegans* embryos.

Introduction

From very large-scale screens for maternal-effect embryonic-lethal mutants, a number of mutants that display excessive endoderm tissue and defects in cell polarity and cell fate specification with no obvious larval phenotypes were isolated. Genetic and molecular analyses revealed that these new mutants include one allele of the Dyrk family kinase homolog *mbk-2(ne3442)*, two gain-of-function alleles of *oma-1(ne411, ne3800)*, two alleles of the cyclin-dependent protein kinase *cdk-1(ne236, ne2257)*, and one allele of a highly conserved CDK-1 interacting protein, *cks-1(ne549)*. All these mutants are similar to the phenotype caused by depletion of the conserved protein kinase GSK-3 (Schlesinger et al., 1999).

MBK-2 is a homolog of the Dyrk family kinase, which is required for microtubule stability and spindle positioning (Pang et al., 2004; Pellettieri et al., 2003; Quintin et al., 2003). The *mbk-2(ne3442)* allele is a Ts mutant that has a mutation altering a conserved amino acid located just two amino acids away from an arginine residue required for substrate recognition in proline-directed kinases (Himpel et al., 2000). Both non Ts allele *cdk-1(ne236)* and Ts allele *cdk-1(ne2626)* have mutations in the cyclin binding region, the T loop (or activation loop). Its binding partner *cks-1(ne549)* has a mutation in the residue which forms single intra hydrogen bond. While these molecules have well known function in cell cycle regulation, the alleles of *cdk-1(ne236, ne2626)* and *cks-1(ne549)* do not show cell-cycle related phenotypes.

OMA-1 is essential for oocyte maturation and expressed in high level in oocytes and newly fertilized embryos, which is degraded rapidly after the first mitotic division (Lin, 2003). In the gain-of-function alleles of *oma-1(zu405, ne411)*, the degradation of OMA-1 is delayed (Lin, 2003; Shirayama et al., 2006). It has been shown that *cks-1(ne549)*, *cdk-1(ne236, ne2257)*, *mbk-2(ne3442)*, and *gsk-3(nr2047*) have defects in OMA-1 degradation (Shirayama et al., 2006). It was found that both MBK-2 and GSK-3 phosphorylate OMA-1 in a precisely-timed manner to regulate the degradation of OMA-1 (Nishi and Lin, 2005; Shirayama et al., 2006). The stabilized OMA-1 leads to mislocalization and stabilization of several maternal proteins important for early

fate determination including PIE-1, POS-1, MEX-1, MEX-3, MEX-5, and SKN-1 (Lin, 2003). Most importantly, delayed degradation of transcription factor SKN-1 in C blastomere is believed to be responsible for the excessive endoderm tissue since it initiates endoderm cells and other mesendodermal tissues.

CKS-1 and CDK-1 do not appear to be directly involved in the phosphorylation of OMA-1 to regulate its degradation (Shirayama et al., 2006), and precise mechanism underlying in this process has not been fully understood. To address this question, we performed a genetic suppressor screen using the *cks-1(ne549)* allele and isolated five independent dominant suppressors. Here we describe that one suppressor has a point mutation in *npp-10*, a homolog of vertebrate NUP98-NUP96 nucleoporin (NUP) precursor. Auto-proteolytic cleavage of this precursor yields two nuclear pore proteins, NUP98 and NUP96, which has been shown to be important for proper targeting of these NUPs to the nuclear pore complexes (NPCs). A point mutation in *npp-10(ne3774)* changes 811th amino acid from glutamic acid to lysine located in the proteolytic cleavage domain, which appears to disrupt this enzymatic activity weakly *in vitro*. However, we did not detect any visible defects in the structure of NPCs in *npp-10(ne3744)*.

Genetic analysis using RNAi and the deletion allele of *npp-10* showed that it acts in a loss-of-function manner. The *npp-10(ne3744)* allele suppresses other extra-gut mutants, *cdk-*

1(ne236, ne2257), *mbk-2(ne3442)*, and *oma-1(ne411)*, which suggest that *npp-10(ne3744)* functions downstream of these molecules. Consistent with this result, we found that the OMA-1 level was not affected but the SKN-1 level was reduced in the extra-gut mutants with *npp-10(ne3744)* background.

We show here one genetic approach to reveal the function of CDK-1/CKS-1 complex and to identify additional components in the OMA-1 regulation pathway. As a result, we present an identification of *npp-10(ne3744)* as a suppressor of *cks-1(ne549)*. Our general conclusion that can be drawn from this study is that the NPP-10 may play a role in the regulation of SKN-1 level in *C. elegans* early embryo.

Results

Identification of *npp-10* as a suppressor of *cks-1(ne549)* by a maternal-effect suppressor screen

To isolate suppressors of *cks-1(ne549)*, we performed a maternal-effect suppressor screen of *cks-1(ne549)*. Following mutagenesis of *cks-1(ne549)* by EMS (**E**thyl **M**ethane **S**ulfonate), we

look for suppressors in F1 generation to obtain dominant suppressors, and F2 generation for recessive ones at the non-permissive temperature 25 °C (Figure 38). In F2 generation screening, we were able to isolate five suppressors, *SK23, SK26, SK29, SK36, SK57*, which suppress *cks-1(ne549)* to full viability (Table 7). By linkage analysis combined with SNP (**S**ingle **N**ucleotide **P**olymorphism) mapping method, we determined the approximate chromosomal location of the suppressors. None of them appeared to be linked to *cks-1*, which suggests that all of them are extragenic suppressors. *SK36* was further pursued for mapping.

SK36 appeared to be in the center of chromosome III, and to perform a fine mapping, three-point mapping technique was used. We constructed a strain containing *unc-32(e189)* and *dpy-17(e164)* in the *cks-1(ne549)* background, which covers the location on chromosome III from -2.16 to 0. The recombination event between these two markers produce recombinants which are informative to map the mutation site between them, and by analyzing about 150 recombinants, we were able to narrow it down to four genes in cosmid ZK328. ORFs of four genes were sequenced, and a point mutation that results in the 811th amino acid residue change from glutamic acid to lysine was found in *npp-10* (ZK328.5), a member of the NUP98-NUP96 precursor family of FG-rich nucleoporins (Figure 39). NUP98-NUP96 encodes precursor protein that generates two nucleoporins, NUP98 and NUP96 by auto-proteolytic cleavage (Figure 40). Like many

nucleoporins, NUP98 has a well-defined domain organization, including; 1) GLEBS domain capable of binding the GLE2 in *Saccharomyces cerevisiae* and hRae1 in human (Bailer et al., 1998; Pritchard et al., 1999) 2) auto-proteolytic domain that is required for cleavage of the NUP98/NUP96 precursor (Fontoura et al., 1999; Rosenblum and Blobel, 1999). The *npp-10(ne3744)* allele has a mutation in the auto-proteolytic cleavage domain, implying that this function might be impaired.

npp-10(ne3744) is a loss-of-function allele

To find how *npp-10(ne3744)* functions to suppress *cks-1(ne549)*, we tried to determine if it acts in a loss or gain-of-function manner. A deletion allele *npp-10(ok467)* was used to test *npp-10(ok467) /* + and *npp-10(ok467) / npp-10(ne3744)* for effect on the suppression of *cks-1(ne549)*. We found that both suppressed the *cks-1(ne549)* embryos to viability (Table 8).

Then we tried to see if injecting *npp-10* dsRNA has an effect on suppression of *cks-1(ne549)*. When the diluted dsRNA was injected to the *cks-1(ne549)* worms, about 40% embryos were enclosed compared to 5% in not injected control, suggesting *npp-1(RNAi)* rescues *cks-1(ne549)* (Table 8). These results imply *npp-10(ne3744)* is a loss-of-function allele for suppression of *cks-1(ne549)*.

***npp-10(ne3744)* has a mild defect in the auto-proteolytic activity**

The auto-proteolytic activity of NUP98-NUP96 is conserved among species (Figure 40) (Emtage et al., 1997; Fontoura et al., 1999; Rosenblum and Blobel, 1999). The residues important for cleavage activity in the enzymatic catalytic sites are H862, S864 in hNUP98 (Hodel et al., 2002). Also K791 and N799 in hNUP98 have a weak effect on this function. The mutated residue of *npp-10(ne3744)* interacts with the residue in the tail domain (NUP98-C) that has a weak effect on the proteolytic activity when mutated, suggesting the mutation (E811K) in *npp-10(ne3744)* may have a similar effect (Rosenblum and Blobel, 1999).

To test this idea, the NUP98 minimal domain for auto-proteolysis (769-942) was cloned into an expression vector in-frame with Glutathione-S-transferase (GST) upstream and green fluorescent protein (GFP) downstream as previously shown (Figure 41a) (Rosenblum and Blobel, 1999). This allowed us to easily identify about 30 KDa NUP98-C fragment compared to 6 KDa without GFP fusion. Then we used *in vitro* transcription/translation system with these constructs. As expected, wild type kinase domain was completely cleaved with two expected sized fragments, ~60 KDa GST-NUP98-N and ~40KDa NUP98-C-GFP. Similar to the previous report, we observed a strong defect of the cleavage activity when we used the construct with

H893Q/S895C mutations. The mutation E811K in *npp-10(ne3744)* indeed shows a very weak disruption in the proteolytic activity as expected (Figure 41b). Considering that *npp-10(ne3744)* does not have any obvious phenotype, this result is reasonable since the strong defect in proteolytic activity will lead to embryonic lethality due to the severe defects in the structure of NPCs.

npp-10(ne3744) **does not have visible defects in the NPCs**

To examine the localization of NUP98 in *npp-10(ne3744)* and extra-gut mutants, we performed an antibody staining experiment using NUP98 antibody (Galy et al., 2003). As shown in the previous study (Galy et al., 2003), we observed the strong punctuate signal in the nuclear membrane in wild type embryos as well as in *npp-10(ne3744)* (Figure 42a). Also in both *cks-1(ne549)* and *cdk-1(ne2257)*, we observed strong nuclear envelope staining as shown in wild type (Figure 42a), suggesting that *npp-10(ne3744)*, *cks-1(ne549) and cdk-1(ne2257)* did not have any visible defects in NUP98 structure.

Previous study in knock-out mice showed that the disruption of NUP98 caused selective changes in the stoichiometry and function of the NPCs (Wu et al., 2001). Therefore we investigated the structural change of the NPCs that may be caused by *npp-10(ne3744)*. For this

purpose, we used mAB414 antibody that detects FG nucleoporins, widely used for examining the structure of the NPCs (Wu et al., 2001). In this staining, we also could not find any visible defects in *npp-10(ne3774)* (Figure 42b). The staining on *cks-1(ne549)*, *cdk-1(ne2257),* and *mbk-2(ne3442)* mutant embryos appeared to be normal as well as their genetic doubles with *npp-10(ne3744)* (Figure 42b). These results indicate that the structure of NPCs in these mutants do not have visible defects although we cannot exclude the possibility that they may have structural defects which cannot be seen by these antibody stainings or that some of functional aspects of the NPC may be impaired.

npp-10(ne3744) **suppresses other extra-gut mutants**

Since *npp-10(ne3744)* rescues one of the extra-gut mutants, *cks-1(ne549)*, we wanted to see if it suppresses other extra-gut mutants. We made the genetic doubles *cdk-1(ne236) npp-10(ne3744)*, *cdk-1(ne2257) npp-10(ne3744)*, *oma-1(ne411) npp-10(ne3744)*, *mbk-2(ne3442) npp-10(ne3744)*, and *gsk-3(nr2047) npp-10(ne3744)*, and tested for suppression. *npp-10(ne3744)* suppressed all the extra-gut mutants tested in terms of viability or enclosure, except *gsk-3(nr2047)* (Table 9). This result suggests that *npp-10(ne3744)* acts in the downstream of *cdk-1, oma-1, and mbk-2* in this pathway.

***npp-10(ne3744)* does not suppress high OMA-1 levels in extra-gut mutants**

Next we wanted to see if high OMA-1 levels observed in extra-gut mutants are reduced by *npp-10(ne3744)*. The OMA-1::GFP fluorescence in the developing oocytes and 1-cell embryos often includes a punctuate pattern of fluorescence and resembles the characteristic pattern of germ-line P granules (Figure 43). Starting with the onset of the first mitotic division, the intensity of OMA-1::GFP fluorescence rapidly decreased, and by the time the division is complete, only approximately 10% remains, which predominantly exists in the germ-line precursors P1, associated with what appeared to be P granules. The GFP signal continued to decrease in 2-cell embryos and again was asymmetric after the next division, with most of the remaining fluorescence segregated to P2, where it was also predominantly associated with granules. The OMA-1::GFP signal became too weak to detect in the embryos after the 4-cell stage.

Embryos of *cdk-1(ne2257)* and *mbk-2(ne3442)* with *npp-10(ne3744)* background, and we found that OMA-1 level still remains high in *npp-10(ne3744)* background (Figure 43). Also OMA-1 antibody (Lin, 2003) was used to stain the embryos of *cks-1(ne549) npp-10(ne3744)*, and OMA-1 still remained high (data not shown).

***npp-10(ne3744)* suppresses high SKN-1 levels in extra-gut mutants**

Previous study shows that the degradation of the maternal SKN-1 protein is delayed in *oma-1(zu405)* (Lin, 2003). Therefore, we wanted to see if the SKN-1 level is elevated in other extra-gut mutants. We performed an antibody staining using the SKN-1 antibody. As expected, we found that SKN-1 is not degraded after the 4-cell stage embryos in *cdk-1(ne2257)* and *gsk-3(RNAi)* (Figure 44).

Next, we tested if the SKN-1 level is reduced by *npp-10(ne3744)* to suppress the extra-gut phenotype. We found that the SKN-1 levels were decreased in the 8- and 12-cell stage embryos of *cdk-1(ne2257) npp-10(ne3744)* and *cks-1(ne549) npp-10(ne3744)* (Figure 44), implying that the change in the NPCs induced by the mutation in *npp-10(ne3744)* is responsible for the reduction of nuclear SKN-1 level and rescue of extra-gut mutants.

Discussion

In this study, we present a result of a suppressor genetic screen of *cks-1(ne549)*. We determined that one of the suppressors was mapped to *npp-10(ne3744)*, a homolog of mammalian NUP98/96.

Nuclear pore complexes and NUP98/96

Nuclear pore complexes (NPCs) are large proteinaceous assemblies with a calculated mass of 40 and 60 MDa in yeast and vertebrates, respectively (Cronshaw et al., 2002; Rout et al., 2000). Despite the differences in size, the basic architecture of the NPCs is conserved among the species. Communication between the nucleus and cytoplasm of a eukaryotic cell is mediated by the NPCs, which act as selective molecular gateways (Gorlich and Kutay, 1999; Ryan and Wente, 2000). NPCs have a modular architecture with substructures that include an eightfold symmetric spoke-ring complex anchored in the membrane, cytoplasmic and nuclear annular rings, and asymmetrical cytoplasmic and nuclear filamentous structures (Figure 45) (Bagley et al., 2000; Stoffler et al., 1999). Since the NPCs are the only known portals between the nucleus and

cytoplasm, it affects all the aspects of cellular physiology that require transport including gene expression, growth and proliferation, signaling, cell cycle control, and death.

To date, 28 mammalian genes encoding in total 30 nucleoporins (NUPs) have been described (Cronshaw et al., 2002), and among them ~50% are essential for viability. In *C. elegans*, there are 20 potential homologs of vertebrate nucleoporins, and the majority of these nucleoporins are also essential for viability (Galy et al., 2003). These NUPs have long been classified into groups based on the presence or absence of primary sequence motifs. One of groups known as FG NUPs comprises at least a third of the total NPC mass and contains at least one domain with multiple glycine-leucine-phenylalanine-glycine (GLFG), FXFG, and/or FG (FG repeats), which is thought to serve as a docking site for karyopherin/substrate complexes as they traverse the NPCs (Radu et al., 1995; Rexach and Blobel, 1995).

One of the FG NUPs, *npp-10*, encodes the precursor proteins that generate two nucleoporins, NUP98 and NUP96, from the posttranslational processing by auto-proteolysis. Interestingly, this mechanism is conserved among species that NUP98 and Nup96 in vertebrates, and NUP145N and NUP145C in budding yeast demonstrate same auto-proteolytic activity. The correct targeting of both NUP98 and NUP96 to the NPCs is dependent on this proteolytic cleavage (Fontoura et al., 1999).

Unlike NUP96 which appears to be nucleoplasmic, NUP98 moves between the nuclear interior and the pore, as well as between the nucleus and the cytoplasm, and plays a critical part in nuclear trafficking. First, NUP98 has been implicated in the transport of RNA across the pore since injection of antibodies to NUP98 into the nucleus blocks the export of most RNAs (Fabre et al., 1994; Powers et al., 1997; Teixeira et al., 1997). Second, NUP98 binds Karyopherin β2 (Kapβ2, transportin) to mediate nuclear import at the nuclear side of the NPCs (Fontoura et al., 2000).

Potential function of the NPCs in the regulation of SKN-1 level

In addition to its role in the specification of gut tissue in the embryos, SKN-1 functions in the digestive system to resist oxidative stress in the adult worms (An and Blackwell, 2003). SKN-1 regulates a key phase II detoxification gene through the constitutive and stress-inducible mechanisms in the ASI chemosensory neurons and intestine, respectively. Upon oxidative stress, SKN-1 accumulates in the intestinal nuclei rapidly, which is regulated positively by PMK-1 p38 MAPK pathway (Inoue et al., 2005) and negatively by GSK-3 (An et al., 2005). This rapid nuclear translocation is not dependent on CRM-1 or NLS (**N**uclear **L**ocalization **S**ignal),

suggesting that it may not be through the common nuclear import/export mechanism (Inoue et al., 2005).

Our data shows the change in the NPCs induced by the mutation in *npp-10(ne3744)* reduces the SKN-1 level in the embryonic cells to rescue extra-gut phenotype. NUP98 has been shown to mediate nuclear transport via karyopherin β2 which is not dependent on NLS signal (Fontoura et al., 2000), therefore it is possible that it may affect SKN-1 nuclear translocation through karyopherin β2. NUP98 itself also appears to be a mobile protein involved in nuclear trafficking (Griffis et al., 2002), suggesting that NUP98 may directly transport SKN-1 in and out of the nucleus. Alternatively the change in NPCs induced by *npp-10(ne3744)* may indirectly regulate the localization of WRM-1. Intriguingly, NUP98 was shown to be regulated by phosphorylation by NIMA kinase in fungus to promote mitosis by regulating the localization of mitotic regulators (De Souza et al., 2003). This observation suggests an interesting possibility that npp-10 may be regulated by kinases such as GSK-3 or PMK-3 for the nuclear translocation of important regulators, for example, SKN-1. As a conclusion, our results here suggest that the nuclear localization of SKN-1 may be regulated by NPP-10-mediated mechanism.

Materials and methods

Genetics and Strains

All strains were handled and cultured as described previously (Brenner, 1974). Strains used were: *cdk-1(ne236 and ne2257)* (III), *mbk-2(ne3442)* (IV), *cks-1(ne549)* (IV), VC316 *+/mT1* II; *npp-10(ok467)/mT1[dpy-10(e128)]* III.

EMS mutagenesis screen for suppressors of *cks-1(ne549)*

The Ts allele *cks-1(ne549)* in the background of the Hawaiian CB4856-derived *lin-11(ne832)* egg-laying deficient strain (WM59) was used for suppressor screen. L4 animals mutagenized with EMS (**E**thyl **M**ethane **S**ulfonate) were grown at 15°C. Half of F1 progenies were shifted to 25 °C at the L4 stage to look for F1 dominant suppressors, and the other half was maintained to produce F2 progenies. F2 animals at the L4 stage were shifted to 25°C for screening F2 recessive suppressors.

RNAi assays

RNAi was performed as described previously by injecting dsRNA (Bei et al., 2002). The *ifg-1* dsRNA was prepared from a full length genomic DNA. Embryos collected 24 hr after injection were scored for the suppression of extra-gut mutants at the appropriate temperature.

Antibody staining

Worms with embryos from wild type and mutants, *npp-10(ne3744)*, *cdk-1(ne2257)*, *cks-1(ne549)*, *mbk-2(ne3442), csk-1(ne549) npp-10(ne3744), cdk-1(ne2257) npp-10(ne3744)*, *mbk-2(ne3442) npp-10(ne3744)*, were dissected directly on poly-L-lysine-coated glass slides. Fixation protocols for αSKN-1 (Lin et al., 1998), αNUP98 (Galy et al., 2003), mAb414 against nucleoporins (Jackson Immunoresearch Laboratories, West Grove, PA) (Galy et al., 2003) were as described. Antibody dilutions used were: SKN-1 monoclonal F2A+ F4C, no dilution (Bowerman et al., 1993); NUP98 polyclonal 1:500 (Galy et al., 2003); mAb414 monoclonal 1:500.

***In vitro* transcription/translation assay**

All wild-type and NUP98 mutant proteins were *in vitro* transcribed and translated using a coupled reticulocyte lysate transcription/translation system (Promega Corp., Madison, WI), in the presence of [^{35}S] methionine, according to manufacturer's instructions. They were separated on SDS-PAGE, and the gels were analyzed by autoradiography.

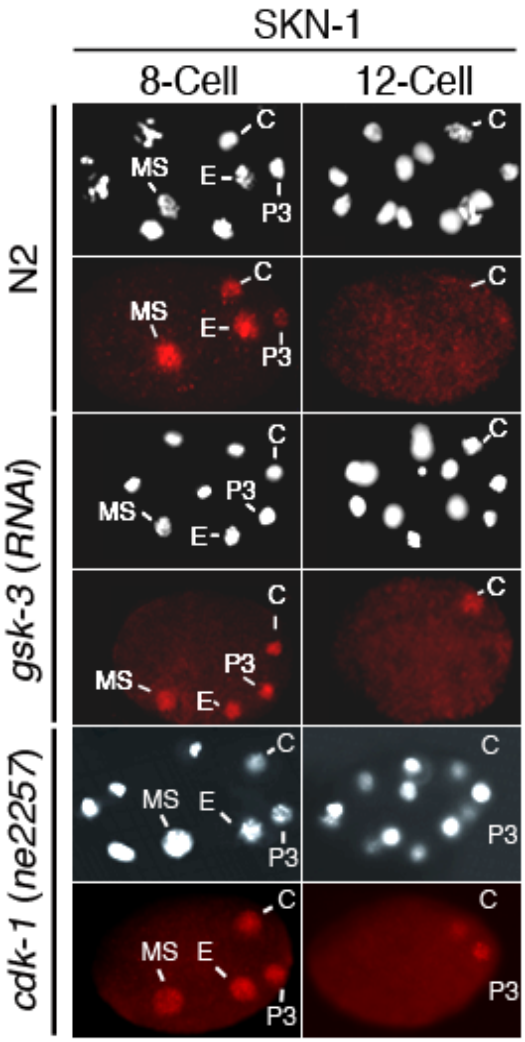

Figure 37. Degradation of SKN-1 is delayed in extra-gut mutants.

Micrographs showing α-SKN-1 staining in wild type, *gsk-3(RNAi)*, and *cdk-1(ne2257)* embryos. Lower panels show SKN-1 immunofluorescence, and upper panels indicate cell stage via DAPI staining. The SKN-1 protein persist at high levels in the C-lineage of *cdk-1(ne2257)* and *gsk-3(RNAi)* embryos at the 12-cell stage, while the SKN-1 staining is not observed in wild type embryos at this stage.

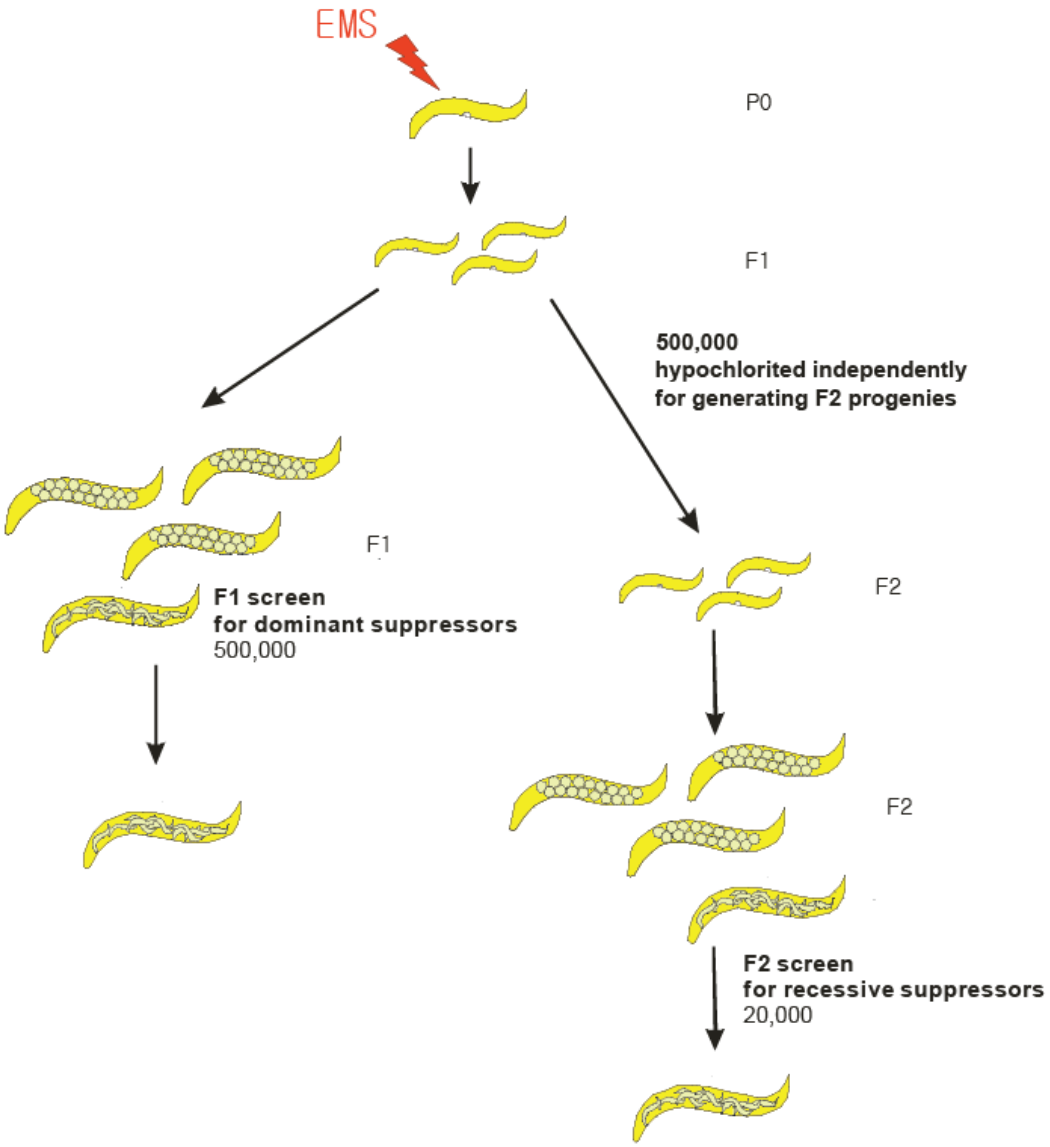

Figure 38. Schematic diagram of the screen for maternal-effect suppressors of *cks-1(ne549)*.

P0 *cks-1(ne549)* animals in *lin-11* Hawaiian (CB4856) background were mutagenized by EMS (**E**thyl **M**ethane **S**ulfonate). After growing at permissive temperature (15°C), the F1 L4 stage animals were shifted to 25°C for 27 hrs then screened for worms with viable embryos, F1

suppressors. For F2 suppressors, the F2 L4 stage animals were shifted to 25°C for 27 hrs to look for animals with viable embryos inside the mother worms. See Table 7 for the results of these suppressor screens.

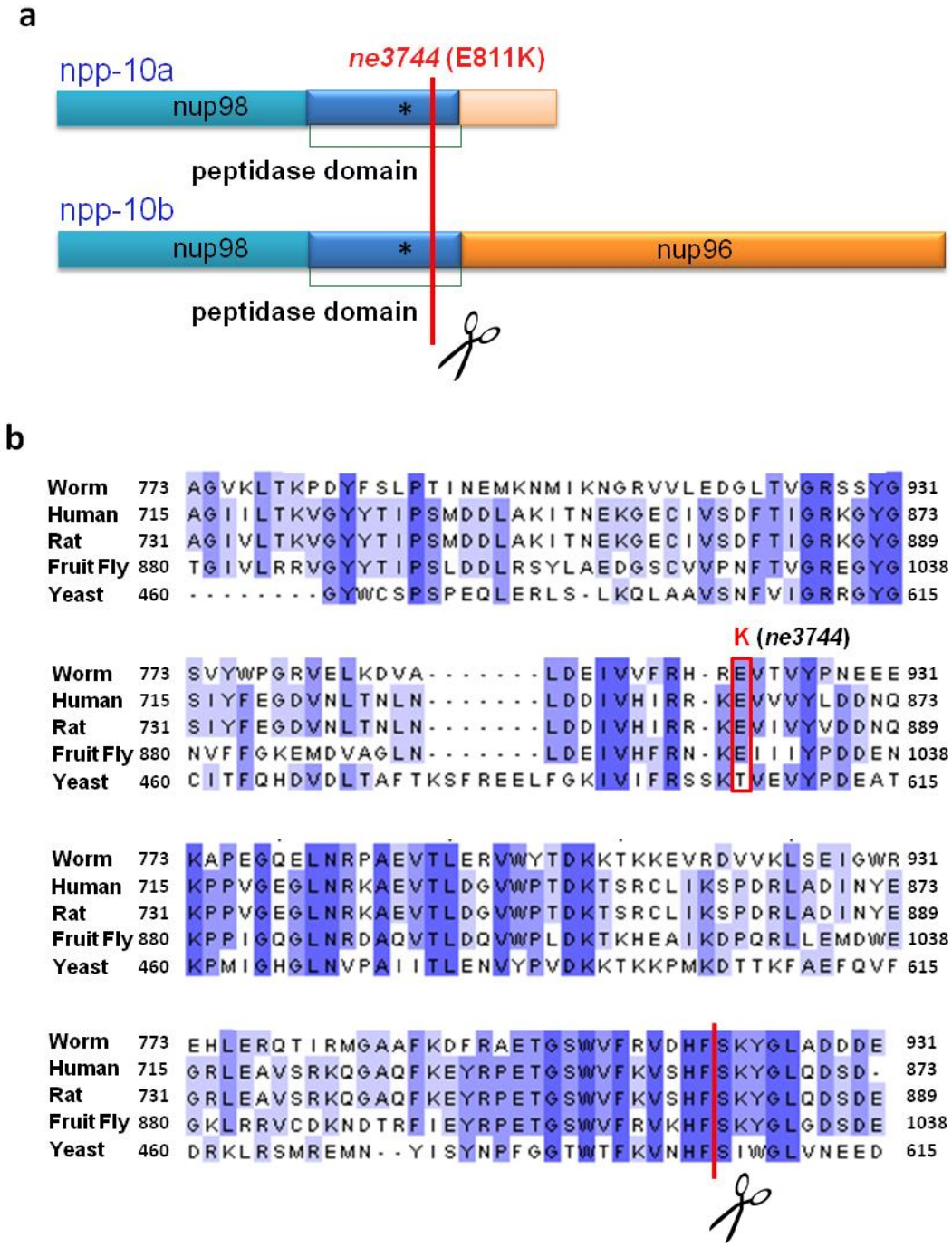

Figure 39. Identification of *SK36* as a point mutation of gene *NUP98-NUP96 (npp-10)*.

a, Schematic representation of two alternatively spliced NUP98-NUP96 precursor proteins. *npp-10* encodes precursor proteins that generate two nucleoporins, NUP98 and NUP96, by auto-proteolytic cleavage. The middle blue box shows the minimal domain for NUP98 cleavage (peptidase domain), where the amino acid substitution in *npp-10(ne3744)* resides. **b**, Amino acid alignments of highly conserved peptidase domain. Red box and letters show the mutated residue. Red line with scissors represents the auto-cleavage site. Conserved residues are shaded, with the darker shade represent the fully conserved residues.

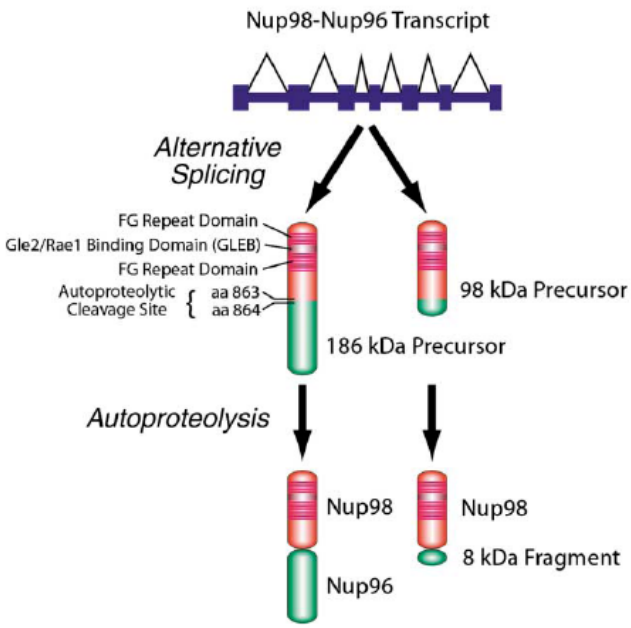

Figure 40. . NUP98-NUP96.

Alternative splicing and auto-proteolysis steps lead to the production of NUP98, Nup96 and an 8KD fragment in humans. This process is conserved among species (Emtage et al., 1997; Fontoura et al., 1999; Rosenblum and Blobel, 1999; Teixeira et al., 1997) .

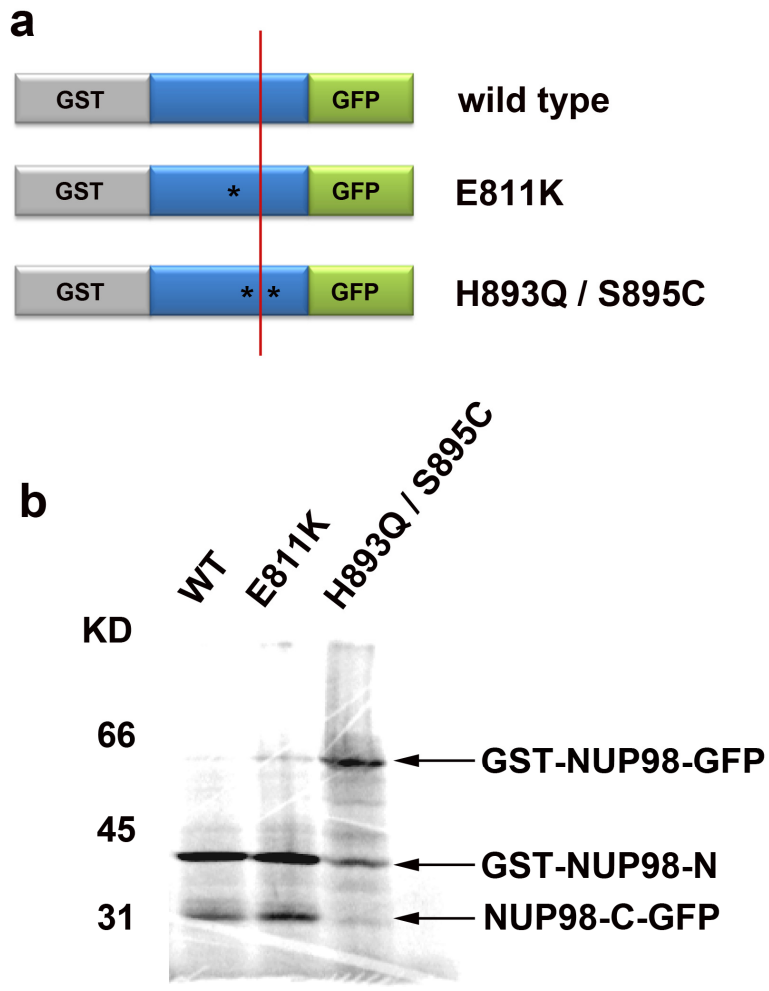

Figure 41. *npp-10(ne3744)* shows a weak defective auto-proteolytic activity *in vitro*.

a, Wild type or mutated NUP98 peptidase domain (769-942) was fused to GST and GFP as shown. Blue box indicates the autocleavage domain in NUP98. Red line represents the autoproteolytic cleavage site. Asterisks show the positions of the mutated residues. **b**, *In vitro* transcription/translation assay shows that the mutation in *ne3744* has a weak cleavage defect.

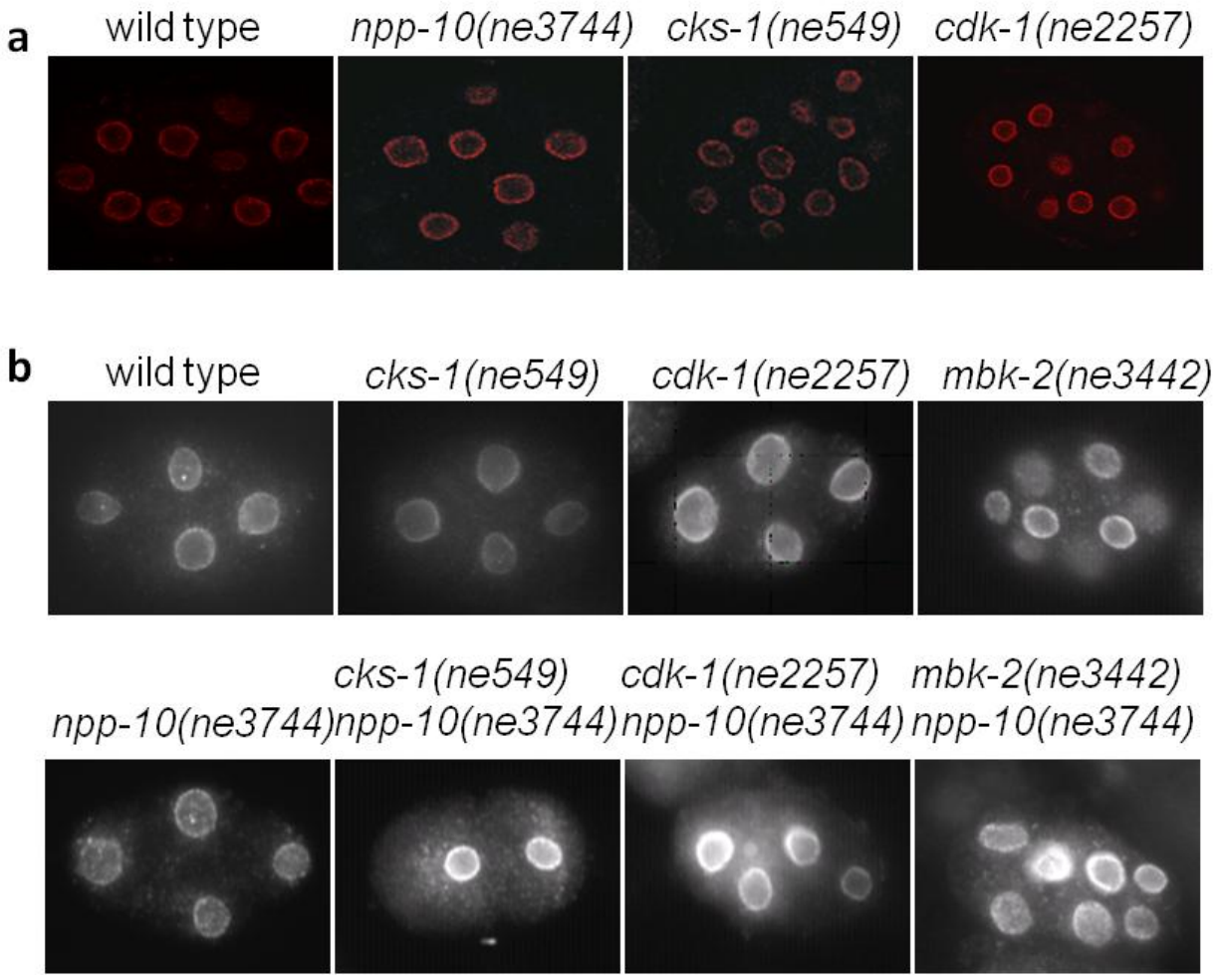

Figure 42. Immunofluorescence of NPCs.

Micrographs showing the structure of NPCs in *cks-1(ne549), cdk-1(ne2257), npp-10(ne3744)*, and genetic doubles *cks-1(ne549) npp-10(ne3744)* and *cdk-1(ne549) npp-10(ne3744)*. No visible defects were detected. **a**, NUP98 antibody staining. **b**, mAB414 antibody staining.

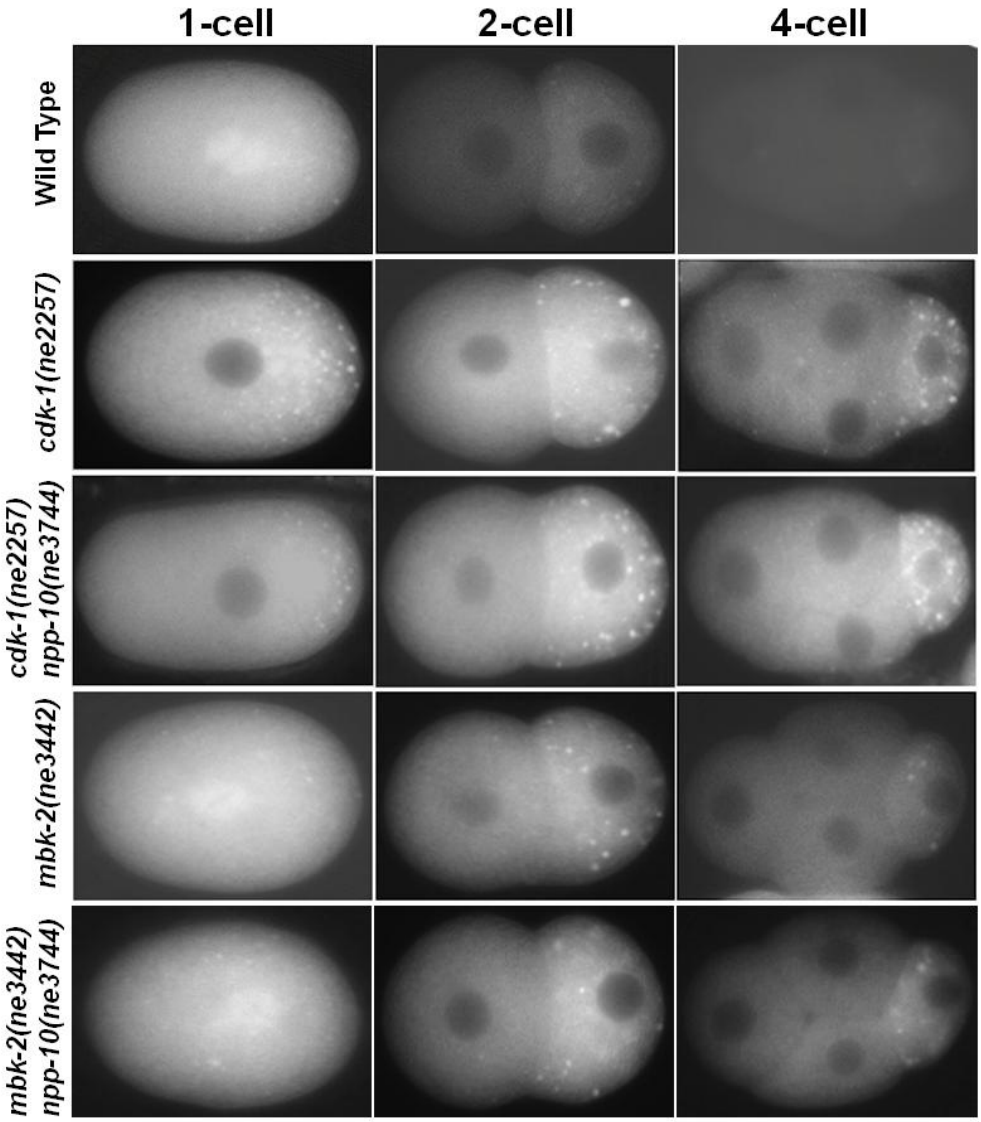

Figure 43. *npp-10(ne3744)* does not suppress high OMA-1 levels in extra-gut mutants.

Micrographs showing OMA-1::GFP in *cdk-1(ne2257)*, *mbk-2(ne3442)*, and their genetic doubles with *npp-10(ne3744)*. Anterior is to the left and dorsal is up. OMA-1 is not reduced in *npp-10(ne3744) cdk-1(ne2257)*, and *npp-10(ne3744) mbk-2(ne3442)*.

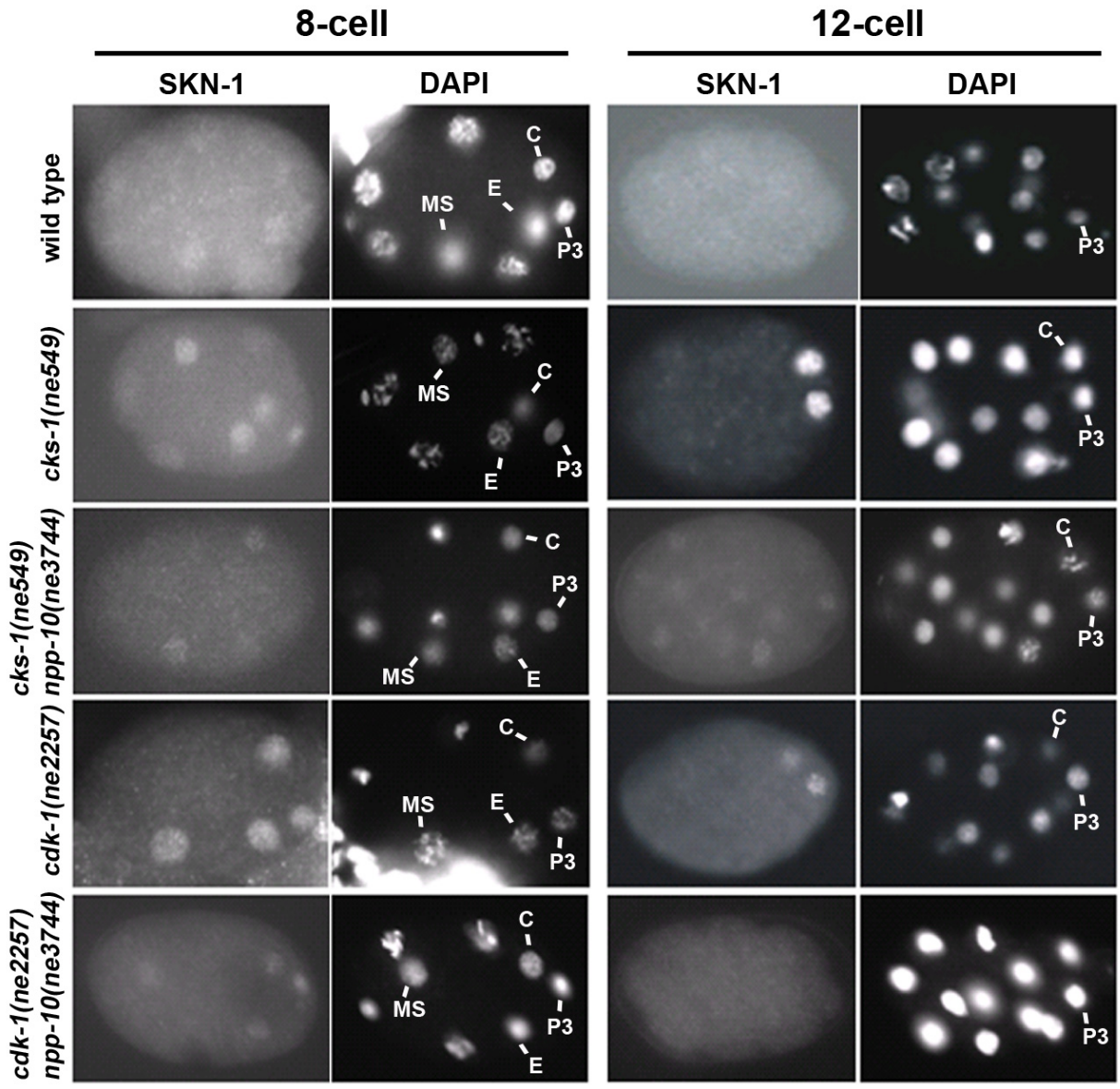

Figure 44. *npp-10(ne3744)* reduces SKN-1 levels in extra-gut mutants.

Micrographs showing α-SKN-1 staining of the embryos of *cks-1(ne549)*, *cdk-1(ne2257)*, and their genetic doubles with *npp-10(ne3744)*. High SKN-1 levels in *cks-1(ne549)* and *cdk-1(ne2257)* are reduced by *npp-10(ne3744)*.

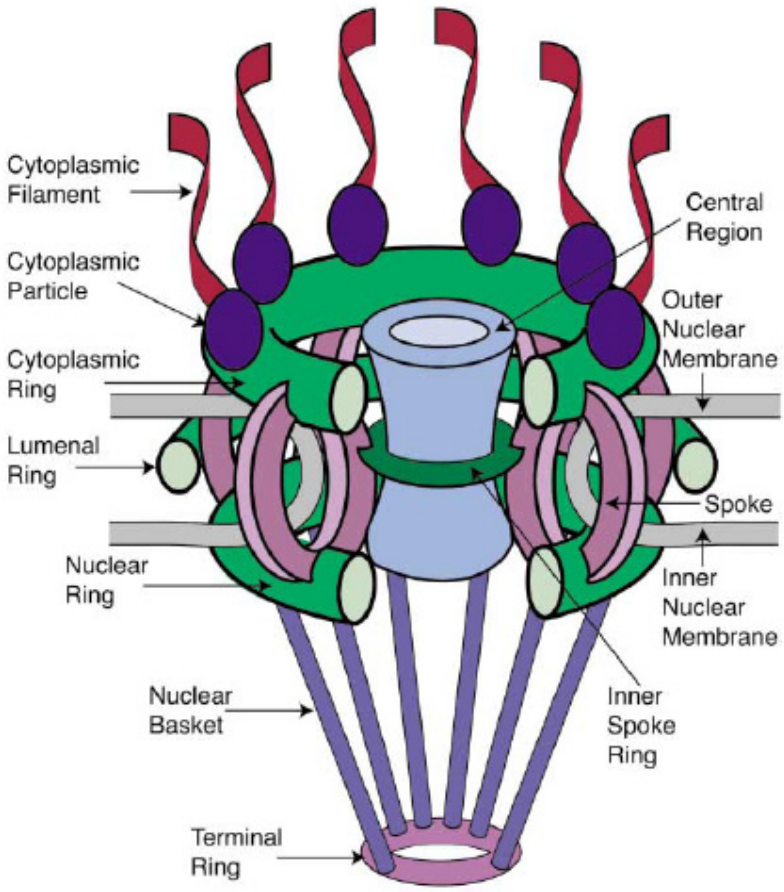

Figure 45. Schematic diagram of NPC substructures.

The structure has an apparent 8-fold rotational symmetry perpendicular to the plane of the nuclear membrane; however, certain facing portions are removed in this diagram to reveal the architecture of the central region. Labels for all the structures found in vertebrate NPCs are included, with the cytoplasmic face on top (Suntharalingam and Wente, 2003).

Suppressor	screen	Number of worms screened	Dominant/Recessive	Chromosomal location
SK23	F2 screen	20,000	Dominant	I
SK26	F1 screen	500,000	Dominant	II
SK29	F2 screen	20,000	Dominant	III
SK36	F2 screen	20,000	Dominant	III
SK57	F1 screen	500,000	Dominant	V

Table 7. Isolated suppressors from the *cks-1(ne549)* suppressor screening.

	% Suppression on *cks-1(ne549)* in viability (n)
npp-10(ne3744)/npp-10(ne3744); cks-1(ne549)/cks-1(ne549)	100 (1030)
npp-10(ne3744)/+; cks-1(ne549)/cks-1(ne549)	100 (879)
npp-10(ok467)/+; cks-1(ne549)/cks-1(ne549)	98 (983)
npp-10(ok467)/npp-10(ne3744); cks-1(ne549)/cks-1(ne549)	12 (865)

Table 8. *npp-10(ne3744)* is a strong dominant suppressor and acts in a loss-of-function manner.

Heterozygote for the deletion allele *npp-10(ok467)* suppresses *cks-1(ne549)*.

Embryo type	% Rescue (n)	Rescue type
cks-1(ne549)	4 (988)	viability at 25°C
cks-1(ne549) npp-10(ne3744)	100 (1035)	
cdk-1(ne2257)	2 (1401)	viability at 23°C
cdk-1(ne2257) npp-10(ne3744)	88 (876)	
cdk-1(ne236)	0 (973)	enclosure[a]
cdk-1(ne236) npp-10(ne3744)	21 (110)	
mbk-2(ne3442)	9 (873)	viability at 25°C
mbk-2(ne3442) npp-10(ne3744)	73 (496)	
oma-1(ne411)	0 (948)	viability at 23°C
oma-1(ne411) npp-10(ne3744)	11 (905)	
gsk-3(nr2047)	47 (19)	extra-gut phenotype suppression[b]
gsk-3(nr2047) npp-10(ne3744)	56 (27)	

Table 9. *npp-10(ne3744)* suppresses other extra-gut mutants.

The suppression rate was checked at the indicated conditions.

[a] *cdk-1(ne236)* is a non Ts allele which does not require temperature control.

[b] laser ablation assay was performed to check the suppression of extra-gut phenotype.

CHAPTER V

SUMMARY AND FUTURE DIRECTIONS

Relays at the membrane in P2/EMS signaling

The process of signal transduction allows a cell to receive messages from its environment and transfer this signal from membrane through the cytoplasm and into the nucleus in a timely manner. In Chapter II, we studied the key mediator WRM-1/β-catenin *in vivo* in the P2/EMS signaling pathway comprised of the Wnt, MAPK-like, and Src pathways. These studies provide insights into how WRM-1integrates the cortical signals and the cell cycle to regulate a polarized cell division in *C. elegans*.

Our results show that CDK-1, GSK-3, and LIT-1 phosphorylate WRM-1 to regulate its localization at the membrane as well as in the nucleus. SRC-1 also contributes to the localization of WRM-1. These observations provide several new insights into the mechanism of P2/EMS signaling. First, the involvement of cell-cycle regulator CDK-1in releasing WRM-1 from membrane explains how the polarized single cell division is perfectly coordinated with the signaling event. Second, we showed the direct involvement of GSK-3 in the P2/EMS signaling pathway, in which the phosphorylation by CDK-1 serves as a priming site for subsequent phosphorylation by GSK-3. Before this study, the role of GSK-3 in P2/EMS signaling pathway was obscure since GSK-3 may function through OMA-1 to exhibit P2/EMS signaling related roles. Third, a novel function of the MAPK-like pathway in modulating the Wnt signaling

pathway was presented in this thesis. WRM-1 is sequestered in the membrane by MOM-4 and LIT-1 until signaling releases it for its nuclear translocation. This result suggests that one of the roles of the MAPK-like pathway is to isolate WRM-1 in the cortex, enabling it to receive the signal from the signal-sending cell P2 and reduce the background level of WRM-1 in the non-signal receiving anterior part. Fourth, SRC-1 contributes to WRM-1 localization. A previous study suggested that the Wnt and Src pathways interact genetically, and predicted that SRC-1 may converge on multiple targets in the Wnt pathway (Bei et al., 2002). Our result shows that SRC-1 phosphorylates WRM-1 *in vitro*, implying WRM-1 may be one of its targets although direct evidence is necessary to prove this hypothesis. Lastly, our *in vitro* data implies that these phosphorylation events by CDK-1, GSK-3 and LIT-1 do not influence the activity of the kinase complex for its downstream target POP-1/TCF, but as shown, affect the nuclear localization of WRM-1.

While our results shed light on the fundamental mechanism by which WRM-1 plays a central role during polarized EMS cell division, they also raise further intriguing questions. First, it is not known whether CDK-1 or GSK-3 activity is regulated or whether these kinases become physically associated with WRM-1 in the cortex. One possibility is that MOM-2/Wnt binding to its receptor MOM-5/Frizzled may bring WRM-1, CDK-1, and GSK-3 into close proximity

promoting their sequential phosphorylation. Alternatively, the activity of these kinases may be regulated by Wnt signaling pathway. Second, we do not know how WRM-1, LIT-1, and GSK-3 are tethered in the cortex. WRM-1 does not bind HMR-1/Cadherin (Costa et al., 1998; Korswagen et al., 2000; Natarajan et al., 2001), and GSK-3 localization in the cortex was visualized for the first time in our study. It would be intriguing to see how these molecules are localized and regulated in the membrane. Third, it is not clear how WRM-1 is transported to the nucleus. Our result implies that the phosphorylation status of WRM-1 affects its nuclear localization, suggesting that phosphorylation may facilitate WRM-1 recognition by nuclear transport regulatory factors such as APR-1. Finally, we still do not completely understand how MOM-2 binding to its receptor causes transmission of the signal. This has been a challenging question in the field of Wnt pathway studies, which is still poorly understood. In the canonical Wnt pathway, ligand binding triggers the formation of a receptor complex and protein kinases modify the receptor tails, leading to the recruitment of negative regulators including Axin in the cytoplasm (He et al., 2004; Mao et al., 2001; Tolwinski et al., 2003; Zeng et al., 2005). The Wnt pathway functioning in P2/EMS signaling works differently in detail, but may have a similar fundamental mechanism. For example, MOM-2 binding to its receptor MOM-5 triggers CDK-1 to modify its target WRM-1 to overcome negative regulation by LIT-1 to release it from the

membrane. In both the canonical pathway and in the Wnt pathway in P2/EMS signaling, it is unknown how Wnt binding induces the activity of kinases, or whether other components are directly affected.

Interestingly, in addition to the Wnt signaling pathway, GSK-3 and CDK-1 are also involved in the degradation of CCCH-type zinc finger protein OMA-1 (Nishi and Lin, 2005; Shirayama et al., 2006). GSK-3 directly phosphorylates OMA-1, while we still do not know the molecular mechanism by which CDK-1 regulates OMA-1 (Shirayama et al., 2006). The mutation in *oma-1* exhibits not only defects in OMA-1 degradation, but also Wnt phenotypes such as a partial penetrance of gutless and EMS spindle orientation problems. Currently it is not understood how stabilized OMA-1 interferes with P2/EMS signaling. One clue comes from the observation that OMA-1 disturbs GSK-3 localization in the germ-line (our unpublished data), suggesting that OMA-1 may also disrupt the localization of GSK-3 in embryonic cells. However our experiment indicates that OMA-1 does not affect the localization of GSK-3 in early embryos (our unpublished data). Nevertheless, it is still possible that OMA-1 may inhibit the activity of GSK-3, a possibility which needs to be tested. Alternatively, OMA-1 may indirectly influence P2/EMS signaling through other maternal determinants disrupted by OMA-1. In any case, it

would be interesting to see how CCCH-type zinc protein such as OMA-1 affects P2/EMS signaling event.

Collaboration between the Wnt signaling pathway and the cell cycle machinery during polarized cell division has not been clearly demonstrated in other organisms. This is partially due to the relatively complex manifestation of this signaling process in a group of cells instead of a single cell as in *C. elegans*. Nevertheless, there could be a direct application of our results during the fate specification of neuroblasts in *Drosophila*. Some neuroblasts which undergo polarized cell division in the *Drosophila* CNS are specified by the Wingless signaling pathway (Chu-LaGraff and Doe, 1993; McCartney et al., 1999). In addition, the CDK-1 homolog CDC2 is also required for the asymmetric localization of fate determinants during this developmental process (Tio et al., 2001). The mechanism by which Wingless or CDC2 regulate this polarized division, if indeed they cooperate, is not understood. Our results provide the first example of cooperation between the Wnt pathway and the cell cycle machinery during asymmetric cell division, which may be a general theme that extends throughout animal biology.

Suppressor screens in the Wnt signaling pathway and OMA-1 pathway

We attempted genetic suppressor screens to identify additional components in the Wnt signaling and OMA-1 regulation pathways. The types of original mutations that are suitable for suppressor screens are partial loss-of-function or weak alleles. Strong alleles such as complete loss-of-function alleles would not work well due to total removal of the protein or its activities. Therefore our temperature-sensitive alleles with their partial functions remaining in specific pathways provide an optimum starting mutant for this type of screening.

Although we identified potentially remarkable candidates in these pathways, more candidates may remain to be identified since only a few of the suppressors were cloned. The major limitation is that the highly labor-intensive screening process generated only a limited number of genes in the pathway. One way to circumvent this difficulty is reverse genetics. The availability of a complete RNAi library has made whole-genome screening feasible, and many papers have been published presenting various possible candidates in a number of pathways. Therefore conducting genome-wide RNAi screening would be helpful to identify a whole set of related components in the pathway, and would complement a conventional suppressor genetics.

REFERENCES

Aberle, H., Bauer, A., Stappert, J., Kispert, A., and Kemler, R. (1997). beta-catenin is a target for the ubiquitin-proteasome pathway. The EMBO journal *16*, 3797-3804.

Ahumada, A., Slusarski, D.C., Liu, X., Moon, R.T., Malbon, C.C., and Wang, H.Y. (2002). Signaling of rat Frizzled-2 through phosphodiesterase and cyclic GMP. Science *298*, 2006-2010.

Amit, S., Hatzubai, A., Birman, Y., Andersen, J.S., Ben-Shushan, E., Mann, M., Ben-Neriah, Y., and Alkalay, I. (2002). Axin-mediated CKI phosphorylation of beta-catenin at Ser 45: a molecular switch for the Wnt pathway. Genes & development *16*, 1066-1076.

An, J.H., and Blackwell, T.K. (2003). SKN-1 links C. elegans mesendodermal specification to a conserved oxidative stress response. Genes & development *17*, 1882-1893.

An, J.H., Vranas, K., Lucke, M., Inoue, H., Hisamoto, N., Matsumoto, K., and Blackwell, T.K. (2005). Regulation of the Caenorhabditis elegans oxidative stress defense protein SKN-1 by glycogen synthase kinase-3. Proceedings of the National Academy of Sciences of the United States of America *102*, 16275-16280.

Arthur, W.T., Petch, L.A., and Burridge, K. (2000). Integrin engagement suppresses RhoA activity via a c-Src-dependent mechanism. Curr Biol *10*, 719-722.

Bagley, S., Goldberg, M.W., Cronshaw, J.M., Rutherford, S., and Allen, T.D. (2000). The nuclear pore complex. Journal of cell science *113 (Pt 22)*, 3885-3886.

Bailer, S.M., Siniossoglou, S., Podtelejnikov, A., Hellwig, A., Mann, M., and Hurt, E. (1998). Nup116p and nup100p are interchangeable through a conserved motif which constitutes a docking site for the mRNA transport factor gle2p. The EMBO journal *17*, 1107-1119.

Banziger, C., Soldini, D., Schutt, C., Zipperlen, P., Hausmann, G., and Basler, K. (2006). Wntless, a conserved membrane protein dedicated to the secretion of Wnt proteins from signaling cells. Cell *125*, 509-522.

Barker, N., and Clevers, H. (2006). Mining the Wnt pathway for cancer therapeutics. Nat Rev Drug Discov *5*, 997-1014.

Barker, N., Hurlstone, A., Musisi, H., Miles, A., Bienz, M., and Clevers, H. (2001). The chromatin remodelling factor Brg-1 interacts with beta-catenin to promote target gene activation. The EMBO journal *20*, 4935-4943.

Bauer, A., Chauvet, S., Huber, O., Usseglio, F., Rothbacher, U., Aragnol, D., Kemler, R., and Pradel, J. (2000). Pontin52 and reptin52 function as antagonistic regulators of beta-catenin signalling activity. The EMBO journal *19*, 6121-6130.

Behrens, J., von Kries, J.P., Kuhl, M., Bruhn, L., Wedlich, D., Grosschedl, R., and Birchmeier, W. (1996). Functional interaction of beta-catenin with the transcription factor LEF-1. Nature *382*, 638-642.

Bei, Y., Hogan, J., Berkowitz, L.A., Soto, M., Rocheleau, C.E., Pang, K.M., Collins, J., and Mello, C.C. (2002). SRC-1 and Wnt signaling act together to specify endoderm and to control cleavage orientation in early C. elegans embryos. Developmental cell *3*, 113-125.

Berkowitz, L.A., and Strome, S. (2000). MES-1, a protein required for unequal divisions of the germline in early C. elegans embryos, resembles receptor tyrosine kinases and is localized to the boundary between the germline and gut cells. Development *127*, 4419-4431.

Bhanot, P., Brink, M., Samos, C.H., Hsieh, J.C., Wang, Y., Macke, J.P., Andrew, D., Nathans, J., and Nusse, R. (1996). A new member of the frizzled family from Drosophila functions as a Wingless receptor. Nature *382*, 225-230.

Bhardwaj, G., Murdoch, B., Wu, D., Baker, D.P., Williams, K.P., Chadwick, K., Ling, L.E., Karanu, F.N., and Bhatia, M. (2001). Sonic hedgehog induces the proliferation of primitive human hematopoietic cells via BMP regulation. Nat Immunol *2*, 172-180.

Bienz, M. (1998). TCF: transcriptional activator or repressor? Current opinion in cell biology *10*, 366-372.

Bienz, M. (2005). beta-Catenin: a pivot between cell adhesion and Wnt signalling. Curr Biol *15*, R64-67.

Bienz, M., and Hamada, F. (2004). Adenomatous polyposis coli proteins and cell adhesion. Current opinion in cell biology *16*, 528-535.

Bilic, J., Huang, Y.L., Davidson, G., Zimmermann, T., Cruciat, C.M., Bienz, M., and Niehrs, C. (2007). Wnt induces LRP6 signalosomes and promotes dishevelled-dependent LRP6 phosphorylation. Science *316*, 1619-1622.

Billuart, P., Winter, C.G., Maresh, A., Zhao, X., and Luo, L. (2001). Regulating axon branch stability: the role of p190 RhoGAP in repressing a retraction signaling pathway. Cell *107*, 195-207.

Blackwell, T.K., Bowerman, B., Priess, J.R., and Weintraub, H. (1994). Formation of a monomeric DNA binding domain by Skn-1 bZIP and homeodomain elements. Science *266*, 621-628.

Bourne, Y., Watson, M.H., Hickey, M.J., Holmes, W., Rocque, W., Reed, S.I., and Tainer, J.A. (1996). Crystal structure and mutational analysis of the human CDK2 kinase complex with cell cycle-regulatory protein CksHs1. Cell *84*, 863-874.

Bowerman, B., Draper, B.W., Mello, C.C., and Priess, J.R. (1993). The maternal gene skn-1 encodes a protein that is distributed unequally in early C. elegans embryos. Cell *74*, 443-452.

Boxem, M., Srinivasan, D.G., and van den Heuvel, S. (1999). The Caenorhabditis elegans gene ncc-1 encodes a cdc2-related kinase required for M phase in meiotic and mitotic cell divisions, but not for S phase. Development *126*, 2227-2239.

Brantjes, H., Barker, N., van Es, J., and Clevers, H. (2002). TCF: Lady Justice casting the final verdict on the outcome of Wnt signalling. Biol Chem *383*, 255-261.

Brembeck, F.H., Rosario, M., and Birchmeier, W. (2006). Balancing cell adhesion and Wnt signaling, the key role of beta-catenin. Curr Opin Genet Dev *16*, 51-59.

Brembeck, F.H., Schwarz-Romond, T., Bakkers, J., Wilhelm, S., Hammerschmidt, M., and Birchmeier, W. (2004). Essential role of BCL9-2 in the switch between beta-catenin's adhesive and transcriptional functions. Genes & development *18*, 2225-2230.

Brenner, S. (1974). The genetics of Caenorhabditis elegans. Genetics *77*, 71-94.

Browning, K.S. (1996). The plant translational apparatus. Plant molecular biology *32*, 107-144.

Bullions, L.C., and Levine, A.J. (1998). The role of beta-catenin in cell adhesion, signal transduction, and cancer. Curr Opin Oncol *10*, 81-87.

Cabrera, C.V., Alonso, M.C., Johnston, P., Phillips, R.G., and Lawrence, P.A. (1987). Phenocopies induced with antisense RNA identify the wingless gene. Cell *50*, 659-663.

Cadigan, K.M., and Liu, Y.I. (2006). Wnt signaling: complexity at the surface. Journal of cell science *119*, 395-402.

Cavallo, R.A., Cox, R.T., Moline, M.M., Roose, J., Polevoy, G.A., Clevers, H., Peifer, M., and Bejsovec, A. (1998). Drosophila Tcf and Groucho interact to repress Wingless signalling activity. Nature *395*, 604-608.

Chen, G., Fernandez, J., Mische, S., and Courey, A.J. (1999). A functional interaction between the histone deacetylase Rpd3 and the corepressor groucho in Drosophila development. Genes & development *13*, 2218-2230.

Chu-LaGraff, Q., and Doe, C.Q. (1993). Neuroblast specification and formation regulated by wingless in the Drosophila CNS. Science *261*, 1594-1597.

Clevers, H., and van de Wetering, M. (1997). TCF/LEF factor earn their wings. Trends Genet *13*, 485-489.

Cliffe, A., Hamada, F., and Bienz, M. (2003). A role of Dishevelled in relocating Axin to the plasma membrane during wingless signaling. Curr Biol *13*, 960-966.

Costa, M., Raich, W., Agbunag, C., Leung, B., Hardin, J., and Priess, J.R. (1998). A putative catenin-cadherin system mediates morphogenesis of the Caenorhabditis elegans embryo. The Journal of cell biology *141*, 297-308.

Crespo, P., Schuebel, K.E., Ostrom, A.A., Gutkind, J.S., and Bustelo, X.R. (1997). Phosphotyrosine-dependent activation of Rac-1 GDP/GTP exchange by the vav proto-oncogene product. Nature *385*, 169-172.

Cronshaw, J.M., Krutchinsky, A.N., Zhang, W., Chait, B.T., and Matunis, M.J. (2002). Proteomic analysis of the mammalian nuclear pore complex. The Journal of cell biology *158*, 915-927.

Daniels, D.L., and Weis, W.I. (2005). Beta-catenin directly displaces Groucho/TLE repressors from Tcf/Lef in Wnt-mediated transcription activation. Nat Struct Mol Biol *12*, 364-371.

DasGupta, R., Kaykas, A., Moon, R.T., and Perrimon, N. (2005). Functional genomic analysis of the Wnt-wingless signaling pathway. Science *308*, 826-833.

Davidson, G., Wu, W., Shen, J., Bilic, J., Fenger, U., Stannek, P., Glinka, A., and Niehrs, C. (2005). Casein kinase 1 gamma couples Wnt receptor activation to cytoplasmic signal transduction. Nature *438*, 867-872.

de la Roche, M., and Bienz, M. (2007). Wingless-independent association of Pygopus with dTCF target genes. Curr Biol *17*, 556-561.

De Souza, C.P., Horn, K.P., Masker, K., and Osmani, S.A. (2003). The SONB(NUP98) nucleoporin interacts with the NIMA kinase in Aspergillus nidulans. Genetics *165*, 1071-1081.

Detwiler, M.R., Reuben, M., Li, X., Rogers, E., and Lin, R. (2001). Two zinc finger proteins, OMA-1 and OMA-2, are redundantly required for oocyte maturation in C. elegans. Developmental cell *1*, 187-199.

Embi, N., Rylatt, D.B., and Cohen, P. (1980). Glycogen synthase kinase-3 from rabbit skeletal muscle. Separation from cyclic-AMP-dependent protein kinase and phosphorylase kinase. Eur J Biochem *107*, 519-527.

Emtage, J.L., Bucci, M., Watkins, J.L., and Wente, S.R. (1997). Defining the essential functional regions of the nucleoporin Nup145p. Journal of cell science *110 (Pt 7)*, 911-925.

Fabre, E., Boelens, W.C., Wimmer, C., Mattaj, I.W., and Hurt, E.C. (1994). Nup145p is required for nuclear export of mRNA and binds homopolymeric RNA in vitro via a novel conserved motif. Cell *78*, 275-289.

Fagotto, F., Gluck, U., and Gumbiner, B.M. (1998). Nuclear localization signal-independent and importin/karyopherin-independent nuclear import of beta-catenin. Curr Biol *8*, 181-190.

Fanto, M., and McNeill, H. (2004). Planar polarity from flies to vertebrates. Journal of cell science *117*, 527-533.

Ferraiuolo, M.A., Lee, C.S., Ler, L.W., Hsu, J.L., Costa-Mattioli, M., Luo, M.J., Reed, R., and Sonenberg, N. (2004). A nuclear translation-like factor eIF4AIII is recruited to the mRNA during splicing and functions in nonsense-mediated decay. Proceedings of the National Academy of Sciences of the United States of America *101*, 4118-4123.

Fire, A., Xu, S., Montgomery, M.K., Kostas, S.A., Driver, S.E., and Mello, C.C. (1998). Potent and specific genetic interference by double-stranded RNA in Caenorhabditis elegans. Nature *391*, 806-811.

Fontoura, B.M., Blobel, G., and Matunis, M.J. (1999). A conserved biogenesis pathway for nucleoporins: proteolytic processing of a 186-kilodalton precursor generates Nup98 and the novel nucleoporin, Nup96. The Journal of cell biology *144*, 1097-1112.

Fontoura, B.M., Blobel, G., and Yaseen, N.R. (2000). The nucleoporin Nup98 is a site for GDP/GTP exchange on ran and termination of karyopherin beta 2-mediated nuclear import. The Journal of biological chemistry *275*, 31289-31296.

Frame, S., and Cohen, P. (2001). GSK3 takes centre stage more than 20 years after its discovery. Biochem J *359*, 1-16.

Galy, V., Mattaj, I.W., and Askjaer, P. (2003). Caenorhabditis elegans nucleoporins Nup93 and Nup205 determine the limit of nuclear pore complex size exclusion in vivo. Molecular biology of the cell *14*, 5104-5115.

Giarre, M., Semenov, M.V., and Brown, A.M. (1998). Wnt signaling stabilizes the dual-function protein beta-catenin in diverse cell types. Ann N Y Acad Sci *857*, 43-55.

Gingras, A.C., Raught, B., and Sonenberg, N. (1999). eIF4 initiation factors: effectors of mRNA recruitment to ribosomes and regulators of translation. Annu Rev Biochem *68*, 913-963.

Goldstein, B. (1992). Induction of gut in Caenorhabditis elegans embryos. Nature *357*, 255-257.

Goldstein, B. (1993). Establishment of gut fate in the E lineage of C. elegans: the roles of lineage-dependent mechanisms and cell interactions. Development *118*, 1267-1277.

Goldstein, B. (1995a). An analysis of the response to gut induction in the C. elegans embryo. Development *121*, 1227-1236.

Goldstein, B. (1995b). Cell contacts orient some cell division axes in the Caenorhabditis elegans embryo. The Journal of cell biology *129*, 1071-1080.

Goldstein, B., Takeshita, H., Mizumoto, K., and Sawa, H. (2006). Wnt signals can function as positional cues in establishing cell polarity. Developmental cell *10*, 391-396.

Gorlich, D., and Kutay, U. (1999). Transport between the cell nucleus and the cytoplasm. Annual review of cell and developmental biology *15*, 607-660.

Goyer, C., Altmann, M., Lee, H.S., Blanc, A., Deshmukh, M., Woolford, J.L., Jr., Trachsel, H., and Sonenberg, N. (1993). TIF4631 and TIF4632: two yeast genes encoding the high-molecular-weight subunits of the cap-binding protein complex (eukaryotic initiation factor 4F) contain an RNA recognition motif-like sequence and carry out an essential function. Molecular and cellular biology *13*, 4860-4874.

Gradi, A., Imataka, H., Svitkin, Y.V., Rom, E., Raught, B., Morino, S., and Sonenberg, N. (1998). A novel functional human eukaryotic translation initiation factor 4G. Molecular and cellular biology *18*, 334-342.

Graham, T.A., Weaver, C., Mao, F., Kimelman, D., and Xu, W. (2000). Crystal structure of a beta-catenin/Tcf complex. Cell *103*, 885-896.

Griffis, E.R., Altan, N., Lippincott-Schwartz, J., and Powers, M.A. (2002). Nup98 is a mobile nucleoporin with transcription-dependent dynamics. Molecular biology of the cell *13*, 1282-1297.

Ha, N.C., Tonozuka, T., Stamos, J.L., Choi, H.J., and Weis, W.I. (2004). Mechanism of phosphorylation-dependent binding of APC to beta-catenin and its role in beta-catenin degradation. Molecular cell *15*, 511-521.

Habas, R., Kato, Y., and He, X. (2001). Wnt/Frizzled activation of Rho regulates vertebrate gastrulation and requires a novel Formin homology protein Daam1. Cell *107*, 843-854.

Hadwiger, J.A., Wittenberg, C., Mendenhall, M.D., and Reed, S.I. (1989). The Saccharomyces cerevisiae CKS1 gene, a homolog of the Schizosaccharomyces pombe suc1+ gene, encodes a subunit of the Cdc28 protein kinase complex. Molecular and cellular biology *9*, 2034-2041.

Hart, M., Concordet, J.P., Lassot, I., Albert, I., del los Santos, R., Durand, H., Perret, C., Rubinfeld, B., Margottin, F., Benarous, R.*, et al.* (1999). The F-box protein beta-TrCP associates with phosphorylated beta-catenin and regulates its activity in the cell. Curr Biol *9*, 207-210.

Hawkins, N.C., Ellis, G.C., Bowerman, B., and Garriga, G. (2005). MOM-5 frizzled regulates the distribution of DSH-2 to control C. elegans asymmetric neuroblast divisions. Developmental biology *284*, 246-259.

Hayles, J., Beach, D., Durkacz, B., and Nurse, P. (1986). The fission yeast cell cycle control gene cdc2: isolation of a sequence suc1 that suppresses cdc2 mutant function. Mol Gen Genet *202*, 291-293.

He, X., Semenov, M., Tamai, K., and Zeng, X. (2004). LDL receptor-related proteins 5 and 6 in Wnt/beta-catenin signaling: arrows point the way. Development *131*, 1663-1677.

Hecht, A., Litterst, C.M., Huber, O., and Kemler, R. (1999). Functional characterization of multiple transactivating elements in beta-catenin, some of which interact with the TATA-binding protein in vitro. The Journal of biological chemistry *274*, 18017-18025.

Himpel, S., Tegge, W., Frank, R., Leder, S., Joost, H.G., and Becker, W. (2000). Specificity determinants of substrate recognition by the protein kinase DYRK1A. The Journal of biological chemistry *275*, 2431-2438.

Hinck, L., Nathke, I.S., Papkoff, J., and Nelson, W.J. (1994). Beta-catenin: a common target for the regulation of cell adhesion by Wnt-1 and Src signaling pathways. Trends Biochem Sci *19*, 538-542.

Hodel, A.E., Hodel, M.R., Griffis, E.R., Hennig, K.A., Ratner, G.A., Xu, S., and Powers, M.A. (2002). The three-dimensional structure of the autoproteolytic, nuclear pore-targeting domain of the human nucleoporin Nup98. Molecular cell *10*, 347-358.

Hoffmans, R., Stadeli, R., and Basler, K. (2005). Pygopus and legless provide essential transcriptional coactivator functions to armadillo/beta-catenin. Curr Biol *15*, 1207-1211.

Hofmann, K. (2000). A superfamily of membrane-bound O-acyltransferases with implications for wnt signaling. Trends Biochem Sci *25*, 111-112.

Huber, A.H., and Weis, W.I. (2001). The structure of the beta-catenin/E-cadherin complex and the molecular basis of diverse ligand recognition by beta-catenin. Cell *105*, 391-402.

Hughes, K., Nikolakaki, E., Plyte, S.E., Totty, N.F., and Woodgett, J.R. (1993). Modulation of the glycogen synthase kinase-3 family by tyrosine phosphorylation. The EMBO journal *12*, 803-808.

Hulsken, J., Birchmeier, W., and Behrens, J. (1994). E-cadherin and APC compete for the interaction with beta-catenin and the cytoskeleton. The Journal of cell biology *127*, 2061-2069.

Hunter, C.P., and Kenyon, C. (1996). Spatial and temporal controls target pal-1 blastomere-specification activity to a single blastomere lineage in C. elegans embryos. Cell *87*, 217-226.

Hyman, A.A., and White, J.G. (1987). Determination of cell division axes in the early embryogenesis of Caenorhabditis elegans. The Journal of cell biology *105*, 2123-2135.

Inoue, H., Hisamoto, N., An, J.H., Oliveira, R.P., Nishida, E., Blackwell, T.K., and Matsumoto, K. (2005). The C. elegans p38 MAPK pathway regulates nuclear localization of the transcription factor SKN-1 in oxidative stress response. Genes & development *19*, 2278-2283.

Inoue, T., Oz, H.S., Wiland, D., Gharib, S., Deshpande, R., Hill, R.J., Katz, W.S., and Sternberg, P.W. (2004). C. elegans LIN-18 is a Ryk ortholog and functions in parallel to LIN-17/Frizzled in Wnt signaling. Cell *118*, 795-806.

Ishitani, T., Ninomiya-Tsuji, J., Nagai, S., Nishita, M., Meneghini, M., Barker, N., Waterman, M., Bowerman, B., Clevers, H., Shibuya, H.*, et al.* (1999). The TAK1-NLK-MAPK-related

pathway antagonizes signalling between beta-catenin and transcription factor TCF. Nature *399*, 798-802.

Jeffrey, P.D., Russo, A.A., Polyak, K., Gibbs, E., Hurwitz, J., Massague, J., and Pavletich, N.P. (1995). Mechanism of CDK activation revealed by the structure of a cyclinA-CDK2 complex. Nature *376*, 313-320.

Kaletta, T., Schnabel, H., and Schnabel, R. (1997). Binary specification of the embryonic lineage in Caenorhabditis elegans. Nature *390*, 294-298.

Kamath, R.S., Fraser, A.G., Dong, Y., Poulin, G., Durbin, R., Gotta, M., Kanapin, A., Le Bot, N., Moreno, S., Sohrmann, M.*, et al.* (2003). Systematic functional analysis of the Caenorhabditis elegans genome using RNAi. Nature *421*, 231-237.

Katanaev, V.L., Ponzielli, R., Semeriva, M., and Tomlinson, A. (2005). Trimeric G protein-dependent frizzled signaling in Drosophila. Cell *120*, 111-122.

Kemler, R. (1993). From cadherins to catenins: cytoplasmic protein interactions and regulation of cell adhesion. Trends Genet *9*, 317-321.

Kemphues, K.J., Priess, J.R., Morton, D.G., and Cheng, N.S. (1988). Identification of genes required for cytoplasmic localization in early C. elegans embryos. Cell *52*, 311-320.

Kidd, A.R., 3rd, Miskowski, J.A., Siegfried, K.R., Sawa, H., and Kimble, J. (2005). A beta-catenin identified by functional rather than sequence criteria and its role in Wnt/MAPK signaling. Cell *121*, 761-772.

Kim, L., Liu, J., and Kimmel, A.R. (1999). The novel tyrosine kinase ZAK1 activates GSK3 to direct cell fate specification. Cell *99*, 399-408.

Korneeva, N.L., Lamphear, B.J., Hennigan, F.L., Merrick, W.C., and Rhoads, R.E. (2001). Characterization of the two eIF4A-binding sites on human eIF4G-1. The Journal of biological chemistry *276*, 2872-2879.

Korswagen, H.C. (2002). Canonical and non-canonical Wnt signaling pathways in Caenorhabditis elegans: variations on a common signaling theme. Bioessays *24*, 801-810.

Korswagen, H.C., Herman, M.A., and Clevers, H.C. (2000). Distinct beta-catenins mediate adhesion and signalling functions in C. elegans. Nature *406*, 527-532.

Kramps, T., Peter, O., Brunner, E., Nellen, D., Froesch, B., Chatterjee, S., Murone, M., Zullig, S., and Basler, K. (2002). Wnt/wingless signaling requires BCL9/legless-mediated recruitment of pygopus to the nuclear beta-catenin-TCF complex. Cell *109*, 47-60.

Krieghoff, E., Behrens, J., and Mayr, B. (2006). Nucleo-cytoplasmic distribution of beta-catenin is regulated by retention. Journal of cell science *119*, 1453-1463.

Kuhl, M., Geis, K., Sheldahl, L.C., Pukrop, T., Moon, R.T., and Wedlich, D. (2001). Antagonistic regulation of convergent extension movements in Xenopus by Wnt/beta-catenin and Wnt/Ca2+ signaling. Mechanisms of development *106*, 61-76.

Li, J., and Li, W.X. (2006). A novel function of Drosophila eIF4A as a negative regulator of Dpp/BMP signalling that mediates SMAD degradation. Nature cell biology *8*, 1407-1414.

Li, J., Li, W.X., and Gelbart, W.M. (2005). A genetic screen for maternal-effect suppressors of decapentaplegic identifies the eukaryotic translation initiation factor 4A in Drosophila. Genetics *171*, 1629-1641.

Li, L., Yuan, H., Weaver, C.D., Mao, J., Farr, G.H., 3rd, Sussman, D.J., Jonkers, J., Kimelman, D., and Wu, D. (1999). Axin and Frat1 interact with dvl and GSK, bridging Dvl to GSK in Wnt-mediated regulation of LEF-1. The EMBO journal *18*, 4233-4240.

Lin, R. (2003). A gain-of-function mutation in oma-1, a C. elegans gene required for oocyte maturation, results in delayed degradation of maternal proteins and embryonic lethality. Developmental biology *258*, 226-239.

Lin, R., Hill, R.J., and Priess, J.R. (1998). POP-1 and anterior-posterior fate decisions in C. elegans embryos. Cell *92*, 229-239.

Lin, R., Thompson, S., and Priess, J.R. (1995). pop-1 encodes an HMG box protein required for the specification of a mesoderm precursor in early C. elegans embryos. Cell *83*, 599-609.

Liu, C., Li, Y., Semenov, M., Han, C., Baeg, G.H., Tan, Y., Zhang, Z., Lin, X., and He, X. (2002). Control of beta-catenin phosphorylation/degradation by a dual-kinase mechanism. Cell *108*, 837-847.

Liu, X., Rubin, J.S., and Kimmel, A.R. (2005). Rapid, Wnt-induced changes in GSK3beta associations that regulate beta-catenin stabilization are mediated by Galpha proteins. Curr Biol *15*, 1989-1997.

Lo, M.C., Gay, F., Odom, R., Shi, Y., and Lin, R. (2004). Phosphorylation by the beta-catenin/MAPK complex promotes 14-3-3-mediated nuclear export of TCF/POP-1 in signal-responsive cells in C. elegans. Cell *117*, 95-106.

Logan, C.Y., and Nusse, R. (2004). The Wnt signaling pathway in development and disease. Annual review of cell and developmental biology *20*, 781-810.

Lomakin, I.B., Hellen, C.U., and Pestova, T.V. (2000). Physical association of eukaryotic initiation factor 4G (eIF4G) with eIF4A strongly enhances binding of eIF4G to the internal ribosomal entry site of encephalomyocarditis virus and is required for internal initiation of translation. Molecular and cellular biology *20*, 6019-6029.

Long, X., Spycher, C., Han, Z.S., Rose, A.M., Muller, F., and Avruch, J. (2002). TOR deficiency in C. elegans causes developmental arrest and intestinal atrophy by inhibition of mRNA translation. Curr Biol *12*, 1448-1461.

Lu, W., Yamamoto, V., Ortega, B., and Baltimore, D. (2004). Mammalian Ryk is a Wnt coreceptor required for stimulation of neurite outgrowth. Cell *119*, 97-108.

Mao, J., Wang, J., Liu, B., Pan, W., Farr, G.H., 3rd, Flynn, C., Yuan, H., Takada, S., Kimelman, D., Li, L.*, et al.* (2001). Low-density lipoprotein receptor-related protein-5 binds to Axin and regulates the canonical Wnt signaling pathway. Molecular cell *7*, 801-809.

McCarter, J., Bartlett, B., Dang, T., and Schedl, T. (1999). On the control of oocyte meiotic maturation and ovulation in Caenorhabditis elegans. Developmental biology *205*, 111-128.

McCartney, B.M., Dierick, H.A., Kirkpatrick, C., Moline, M.M., Baas, A., Peifer, M., and Bejsovec, A. (1999). Drosophila APC2 is a cytoskeletally-associated protein that regulates wingless signaling in the embryonic epidermis. The Journal of cell biology *146*, 1303-1318.

Mello, C.C., Draper, B.W., Krause, M., Weintraub, H., and Priess, J.R. (1992). The pie-1 and mex-1 genes and maternal control of blastomere identity in early C. elegans embryos. Cell *70*, 163-176.

Meneghini, M.D., Ishitani, T., Carter, J.C., Hisamoto, N., Ninomiya-Tsuji, J., Thorpe, C.J., Hamill, D.R., Matsumoto, K., and Bowerman, B. (1999). MAP kinase and Wnt pathways

converge to downregulate an HMG-domain repressor in Caenorhabditis elegans. Nature *399*, 793-797.

Miller, J.R., Hocking, A.M., Brown, J.D., and Moon, R.T. (1999). Mechanism and function of signal transduction by the Wnt/beta-catenin and Wnt/Ca2+ pathways. Oncogene *18*, 7860-7872.

Mizumoto, K., and Sawa, H. (2007a). Cortical beta-catenin and APC regulate asymmetric nuclear beta-catenin localization during asymmetric cell division in C. elegans. Developmental cell *12*, 287-299.

Mizumoto, K., and Sawa, H. (2007b). Two betas or not two betas: regulation of asymmetric division by beta-catenin. Trends Cell Biol *17*, 465-473.

Molenaar, M., van de Wetering, M., Oosterwegel, M., Peterson-Maduro, J., Godsave, S., Korinek, V., Roose, J., Destree, O., and Clevers, H. (1996). XTcf-3 transcription factor mediates beta-catenin-induced axis formation in Xenopus embryos. Cell *86*, 391-399.

Morino, S., Imataka, H., Svitkin, Y.V., Pestova, T.V., and Sonenberg, N. (2000). Eukaryotic translation initiation factor 4E (eIF4E) binding site and the middle one-third of eIF4GI constitute

the core domain for cap-dependent translation, and the C-terminal one-third functions as a modulatory region. Molecular and cellular biology *20*, 468-477.

Morton, D.G., Roos, J.M., and Kemphues, K.J. (1992). par-4, a gene required for cytoplasmic localization and determination of specific cell types in Caenorhabditis elegans embryogenesis. Genetics *130*, 771-790.

Mosimann, C., Hausmann, G., and Basler, K. (2006). Parafibromin/Hyrax activates Wnt/Wg target gene transcription by direct association with beta-catenin/Armadillo. Cell *125*, 327-341.

Nakamura, K., Kim, S., Ishidate, T., Bei, Y., Pang, K., Shirayama, M., Trzepacz, C., Brownell, D.R., and Mello, C.C. (2005). Wnt signaling drives WRM-1/beta-catenin asymmetries in early C. elegans embryos. Genes & development *19*, 1749-1754.

Natarajan, L., Witwer, N.E., and Eisenmann, D.M. (2001). The divergent Caenorhabditis elegans beta-catenin proteins BAR-1, WRM-1 and HMP-2 make distinct protein interactions but retain functional redundancy in vivo. Genetics *159*, 159-172.

Nelson, W.J., and Nusse, R. (2004). Convergence of Wnt, beta-catenin, and cadherin pathways. Science *303*, 1483-1487.

Nishi, Y., and Lin, R. (2005). DYRK2 and GSK-3 phosphorylate and promote the timely degradation of OMA-1, a key regulator of the oocyte-to-embryo transition in C. elegans. Developmental biology *288*, 139-149.

Nusse, R. (1997). A versatile transcriptional effector of Wingless signaling. Cell *89*, 321-323.

Nusse, R., and Varmus, H.E. (1982). Many tumors induced by the mouse mammary tumor virus contain a provirus integrated in the same region of the host genome. Cell *31*, 99-109.

Obenauer, J.C., Cantley, L.C., and Yaffe, M.B. (2003). Scansite 2.0: Proteome-wide prediction of cell signaling interactions using short sequence motifs. Nucleic Acids Res *31*, 3635-3641.

Palacios, I.M., Gatfield, D., St Johnston, D., and Izaurralde, E. (2004). An eIF4AIII-containing complex required for mRNA localization and nonsense-mediated mRNA decay. Nature *427*, 753-757.

Pang, K.M., Ishidate, T., Nakamura, K., Shirayama, M., Trzepacz, C., Schubert, C.M., Priess, J.R., and Mello, C.C. (2004). The minibrain kinase homolog, mbk-2, is required for spindle positioning and asymmetric cell division in early C. elegans embryos. Developmental biology *265*, 127-139.

Papkoff, J. (1997). Regulation of complexed and free catenin pools by distinct mechanisms. Differential effects of Wnt-1 and v-Src. The Journal of biological chemistry *272*, 4536-4543.

Park, F.D., and Priess, J.R. (2003). Establishment of POP-1 asymmetry in early C. elegans embryos. Development *130*, 3547-3556.

Pellettieri, J., Reinke, V., Kim, S.K., and Seydoux, G. (2003). Coordinate activation of maternal protein degradation during the egg-to-embryo transition in C. elegans. Developmental cell *5*, 451-462.

Peters, J.M., McKay, R.M., McKay, J.P., and Graff, J.M. (1999). Casein kinase I transduces Wnt signals. Nature *401*, 345-350.

Pinson, K.I., Brennan, J., Monkley, S., Avery, B.J., and Skarnes, W.C. (2000). An LDL-receptor-related protein mediates Wnt signalling in mice. Nature *407*, 535-538.

Polakis, P. (2000). Wnt signaling and cancer. Genes & development *14*, 1837-1851.

Polinko, E.S., and Strome, S. (2000). Depletion of a Cks homolog in C. elegans embryos uncovers a post-metaphase role in both meiosis and mitosis. Curr Biol *10*, 1471-1474.

Powers, M.A., Forbes, D.J., Dahlberg, J.E., and Lund, E. (1997). The vertebrate GLFG nucleoporin, Nup98, is an essential component of multiple RNA export pathways. The Journal of cell biology *136*, 241-250.

Praitis, V. (2006). Creation of transgenic lines using microparticle bombardment methods. Methods Mol Biol *351*, 93-107.

Price, M.A. (2006). CKI, there's more than one: casein kinase I family members in Wnt and Hedgehog signaling. Genes & development *20*, 399-410.

Priess, J.R., and Thomson, J.N. (1987). Cellular interactions in early C. elegans embryos. Cell *48*, 241-250.

Pritchard, C.E., Fornerod, M., Kasper, L.H., and van Deursen, J.M. (1999). RAE1 is a shuttling mRNA export factor that binds to a GLEBS-like NUP98 motif at the nuclear pore complex through multiple domains. The Journal of cell biology *145*, 237-254.

Quintin, S., Mains, P.E., Zinke, A., and Hyman, A.A. (2003). The mbk-2 kinase is required for inactivation of MEI-1/katanin in the one-cell Caenorhabditis elegans embryo. EMBO reports *4*, 1175-1181.

Radu, A., Moore, M.S., and Blobel, G. (1995). The peptide repeat domain of nucleoporin Nup98 functions as a docking site in transport across the nuclear pore complex. Cell *81*, 215-222.

Rexach, M., and Blobel, G. (1995). Protein import into nuclei: association and dissociation reactions involving transport substrate, transport factors, and nucleoporins. Cell *83*, 683-692.

Reya, T., Morrison, S.J., Clarke, M.F., and Weissman, I.L. (2001). Stem cells, cancer, and cancer stem cells. Nature *414*, 105-111.

Richardson, H.E., Stueland, C.S., Thomas, J., Russell, P., and Reed, S.I. (1990). Human cDNAs encoding homologs of the small p34Cdc28/Cdc2-associated protein of Saccharomyces cerevisiae and Schizosaccharomyces pombe. Genes & development *4*, 1332-1344.

Rijsewijk, F., Schuermann, M., Wagenaar, E., Parren, P., Weigel, D., and Nusse, R. (1987). The Drosophila homolog of the mouse mammary oncogene int-1 is identical to the segment polarity gene wingless. Cell *50*, 649-657.

Rocheleau, C.E., Downs, W.D., Lin, R., Wittmann, C., Bei, Y., Cha, Y.H., Ali, M., Priess, J.R., and Mello, C.C. (1997). Wnt signaling and an APC-related gene specify endoderm in early C. elegans embryos. Cell *90*, 707-716.

Rocheleau, C.E., Yasuda, J., Shin, T.H., Lin, R., Sawa, H., Okano, H., Priess, J.R., Davis, R.J., and Mello, C.C. (1999). WRM-1 activates the LIT-1 protein kinase to transduce anterior/posterior polarity signals in C. elegans. Cell *97*, 717-726.

Roose, J., Molenaar, M., Peterson, J., Hurenkamp, J., Brantjes, H., Moerer, P., van de Wetering, M., Destree, O., and Clevers, H. (1998). The Xenopus Wnt effector XTcf-3 interacts with Groucho-related transcriptional repressors. Nature *395*, 608-612.

Rose, L.S., and Kemphues, K.J. (1998). Early patterning of the C. elegans embryo. Annu Rev Genet *32*, 521-545.

Rosenblum, J.S., and Blobel, G. (1999). Autoproteolysis in nucleoporin biogenesis. Proceedings of the National Academy of Sciences of the United States of America *96*, 11370-11375.

Rout, M.P., Aitchison, J.D., Suprapto, A., Hjertaas, K., Zhao, Y., and Chait, B.T. (2000). The yeast nuclear pore complex: composition, architecture, and transport mechanism. The Journal of cell biology *148*, 635-651.

Rubinfeld, B., Albert, I., Porfiri, E., Fiol, C., Munemitsu, S., and Polakis, P. (1996). Binding of GSK3beta to the APC-beta-catenin complex and regulation of complex assembly. Science *272*, 1023-1026.

Ryan, K.J., and Wente, S.R. (2000). The nuclear pore complex: a protein machine bridging the nucleus and cytoplasm. Current opinion in cell biology *12*, 361-371.

Sancho, E., Batlle, E., and Clevers, H. (2003). Live and let die in the intestinal epithelium. Current opinion in cell biology *15*, 763-770.

Schierenberg, E. (1987). Reversal of cellular polarity and early cell-cell interaction in the embryos of Caenorhabditis elegans. Developmental biology *122*, 452-463.

Schlesinger, A., Shelton, C.A., Maloof, J.N., Meneghini, M., and Bowerman, B. (1999). Wnt pathway components orient a mitotic spindle in the early Caenorhabditis elegans embryo without requiring gene transcription in the responding cell. Genes & development *13*, 2028-2038.

Schnabel, R., Weigner, C., Hutter, H., Feichtinger, R., and Schnabel, H. (1996). mex-1 and the general partitioning of cell fate in the early C. elegans embryo. Mechanisms of development *54*, 133-147.

Schneider, S.Q., Finnerty, J.R., and Martindale, M.Q. (2003). Protein evolution: structure-function relationships of the oncogene beta-catenin in the evolution of multicellular animals. J Exp Zoolog B Mol Dev Evol *295*, 25-44.

Shibuya, T., Tange, T.O., Sonenberg, N., and Moore, M.J. (2004). eIF4AIII binds spliced mRNA in the exon junction complex and is essential for nonsense-mediated decay. Nat Struct Mol Biol *11*, 346-351.

Shin, T.H., Yasuda, J., Rocheleau, C.E., Lin, R., Soto, M., Bei, Y., Davis, R.J., and Mello, C.C. (1999). MOM-4, a MAP kinase kinase kinase-related protein, activates WRM-1/LIT-1 kinase to transduce anterior/posterior polarity signals in C. elegans. Molecular cell *4*, 275-280.

Shirayama, M., Soto, M.C., Ishidate, T., Kim, S., Nakamura, K., Bei, Y., van den Heuvel, S., and Mello, C.C. (2006). The Conserved Kinases CDK-1, GSK-3, KIN-19, and MBK-2 Promote OMA-1 Destruction to Regulate the Oocyte-to-Embryo Transition in C. elegans. Curr Biol *16*, 47-55.

Sierra, J., Yoshida, T., Joazeiro, C.A., and Jones, K.A. (2006). The APC tumor suppressor counteracts beta-catenin activation and H3K4 methylation at Wnt target genes. Genes & development *20*, 586-600.

Slusarski, D.C., Corces, V.G., and Moon, R.T. (1997). Interaction of Wnt and a Frizzled homologue triggers G-protein-linked phosphatidylinositol signalling. Nature *390*, 410-413.

Stoffler, D., Fahrenkrog, B., and Aebi, U. (1999). The nuclear pore complex: from molecular architecture to functional dynamics. Current opinion in cell biology *11*, 391-401.

Strome, S., Martin, P., Schierenberg, E., and Paulsen, J. (1995). Transformation of the germ line into muscle in mes-1 mutant embryos of C. elegans. Development *121*, 2961-2972.

Suh, E.K., and Gumbiner, B.M. (2003). Translocation of beta-catenin into the nucleus independent of interactions with FG-rich nucleoporins. Exp Cell Res *290*, 447-456.

Sulston, J.E., Schierenberg, E., White, J.G., and Thomson, J.N. (1983). The embryonic cell lineage of the nematode Caenorhabditis elegans. Developmental biology *100*, 64-119.

Suntharalingam, M., and Wente, S.R. (2003). Peering through the pore: nuclear pore complex structure, assembly, and function. Developmental cell *4*, 775-789.

Tabuse, Y., Izumi, Y., Piano, F., Kemphues, K.J., Miwa, J., and Ohno, S. (1998). Atypical protein kinase C cooperates with PAR-3 to establish embryonic polarity in Caenorhabditis elegans. Development *125*, 3607-3614.

Taipale, J., and Beachy, P.A. (2001). The Hedgehog and Wnt signalling pathways in cancer. Nature *411*, 349-354.

Takeshita, H., and Sawa, H. (2005). Asymmetric cortical and nuclear localizations of WRM-1/beta-catenin during asymmetric cell division in C. elegans. Genes & development *19*, 1743-1748.

Tamai, K., Semenov, M., Kato, Y., Spokony, R., Liu, C., Katsuyama, Y., Hess, F., Saint-Jeannet, J.P., and He, X. (2000). LDL-receptor-related proteins in Wnt signal transduction. Nature *407*, 530-535.

Teixeira, M.T., Siniossoglou, S., Podtelejnikov, S., Benichou, J.C., Mann, M., Dujon, B., Hurt, E., and Fabre, E. (1997). Two functionally distinct domains generated by in vivo cleavage of Nup145p: a novel biogenesis pathway for nucleoporins. The EMBO journal *16*, 5086-5097.

Tenenhaus, C., Schubert, C., and Seydoux, G. (1998). Genetic requirements for PIE-1 localization and inhibition of gene expression in the embryonic germ lineage of Caenorhabditis elegans. Developmental biology *200*, 212-224.

Thorpe, C.J., Schlesinger, A., and Bowerman, B. (2000). Wnt signalling in Caenorhabditis elegans: regulating repressors and polarizing the cytoskeleton. Trends Cell Biol *10*, 10-17.

Thorpe, C.J., Schlesinger, A., Carter, J.C., and Bowerman, B. (1997). Wnt signaling polarizes an early C. elegans blastomere to distinguish endoderm from mesoderm. Cell *90*, 695-705.

Tio, M., Udolph, G., Yang, X., and Chia, W. (2001). cdc2 links the Drosophila cell cycle and asymmetric division machineries. Nature *409*, 1063-1067.

Tolwinski, N.S., Wehrli, M., Rives, A., Erdeniz, N., DiNardo, S., and Wieschaus, E. (2003). Wg/Wnt signal can be transmitted through arrow/LRP5,6 and Axin independently of Zw3/Gsk3beta activity. Developmental cell *4*, 407-418.

van de Wetering, M., Cavallo, R., Dooijes, D., van Beest, M., van Es, J., Loureiro, J., Ypma, A., Hursh, D., Jones, T., Bejsovec, A.*, et al.* (1997). Armadillo coactivates transcription driven by the product of the Drosophila segment polarity gene dTCF. Cell *88*, 789-799.

van Ooyen, A., and Nusse, R. (1984). Structure and nucleotide sequence of the putative mammary oncogene int-1; proviral insertions leave the protein-encoding domain intact. Cell *39*, 233-240.

Varnum-Finney, B., Xu, L., Brashem-Stein, C., Nourigat, C., Flowers, D., Bakkour, S., Pear, W.S., and Bernstein, I.D. (2000). Pluripotent, cytokine-dependent, hematopoietic stem cells are immortalized by constitutive Notch1 signaling. Nat Med *6*, 1278-1281.

Wallingford, J.B., and Habas, R. (2005). The developmental biology of Dishevelled: an enigmatic protein governing cell fate and cell polarity. Development *132*, 4421-4436.

Wallingford, J.B., Vogeli, K.M., and Harland, R.M. (2001). Regulation of convergent extension in Xenopus by Wnt5a and Frizzled-8 is independent of the canonical Wnt pathway. Int J Dev Biol *45*, 225-227.

Walston, T., Tuskey, C., Edgar, L., Hawkins, N., Ellis, G., Bowerman, B., Wood, W., and Hardin, J. (2004). Multiple Wnt signaling pathways converge to orient the mitotic spindle in early C. elegans embryos. Developmental cell *7*, 831-841.

Wang, Q.M., Fiol, C.J., DePaoli-Roach, A.A., and Roach, P.J. (1994). Glycogen synthase kinase-3 beta is a dual specificity kinase differentially regulated by tyrosine and serine/threonine phosphorylation. The Journal of biological chemistry *269*, 14566-14574.

Waring, D.A., and Kenyon, C. (1990). Selective silencing of cell communication influences anteroposterior pattern formation in C. elegans. Cell *60*, 123-131.

Watts, J.L., Etemad-Moghadam, B., Guo, S., Boyd, L., Draper, B.W., Mello, C.C., Priess, J.R., and Kemphues, K.J. (1996). par-6, a gene involved in the establishment of asymmetry in early C. elegans embryos, mediates the asymmetric localization of PAR-3. Development *122*, 3133-3140.

Wehrli, M., Dougan, S.T., Caldwell, K., O'Keefe, L., Schwartz, S., Vaizel-Ohayon, D., Schejter, E., Tomlinson, A., and DiNardo, S. (2000). arrow encodes an LDL-receptor-related protein essential for Wingless signalling. Nature *407*, 527-530.

Willert, K., Brown, J.D., Danenberg, E., Duncan, A.W., Weissman, I.L., Reya, T., Yates, J.R., 3rd, and Nusse, R. (2003). Wnt proteins are lipid-modified and can act as stem cell growth factors. Nature *423*, 448-452.

Willert, K., and Jones, K.A. (2006). Wnt signaling: is the party in the nucleus? Genes & development *20*, 1394-1404.

Willert, K., and Nusse, R. (1998). Beta-catenin: a key mediator of Wnt signaling. Curr Opin Genet Dev *8*, 95-102.

Winter, C.G., Wang, B., Ballew, A., Royou, A., Karess, R., Axelrod, J.D., and Luo, L. (2001). Drosophila Rho-associated kinase (Drok) links Frizzled-mediated planar cell polarity signaling to the actin cytoskeleton. Cell *105*, 81-91.

Wood, W.B. (1991). Evidence from reversal of handedness in C. elegans embryos for early cell interactions determining cell fates. Nature *349*, 536-538.

Wu, M., and Herman, M.A. (2007). Asymmetric localizations of LIN-17/Fz and MIG-5/Dsh are involved in the asymmetric B cell division in C. elegans. Developmental biology *303*, 650-662.

Wu, S.L., Staudinger, J., Olson, E.N., and Rubin, C.S. (1998). Structure, expression, and properties of an atypical protein kinase C (PKC3) from Caenorhabditis elegans. PKC3 is required for the normal progression of embryogenesis and viability of the organism. The Journal of biological chemistry *273*, 1130-1143.

Wu, X., Kasper, L.H., Mantcheva, R.T., Mantchev, G.T., Springett, M.J., and van Deursen, J.M. (2001). Disruption of the FG nucleoporin NUP98 causes selective changes in nuclear pore complex stoichiometry and function. Proceedings of the National Academy of Sciences of the United States of America *98*, 3191-3196.

Xing, Y., Clements, W.K., Kimelman, D., and Xu, W. (2003). Crystal structure of a beta-catenin/axin complex suggests a mechanism for the beta-catenin destruction complex. Genes & development *17*, 2753-2764.

Xing, Y., Clements, W.K., Le Trong, I., Hinds, T.R., Stenkamp, R., Kimelman, D., and Xu, W. (2004). Crystal structure of a beta-catenin/APC complex reveals a critical role for APC phosphorylation in APC function. Molecular cell *15*, 523-533.

Yan, R., Rychlik, W., Etchison, D., and Rhoads, R.E. (1992). Amino acid sequence of the human protein synthesis initiation factor eIF-4 gamma. The Journal of biological chemistry *267*, 23226-23231.

Yanagawa, S., Matsuda, Y., Lee, J.S., Matsubayashi, H., Sese, S., Kadowaki, T., and Ishimoto, A. (2002). Casein kinase I phosphorylates the Armadillo protein and induces its degradation in Drosophila. The EMBO journal *21*, 1733-1742.

Yoshikawa, S., McKinnon, R.D., Kokel, M., and Thomas, J.B. (2003). Wnt-mediated axon guidance via the Drosophila Derailed receptor. Nature *422*, 583-588.

Yu, V.P., Baskerville, C., Grunenfelder, B., and Reed, S.I. (2005). A kinase-independent function of Cks1 and Cdk1 in regulation of transcription. Molecular cell *17*, 145-151.

Zapata, J.M., Martinez, M.A., and Sierra, J.M. (1994). Purification and characterization of eukaryotic polypeptide chain initiation factor 4F from Drosophila melanogaster embryos. The Journal of biological chemistry *269*, 18047-18052.

Zeng, X., Tamai, K., Doble, B., Li, S., Huang, H., Habas, R., Okamura, H., Woodgett, J., and He, X. (2005). A dual-kinase mechanism for Wnt co-receptor phosphorylation and activation. Nature *438*, 873-877.

Zhai, L., Chaturvedi, D., and Cumberledge, S. (2004). Drosophila wnt-1 undergoes a hydrophobic modification and is targeted to lipid rafts, a process that requires porcupine. The Journal of biological chemistry *279*, 33220-33227.